THE CRYSTAL STRUCTURE OF CORONENE AND RELATED HYDROCARBONS.

T H E S I S

Presented for the degree of

Doctor of Philosophy

in the

University of Glasgow

by

John Greville White, B.Sc.

September, 1946.

ProQuest LLC.
789 East Eisenhower Parkway
P.O. Box 1346
Ann Arbor, MI 48106 – 1346

THE CRYSTAL STRUCTURE OF CORONENE AND RELATED HYDROCARBONS.

--------oOo--------

PREFACE.

The work described on coronene has been published by the Chemical Society ("The Crystal Structure of Coronene. A Quantitative X-ray Investigation." J.C.S., 1945, 607) and a paper on "The Crystal Structure of Pyrene" has been ordered for publication by the same Society. The work carried out on 1.2:5.6 Dibenzanthracene and also that on errors arising in Fourier projection maps (Part III) is being prepared for publication. All these papers are in conjunction with Prof. J. Monteath Robertson.

The author wishes to thank Prof. J. Monteath Robertson for suggesting the problems for research, and for his constant help and encouragement throughout. Thanks are also due to the Carnegie Trustees for a Scholarship held during part of the work; to Mr. J. Findlay for help in preparing diagrams; and to Mr. E.J. Bowen, F.R.S. and Messrs. I.C.I. Ltd. for samples of the hydrocarbon coronene.

SUMMARY.

The crystal structures of the hydrocarbons coronene, pyrene and the orthorhombic modification of 1:2:5:6 dibenzanthracene have been investigated by X-ray diffraction methods. The experimental data for corenene were measured by the author and those for the other two compounds by Prof. J.M.Robertson. Variations have been found in carbon-carbon bond distances in different parts of the molecules and in the case of coronene these are considered to be beyond experimental error, but in the other compounds the position is less certain in view of unfavourable resolution in the Fourier projection maps.

Errors arising in coordinates obtained from two-dimensional Fourier analyses have been investigated and the results applied to the structure analyses mentioned above.

The bond distances measured in coronene, pyrene and dibenzanthracene are discussed in terms of the stable valency bond structures for the three compounds and a large measure of agreement is found to exist between the measured and calculated values.

THE CRYSTAL STRUCTURE OF CORONENE AND RELATED HYDROCARBONS.

PART I. INTRODUCTION

A. HISTORICAL.

The conception that a regular atomic structure might account for the external properties of crystals arose more than a century before the discovery of X-rays. Haüy, in his "Essai d'une théorie sur la structure des cristaux" (1784) explained the development of certain crystal faces as being due to the stacking together of small rhombs. This would appear to be the first tentative suggestion of the unit cell, or three dimensional unit of pattern. In the following century the mathematical side of the subject developed and between 1885 and 1894 reached near completion with the independent formulation of the 230 possible space groups by Federov, Schoenflies and Barlow. This subject is fully described in Hilton's "Mathematical Crystallography"(1).

The first diffraction experiment with X-rays was carried out in 1912 by Friedrich and Knipping(2) at Munich on a suggestion from von Laue that diffraction by a crystal would establish the wave nature of X-rays. Laue (3) postulated the mathematical relations which must hold for diffraction to take place but W. L. Bragg(4)(5) arrived at a simpler relation by considering that X-rays are reflected from crystal planes. The first structures to be completely analysed were those of potassium and sodium chlorides(6).

The intensity formulae for both the perfect and mosaic crystal were deduced in 1914 by Darwin(7,8) but were almost forgotten for years as this work was so far in advance of the early techniques.

Between 1918 and 1922 the results of space group theory were applied to X-ray analysis by Niggli(9) and Wyckoff(10).

The first emphasis of the early researches was in the field of inorganic chemistry where little was known of the structures. W. H. Bragg's development of the ionisation spectrometer(11) led first to the diamond structure(12) and almost immediately to the structures of many other compounds.

The use of Fourier analysis was suggested in 1915 by W. H. Bragg(13), but it was Compton(14) who showed how the coefficients of the Fourier series might be derived from the intensities of X-ray reflections. The first use of a double Fourier series in crystal analysis was by W. L. Bragg(15) on the structure of diopside in 1929.

In organic chemistry the problem was more difficult as the molecules are in general more complex and the difference in scattering power between atoms of carbon, nitrogen, and oxygen is small. The first Fourier analysis of a complex organic structure was carried out by Robertson(16) on anthracene.

B. THEORETICAL.

Diffraction by the Crystal Lattice. The characteristic of a true crystal is three dimensional periodicity, i.e. a unit of pattern is repeated throughout the crystal in three dimensions. When a beam of X-rays falls on the crystal certain diffracted beams occur in definite directions, due to reinforcement of the waves diffracted in these directions throughout the crystal pattern.

The problem was first considered by analogy with the diffraction of light by a line grating where several images are built up in different directions, corresponding to different orders of spectra. The crystal can be considered as a three dimensional grating diffracting the incident beam. The conditions for the formation of X-ray spectra were first formulated by Laue(3). If the incident beam makes an angle ψ_o with the grating, the spacing of which is a, and the diffracted beam makes an angle ψ with the grating, then the path difference is $a(\cos\psi - \cos\psi_o)$ (see Diag.1), or $a(\alpha - \alpha_o)$ where $\cos\psi = \alpha$, $\cos\psi_o = \alpha_o$ (Diagram 1).

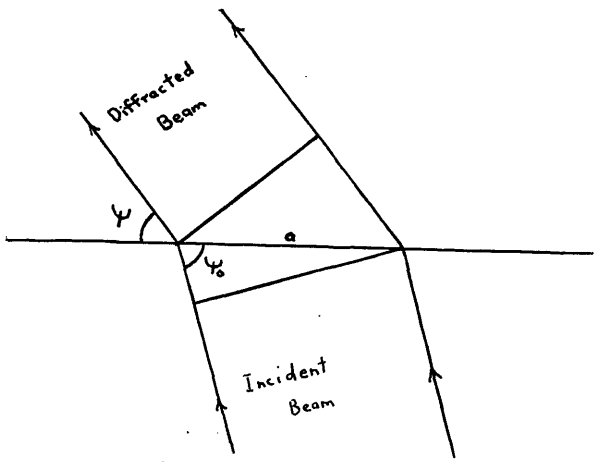

Diagram 1.

The condition that the waves should reinforce is that the path difference should be equal to an integral number of wave lengths, i.e. $a(\alpha - \alpha_o) = n\lambda$ ..... (i)

where λ is the wave length and n an integer. In the three dimensional case three such relations must hold, viz.,

$$a(\alpha - \alpha_o) = h\lambda \quad \text{..... (ii)}$$
$$b(\beta - \beta_o) = k\lambda \quad \text{..... (iii)}$$
$$c(\gamma - \gamma_o) = l\lambda \quad \text{..... (iv).}$$

The order of the spectrum is defined by the three integers (h, k, l).

It was realised by W. L. Bragg that the results of the above treatment are identical with those obtained by a much simpler idea, that the X-ray beam is reflected by successive planes of the crystal lattice. Diagram 2 illustrates the reflection of the incident beam from a series of crystallographic planes whose spacing is d.

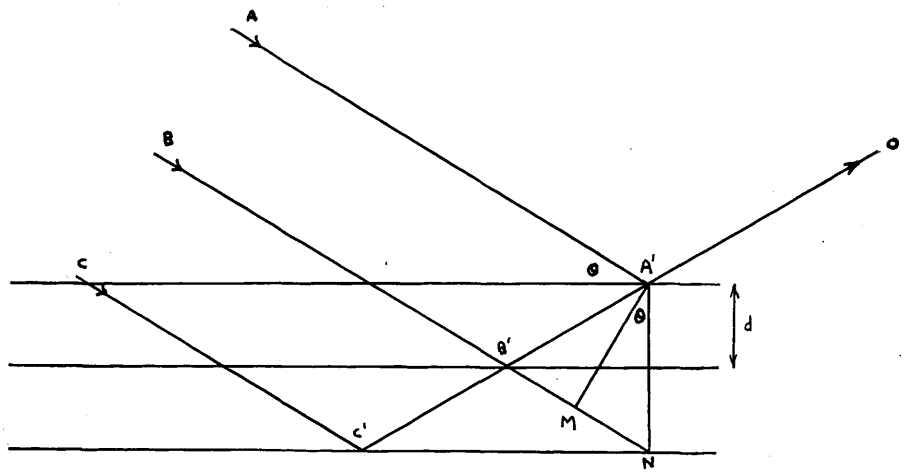

Diagram 2.

If the angle between the planes and the incident beam is θ then the path difference between reflections from successive planes is $B'A' - B'M = B'N - B'M = MN = 2d \sin\theta$. The Bragg Law is thus given by $n\lambda = 2d \sin\theta$ ..... (v).

If the radiation is monochromatic reflection will only occur at values of θ corresponding to integral values of n. This illustrates the essential difference of the three dimensional case from that of the line grating first considered, for in the line grating the successive orders of spectra were present simultaneously, whereas in the case of a crystal, reflection from a series of planes of given spacing will only occur when the crystal is turned into such a position that the Bragg Law is satisfied.

If, however, X-radiation consisting of mixed wave lengths is used, for any position of the crystal a certain series of planes will select the wave length appropriate to the angle of incidence, and reflection will occur. For a given wave length only a finite number of spectra can appear, as $2\sin\theta < 2$.

Determination of Axial Lengths.

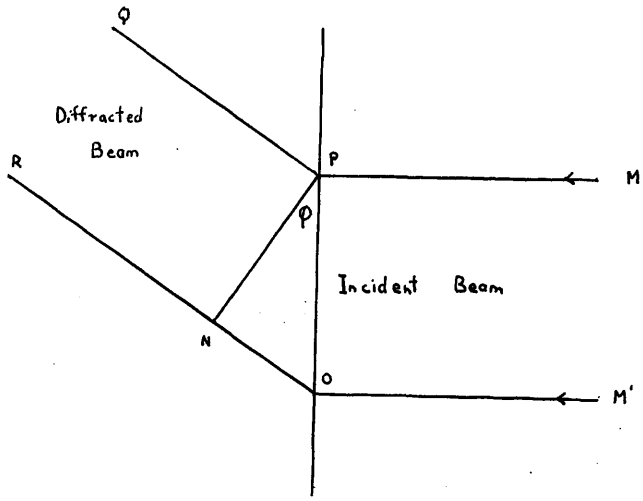

Diagram 3.

Let a crystal be rotated about a certain axis and let the incident beam be normal to that axis. If O and P (Diagram 3) are successive identical points along the axis of rotation then the direction of diffraction will depend on OP according to the relation

$$n\lambda = OP \sin\varphi \quad \ldots\ldots\ldots \quad (vi)$$

as can be seen from Diagram 3. φ is the complement of the angle between the diffracted beam and the axis of rotation. If OP represents the c axis of the crystal then all reflections for which l = a fixed value of n have directions such that they all make the same angle $(90^{\circ} - \varphi)$ with the axis of rotation. Hence all hk1 reflections will lie on a cone with its axis the rotation axis, and all hk2 reflections will lie on a concentric cone of smaller semi-vertical angle.

If a flat plate is used to record the reflections these families of cones intersect the plate in hyperbolas while if a cylindrical film is used, the axis of the cylinder coinciding with the axis of rotation, then the cones intersect the cylinder on circles, which become straight lines when the cylinder is opened out. These straight lines are the characteristic "layer lines" of rotation photographs. The distance between the lines can be measured and from the radius of the camera the angle φ calculated for each layer line. The periodicity along the rotation axis is given by $\frac{n\lambda}{\sin\varphi}$ where n is the order of the layer line above the equatorial and φ the corresponding diffraction angle. Hence periodicities can be obtained in three directions in the crystal and the dimensions of the unit cell found unambiguously.

Structure Amplitude. The structure amplitude is defined as the ratio of the amplitude of the wave scattered by the whole unit cell for a given plane to that which would be scattered by a single electron under the same conditions. The diffracted wave is made up of components from each atom in the cell, hence if we consider an atom of co-ordinates (x, y, z) then the difference in phase of a wave scattered by this atom, compared with an imaginary peak at the origin, will be $2\Pi\left(\frac{hx}{a} + \frac{ky}{b} + \frac{lz}{c}\right)$ ..... (vii)

where a, b and c are the axial lengths of the unit cell.

As the 'structure amplitude' includes both amplitude and phase it can be expressed most compactly by the use of complex numbers, viz.,

$$F(hkl) = \Sigma f e^{2\Pi i\left(\frac{hx}{a} + \frac{ky}{b} + \frac{lz}{c}\right)} \quad \text{.....} \quad \text{(viii)}$$

the summation being carried out over all atoms in the unit cell. f is the scattering efficiency of each atom for the particular plane considered and in order to give F(h kl) in absolute units, in accordance with the above definition, f must be on such a scale that its value when $\sin\theta = 0$ is equal to the total number of electrons in the unit cell. f falls away rapidly with increase of $\frac{\sin\theta}{\lambda}$ as the efficiency of scattering is reduced at large values of θ by phase differences between the component waves scattered by electrons in different parts of the atom.

The scattering of X-rays by an atom of an element depends on the atomic number and f may be calculated from the expression

$$f = \int_0^\infty U(r)\frac{\sin\varphi}{\varphi}dr \quad \text{.....} \quad \text{(ix)}$$

where $\varphi = \frac{4\Pi r \sin\theta}{\lambda}$ and $U(r)dr$ represents the probability of

finding an electron between the radii r and r + dr from the centre of the atom.

Equation (viii) involves sine terms as well as cosine terms but if the structure has a centre of symmetry then an atom in position (x, y, z) will have a related atom at $(\bar{x}, \bar{y}, \bar{z})$ and for each term in the summation $\sin 2\pi(\frac{hx}{a} + \frac{ky}{b} + \frac{lz}{c})$ there will be a corresponding term $\sin 2\pi(\frac{h\bar{x}}{a} + \frac{k\bar{y}}{b} + \frac{l\bar{z}}{c}) = -\sin 2\pi(\frac{hx}{a} + \frac{ky}{b} + \frac{lz}{c})$

Hence the sine terms cancel out and in this special case

$$F(hkl) = \Sigma f \cos 2\pi(\frac{hx}{a} + \frac{ky}{b} + \frac{lz}{c}) \ldots\ldots\ldots (x)$$

Equation (x) applies to structure factors in the two space groups described in Part II, both of which have centres of symmetry.

Space Group Theory. The theory of symmetry relations in a continuous three dimensional lattice was worked out before the discovery of X-rays made any practical application possible. If we consider the external symmetry of a perfect crystal it is found that there are 32 classes (different combinations of symmetry elements) distributed among the seven crystal systems. To extend the theory to a continued lattice two additional elements of symmetry are necessary, the glide plane and screw axis, both involving translations.

It was shown by Federov, Schoenflies and Barlow that the number of symmetry combinations in a space lattice is finite and that there are 230 such arrangements. Certain types of symmetry, such as 5 or 7 fold axes, can be shown to be impossible in a continued network while any possible combination of symmetry elements in a different

form from any of the 230 space groups can be converted into one of them by a change of the crystallographic axes.

As stated above certain symmetry elements involve translations and this fact is used in space group determination by X-rays. Consider a face centred lattice where the equivalent points are given by the co-ordinates $000; 0\frac{b}{2}\frac{c}{2}; \frac{a}{2}0\frac{c}{2};$ and $\frac{a}{2}\frac{b}{2}0$. This arrangement includes a centre of symmetry therefore the expression for the structure factor contains only cosines. Hence

$$F(hkl) = 4f\left[\cos 0 + \cos 2\pi\left(\frac{k}{2} + \frac{l}{2}\right) + \cos 2\pi\left(\frac{h}{2} + \frac{l}{2}\right) + \cos 2\pi\left(\frac{h}{2} + \frac{k}{2}\right)\right]$$

$$= 4f \cos\pi(h + k + 1) \cos\tfrac{1}{2}\pi(k + l) \cos\tfrac{1}{2}\pi(h + l) \cos\tfrac{1}{2}\pi(h + k) \ldots\ldots\ldots \quad \text{(xi)}$$

From (xi) it can be seen that if $h + k$, $k + l$ or $h + l$ are odd the expression for the structure factor vanishes, i.e. reflections can only occur for which $h + k$, $k + l$, $h + l$ are all even. Spectra such as (140) or (230) cannot appear and are designated "missing spectra".

Centred lattices give rise to the most general extinctions involving all (hkl). Glide planes cause a more limited class of missing spectra, only one zone e.g. (h0l) or (0kl) being affected while with screw axes a still smaller class of reflections such as (0k0) are involved.

This is readily understood on analysing an axial glide plane into its two components, a reflection in the plane and a translation parallel to the plane. In normal projections on to the plane itself the half axial translation has its true value while the

reflection cannot be distinguished. In any other projection however the translation component is foreshortened and the reflection becomes noticeable, so that systematic extinctions do not occur. In an n fold screw axis parallel to b there are in the related units y co-ordinates of equal magnitude but opposite sign with respect to the 0n0 planes, hence the only systematic extinctions are in the 0k0 series where only reflections where k is divisible by n occur.

Space group theory has been developed in a form suitable for use in conjunction with X-ray analysis and in the International Tables(17) the 230 space groups are listed and correlated with the missing spectra which they produce. The determination of the space group has thus become almost a matter of routine. Crystal axes are assigned unambiguously by means of rotation photographs. The reflections are then indexed on the basis of these axial lengths and from the systematic extinctions the space group can either be definitely assigned or reduced to one of a few possibilities.

Certain space groups cannot be established conclusively by X-ray methods alone. By Friedel's Law the diffraction effects of X-rays add on a centre of symmetry where this may not occur in the crystal, hence except in a specialised case such as the space group $P2_1/a$, where the combination of symmetry elements is such that they must include a centre of symmetry, pyro- or piezo-electric measurements must be carried out before assigning the higher symmetry to a structure. If such experiments are inconclusive the space group of lower symmetry must be assumed.

Further, only symmetry elements producing translations can cause missing spectra, hence the space groups P2/a and Pa are indistinguishable by X-ray methods alone, as no information about the presence of a two-fold rotation axis can be obtained. General extinctions due to centred lattices imply extinctions in specialised classes, e.g. I222 cannot be distinguished from $I2_12_12_1$; as the characteristic screw axis extinctions of 0k0 with k odd occur in any case because of the extinction of (hkl) with h + k + l odd.

In equation (viii) F(hkl) is obtained by summing over every atom in the unit cell. In a given space group, however, there are usually a number of "equivalent points" and if an atom occurs at one it is automatically reproduced at the others by the symmetry operations of the space group. Hence it is customary to sum the structure factor over the crystallographically independent atoms alone, but this usually necessitates a change in the trignometrical form of the structure factor.

For example, in the space group $P2_1/a$ in which coronene and pyrene (described in Part II) crystallise, there are four such equivalent points:

$$x,y,z;\ \bar{x},\bar{y},\bar{z};\ \tfrac{1}{2}+x,\ \tfrac{1}{2}-y,\ z;\ \tfrac{1}{2}-x,\ \tfrac{1}{2}+y,\ \bar{z}.$$

Each pair are related by a centre of symmetry, hence no sine terms are necessary.

$$F(hkl) = \Sigma\ 2\left[\cos 2\pi\left(\frac{hx}{a} + \frac{ky}{b} + \frac{lz}{c}\right) + \cos 2\pi\left(\frac{hx}{a} - \frac{ky}{b} + \frac{lz}{c} + \frac{h+k}{2}\right)\right]$$

$$= \Sigma\ 4\left[\cos 2\pi\left(\frac{hx}{a} + \frac{lz}{c} + \frac{h+k}{4}\right) \cos 2\pi\left(\frac{ky}{b} - \frac{h+k}{4}\right)\right] \quad \text{(xii)}$$

If k = 0

$$F(h0l) = \Sigma\ 4\ \cos 2\pi\left(\frac{hx}{a} + \frac{lz}{c} + \frac{h}{4}\right) \cos 2\pi\frac{h}{4}$$

$$= 4\Sigma \cos 2\pi\left(\frac{hx}{a} + \frac{lz}{c}\right) \quad \text{(xiii)}$$

If h = 0

$$F(0kl) = \Sigma\ 4\left[\cos 2\pi\left(\frac{lz}{c} + \frac{k}{4}\right) \cos 2\pi\left(\frac{ky}{b} - \frac{k}{4}\right)\right]$$

$$= \Sigma\ 2\left[\cos 2\pi\left(\frac{lz}{c} + \frac{ky}{b}\right) + \cos 2\pi\left(\frac{lz}{c} - \frac{ky}{b} + \frac{k}{2}\right)\right]$$

If k is even

$$F(0kl) = \Sigma\ 2\left[\cos 2\pi\left(\frac{lz}{c} + \frac{ky}{b}\right) + \cos 2\pi\left(\frac{lz}{c} - \frac{ky}{b}\right)\right]$$

$$= 4\Sigma \cos 2\pi\frac{lz}{c} \cos 2\pi\frac{ky}{b} \quad \text{(xiv)}$$

If k is odd

$$F(0kl) = 2\Sigma\left[\cos 2\pi\left(\frac{lz}{c} + \frac{ky}{b}\right) - \cos 2\pi\left(\frac{lz}{c} - \frac{ky}{b}\right)\right]$$

$$= -4\Sigma \sin 2\pi\frac{lz}{c} \sin 2\pi\frac{ky}{b} \quad \text{(xv)}$$

If l = 0

$$F(hk0) = 4\Sigma\left[\cos 2\pi\left(\frac{hx}{a} + \frac{h+k}{4}\right) \cos 2\pi\left(\frac{ky}{b} - \frac{h+k}{4}\right)\right]$$

If h+k even $F(hk0) = 4\Sigma \cos 2\pi\frac{hx}{a} \cos 2\pi\frac{ky}{b}$ ..... (xvi)

If h+k odd $F(hk0) = -4\Sigma \sin 2\pi\frac{hx}{a} \sin 2\pi\frac{ky}{b}$ ..... (xvii)

Intensity of the X-ray reflection.

The calculation of the structure amplitude from a knowledge of atomic co-ordinates is given above (viii) but in practice it is the intensity of the diffracted beam which is observed and this

must be related to the structure amplitude. From the classical theory of electromagnetic waves the amplitude of the wave scattered at a distance r from the source by a free electron is $\frac{A}{r}\frac{e^2}{mc^2}$ .. (xviii) where A is the amplitude of the wave which sets the electron vibrating, c the velocity of light, e the electronic charge and m the mass of the electron. In (xviii) the electric vector is assumed to be normal to the plane containing the incident and diffracted rays but if it lies in this plane the amplitude becomes $\frac{A}{r}\frac{e^2}{mc^2}\cos 2\theta$ ..... (xix) where 2θ is the angle between the incident and diffracted beams. A wave-mechanical treatment leads to very similar results, hence the classical expression can be retained.

Now the diffracted beam does not flash out instantaneously for each plane but is produced on rotation through a small angle depending on the perfection of the crystal specimen. An absolute measurement of the energy of the diffracted beam is given by $\frac{E\omega}{I_o}$ ..... (xx) where E is the energy measured during an angular rotation ω and I_o is the energy of the incident beam. Expressions (xix) and (xx) can be combined to give an absolute measurement of the structure amplitude from the equation

$$\frac{E\omega}{I_o} = \left[N \frac{e^2}{mc^2} F(hkl)\right]^2 \lambda^3 \frac{1 + \cos^2 2\theta}{2 \sin 2\theta} \delta v \ldots\ldots\ldots \text{(xxi)}$$

if the crystal has a very small volume δv of negligible absorption and N is the number of unit cells per unit volume of the crystal. $\frac{1}{2}(1 + \cos^2 2\theta)$ is a factor to correct for the normal unpolarised state of the radiation.

Equation (xxi) gives the intensity-structure amplitude relation

as applied to most crystals which are of the mosaic type, i.e. they consist of small blocks not exactly parallel. Certain crystals, however, such as diamond, are of the "perfect" type and equation (xxii) must be used.

$$\frac{E\omega}{I_o} = \frac{8}{3\Pi} N \frac{e^2}{mc^2} F(hkl) \lambda^2 \frac{1 + |\cos 2\theta|}{2\sin 2\theta} \quad \ldots\ldots\ldots\ldots\ldots \text{(xxii)}$$

F(hkl) enters equation (xxi) as the square while in the perfect crystal the intensity is directly proportional to the structure emplitude.

When relative intensity measurements alone are required the expressions become much simpler, i.e. $\frac{F_1}{F_2} = \sqrt{\left\{ \frac{I_1 P_2 \sin 2\theta_1}{I_2 P_1 \sin 2\theta_2} \right\}}$ ..... (xxiii) where I_1, I_2 are two observed intensities under the same conditions, F_1, F_2 are the required relative structure factors and P_1, P_2 are the corresponding polarisation factors. If the absorption of the beam by the crystal is appreciable the observed intensities are multiplied by $e^{+\mu t}$ where t is the length of the mean path of the crystal and μ is the absorption coefficient of the substance for the wave length employed.

When a crystal approximates to the mosaic type but the substituent blocks are rather large for equation (xxi) to be accurate there is a falling off of intensities of strong reflections. This effect is known as "primary extinction" and may be reduced by quenching in liquid air or by some other method which reduces the perfection of the specimen. "Secondary extinction" is an artificial increase of the absorption coefficient for very strong reflections due to the diffracted beam being reflected back by the upper layer of the crystal.

Intensity measurements may be put on an absolute scale from first

principles by using equation (xxi) or, more commonly, by comparison with a standard crystal which has previously been directly calibrated.

Fourier Analysis.

A periodic function of a variable x which repeats its value when x is increased by a quantity a can be expressed by a sum of cosine terms e.g.

$$F(x) = F_o + F_1 \cos\left(2\pi\frac{x}{a} + \alpha_1\right) + F_2 \cos\left(2\pi\frac{2x}{a} + \alpha_2\right) + \ldots$$
$$= \sum_{o}^{\infty} F_n \cos\left(2\pi\frac{hx}{a} + \alpha_n\right) \quad \ldots\ldots\ldots\ldots\ldots\ldots \quad (xxiv)$$

In a crystal it is the electrons which scatter X-rays and as the same electron distribution is repeated throughout the crystal at intervals corresponding to the dimensions of the unit cell the electron density at a point (x,y,z) can be represented by a triple Fourier series

$$\rho(xyz) = \sum_{-\infty}^{\infty}\sum_{-\infty}^{\infty}\sum_{-\infty}^{\infty} F(hkl) \cos\left(2\pi\frac{hx}{a} + 2\pi\frac{ky}{b} + 2\pi\frac{lz}{c} + \alpha hkl\right) \ldots \quad (xxv)$$

This can be expressed more symmetrically as

$$\rho(xyz) = \sum_{-\infty}^{\infty}\sum_{-\infty}^{\infty}\sum_{-\infty}^{\infty} F^1(hkl) e^{2\pi i\left(\frac{hx}{a} + \frac{ky}{b} + \frac{lz}{c}\right)} \ldots\ldots\ldots\ldots \quad (xxvi)$$

where $F^1(hkl)$ is a complex quantity and $F^1(hkl)$ and $F^1(\bar{h}\bar{k}\bar{l})$ are conjugate i.e. $|F^1(hkl)| = |F^1(\bar{h}\bar{k}\bar{l})|$ but the phases are opposite.

Now the expression for the structure amplitude (viii) was derived from a consideration of scattering matter concentrated at discrete points in the structure, but in order to describe the electron density as a continuous function we must integrate this expression instead of summing it.

Thus
$$F(h^1k^1l^1) = \int_{-\frac{a}{2}}^{\frac{a}{2}}\int_{-\frac{b}{2}}^{\frac{b}{2}}\int_{-\frac{c}{2}}^{\frac{c}{2}} \rho(xyz) e^{2\pi i\left(\frac{h^1x}{a} + \frac{k^1y}{b} + \frac{l^1z}{c}\right)} \times \frac{V dx\, dy\, dz}{abc} \quad (xxvii)$$

where a, b and c are the crystallographic axes.

Substituting (xxvi) for $\rho(xyz)$

$$F(h^1k^1l^1) = \int_{-\frac{a}{2}}^{\frac{a}{2}}\int_{-\frac{b}{2}}^{\frac{b}{2}}\int_{-\frac{c}{2}}^{\frac{c}{2}} \sum_{-\infty}^{\infty}\sum_{-\infty}^{\infty}\sum_{-\infty}^{\infty} F^1(hkl)e^{2\pi i(\frac{hx}{a}+\frac{ky}{b}+\frac{lz}{c})} e^{2\pi i(\frac{h^1x}{a}+\frac{k^1y}{b}+\frac{l^1z}{c})} \times \frac{V dx\, dy\, dz}{abc} \quad \ldots\ldots\ldots \text{(xxviii)}$$

$$= V.F^1(\bar{h}^1, \bar{k}^1, \bar{l}^1) \quad \ldots\ldots\ldots\ldots\ldots\ldots\ldots \text{(xxix)}$$

since every term is zero except that for which

$$h = -h^1, \quad k = -k^1, \quad l = -l^1.$$

Hence $F(hkl)$ and $F(\bar{h}\bar{k}\bar{l})$ are also conjugate except where a wave length near an atomic absorption edge is used and Friedel's Law breaks down.

From (xxvi) and (xxix)

$$\rho(xyz) = \frac{1}{V}\sum_{-\infty}^{\infty}\sum_{-\infty}^{\infty}\sum_{-\infty}^{\infty} F(hkl)e^{-2\pi i(\frac{hx}{a}+\frac{ky}{b}+\frac{lz}{c})} \quad \ldots\ldots \text{(xxx)}$$

All quantities on the right hand side of (xxx) are known with the exception of the phase constants of $F(hkl)$. In certain special cases the phase constants can be determined (e.g. platinum phthalocyanine.[18]) but in the general case this information is necessarily lost in making the experiment. Before calculating the Fourier series, therefore, trial analysis is necessary. This process consists of setting up a reasonable model of the structure, using physical or chemical evidence, which will explain certain outstanding features in the observed intensities of X-ray reflections. Examples are given in detail in Part II under the three compounds analysed.

When the structure is established sufficiently well for most of the phase constants to be known, refinement of the atomic parameters can proceed automatically by Fourier analysis. A limited number of terms can be included in the first series and from the resulting atomic positions the phase constants of weaker reflections, which had

previously been doubtful, can be fixed and the terms added in in a new Fourier summation. The method is thus one of successive approximation, but it should be noted that even where all the observed reflections are included the series is still incomplete as it should be summed to infinity. This incompleteness has the effect of adding false detail to the contour maps and its effect on atomic positions is discussed in Part III.

In practice the evaluation of the triple series (xxx) involves a tremendous amount of labour but this can be reduced by evaluating instead the projection of the electron density on a crystallographic plane.

$$\rho(x\ z) = \frac{1}{B}\sum_{-\infty}^{\infty}\sum_{-\infty}^{\infty} F(h0l)\cos 2\pi\left(\frac{hx}{a} + \frac{lx}{c}\right) \quad \ldots\ldots\ldots \quad (xxxi)$$

$\rho(x\ z)$ is the electron density at the point $(x\ z)$ on the ac plane (010) and B is the area of projection. Two such projections along different axes can theoretically give all atomic co-ordinates, although in some cases projections may be obscured by overlapping of atoms.

One question remains, however, that of whether a structure giving satisfactory agreement between the observed and calculated values of the structure factor is a unique solution of the problem. Patterson(19) has examined the one dimensional case and has found that different periodic distributions along a line can have the same vector distances and would therefore give rise to the same X-ray intensities. This question has been reviewed by Robertson(20) and it is pointed out that if such ambiguities arose with regard to complicated structures, all except the true structure would probably

be ridiculous in terms of chemistry. At the same time, before a structure is accepted as correct, all lines of physical evidence (magnetic susceptibilities, refractive indices etc.) should combine to support that structure deduced from the X-ray data.

Experimental Methods.

The Laue photograph makes use of a stationary crystal and 'white' X-radiation, containing a continuous range of wave lengths. While the method gives useful information about crystal symmetry, its main disadvantage in detailed structural work is that in general the proportions of different wave lengths in the incident beam are not accurately known and correlation of intensities is a difficult matter.

The ionisation spectrometer gives very accurate intensity measurements. Here a homogeneous X-ray beam is reflected from a crystal face and the reflected beam thrown into a chamber containing a gas such as methyl bromide. The ionisation of the gas is measured by means of an electrometer and by making the ionisation chamber rotate in synchronisation with the crystal an integrated value of the intensity can be obtained. Large crystals with well developed faces are required and the individual measurement of reflections is laborious. The ionisation spectrometer is therefore little used now except for making absolute measurements.

Any photographic method of recording X-ray reflections is preferable to the ionisation spectrometer because of the large amount of information contained in one film. Some variation of the rotation method of Schiebold and Polanyi(21) is generally used. In its straightforward application this technique leads to

ambiguities in indexing reflections as for a given reflection all that is known is one index (h, k or l) and the value of 2 sinθ. Several planes in a zone may have approximately the same 2 sinθ value, hence two important modifications of the rotation method have developed in order to overcome this difficulty.

If, instead of having a continuous rotation, the crystal oscillates over a range of a few degrees then only a limited number of reflections can occur and the possibility of wrong indexing is greatly diminished. The problem, however, is still equivalent to solving one equation containing two variables by the use of certain inequality relations.

The most important development of all is that due to Weissenberg (22). All layer lines in a rotation photograph except one are screened off and this one is examined in detail by having the camera move in a direction perpendicular to the crystal rotation axis in synchronisation with the rotation. The layer line is thus spread out over the whole film and the relative angles between different reflections measured directly. Hence the reflections can be indexed automatically and unequivocally. A further advantage of moving film photography is that all scattered radiation comes through a narrow slit between two screens and the background, which limits the accuracy with which intensity measurements can be made, is spread out over the whole film and is thus much less than in the corresponding simple rotation photograph. Detailed methods of indexing X-ray photographs are very fully described in Buerger's "X-Ray Crystallography"(23)

C. PREVIOUS WORK ON THE STRUCTURES OF POLYCYCLIC AROMATIC HYDROCARBONS.

The structure of condensed ring aromatic hydrocarbons has attracted attention since the early days of X-ray crystallography, the earliest investigation of naphthalene ($C_{10}H_8$) and anthracene ($C_{14}H_{10}$) being by W. H. Bragg in 1921(24). The latest theories of organic chemistry suggested a regular, co-planar structure for the benzene ring and it was of great importance to establish this by the direct methods of X-ray analysis and also to ascertain whether any distortions occurred in compounds formed by condensation of two or more aromatic rings.

The expected regular structure for benzene was confirmed in 1931(25) and the carbon-carbon bond distances given as 1.39 ± 0.01A. The first detailed measurements of bond distances in condensed ring aromatic hydrocarbons were made by Robertson(16, 26) on naphthalene(I) and anthracene(II). Two dimensional Fourier series methods were used to their fullest extent, projections of all the principal zones being made.

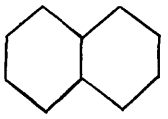

I

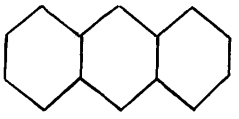

II

The aromatic rings were found to be regular, planar hexagons with mean radius 1.41A in both cases, within the limits of experimental error. In naphthalene it was noted, however, that the central bond distance was about 0.03A longer than the average, but this variation was not considered to be definitely established as errors of about the same magnitude could arise from incompleteness of the Fourier series. More important, much detailed information was lost because

of the unfavourable orientation of the molecules in the crystal which led to overlapping and distortion of certain atoms.

The structure of chrysene ($C_{18}H_{12}$-III) was investigated by Iball(27) and the best average radius of the hexagons found to be 1.41A. Here again lack of resolution in the projections limited the accuracy of the work, and any irregularities lay within the limits of experimental error.

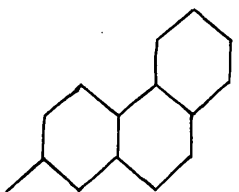

III

On the theoretical side the conception of single bond-double bond resonance had arisen and the experimental data confirmed the idea that carbon-carbon bond lengths might lie between the single bond value of 1.54A(12) and the double bond distance of 1.33A(28). In benzene resonance between the two Kekulé structures (IV,V) would give each bond 50% double bond character. Graphite(29) has a structure consisting of indefinitely extended layers of condensed benzene rings, and each bond could be represented as having 1/3 double bond character corresponding to the experimental value of 1.42A.

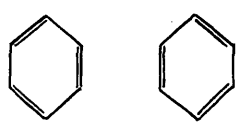

IV V

Pauling and Brockway(30) constructed an empirical curve of double bond character against bond distance using the above data and calculated the bond lengths in naphthalene from the three stable valence bond structures (VI, VII, VIII).

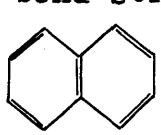

VI

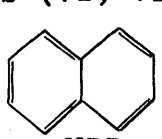

VII

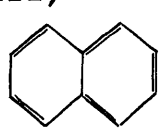

VIII

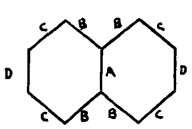

IX

On this basis all bonds would be equal to 1.42A except the C bonds(IX) which were calculated as being shorter. Pauling(31) has

quoted chemical evidence which indicates that these bonds do, in fact, behave more like double bonds than do the D bonds.

This treatment of the problem was criticised by Penney(32) as being too empirical and neglecting the excited structures which must also make some contribution. Penney gave a rigorous quantum-mechanical treatment of naphthalene and predicted values of 1.42A for the A bonds, 1.40 for B, 1.38 for C and 1.40 for D with a mean value of 1.40A. It will be seen that Penney's longest bond distance is for the central bond which Robertson suggested might be rather longer than the others.

These variations in carbon-carbon bond distances over a range of 0.04A cannot be conclusively established for individual bonds by two-dimensional Fourier methods in any but the most favourable cases, and even here the maximum experimental errors might cover such variations.

The present work was undertaken principally in order to measure accurately such deviations in carbon-carbon bond distances and where distortions could not be definitely established for the reasons given above to refine the structure as far as possible by two dimensional Fourier methods as a necessary preliminary stage to possible three dimensional work which might give the required information.

PART II. THE CRYSTAL STRUCTURES OF CORONENE, PYRENE AND THE ORTHORHOMBIC MODIFICATION OF 1.2:5.6 DIBENZANTHRACENE.

A. INTRODUCTION.

Coronene ($C_{24}H_{12}$-X) is the simplest condensed-ring aromatic hydrocarbon in which a central benzene nucleus is completely surrounded by benzene rings. The extremely high symmetry of the molecule, combined with a favourable crystallographic orientation, make this compound very suitable for accurate experimental determination of the molecular dimensions, while at the same time a rigorous quantum-mechanical treatment of the problem can be made. Preliminary details of such a treatment by the molecular orbital method have recently been given by Coulson(33).

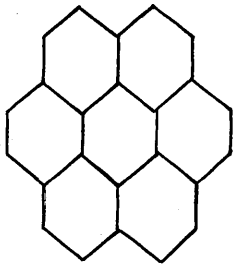

X

The molecule of pyrene ($C_{16}H_{10}$- XI) is simpler than that of coronene but the arrangement of the molecules in the crystal is more complex. Preliminary work has been done on this compound by Dhar and Guha(34) and their work leads to a determination of the cell constants and space group, but not to the detailed structure of the crystal.

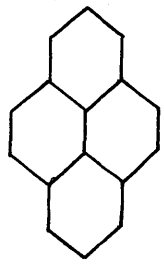

XI

Optical and goniometric crystal data are given by Groth(35). The structure of 1.2:5.6 dibenzanthracene($C_{22}H_{14}$ - XII) is of particular interest because of the carcinogenic properties of the compound. Two distinct crystalline modifications exist, one monoclinic and the other orthorhombic. The second was first described by Krishnan and Banerjee(36) and it is this form which has been included in the present investigation. Iball(37) has measured the cell dimensions and established the space group of the crystal and Krishnan and Banerjee(38) suggest an approximate orientation of the molecules based on measurements of magnetic susceptibility, but atomic positions have not been suggested by these authors.

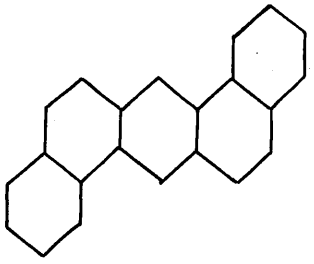

XII

Absolute intensity measurements of the main zones of pyrene and dibenzanthracene were made by Prof. J.M. Robertson and it is almost entirely on the basis of these measurements that the two structures were worked out (see Experimental Section).

Facing p. 25.

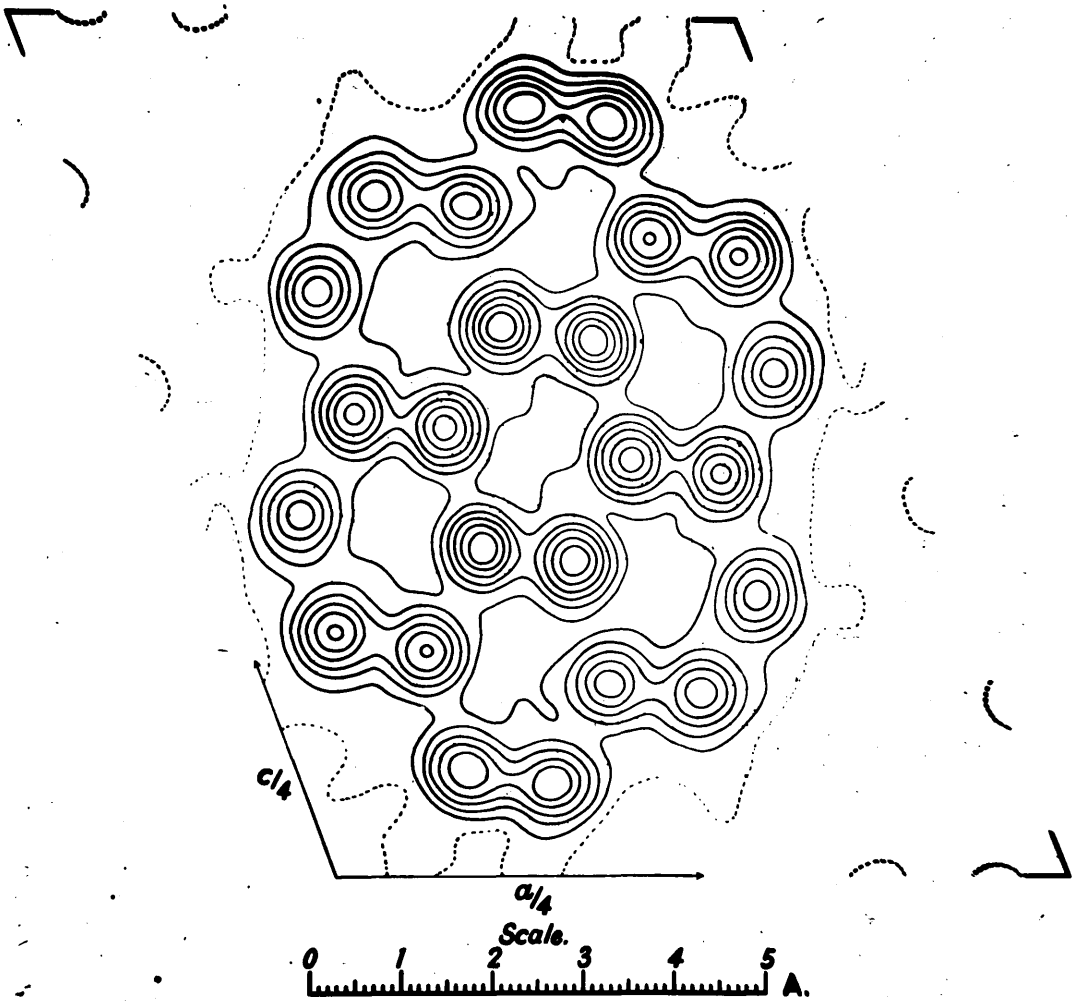

Fig. 1a.

Fig. 1.

Projection of the coronene structure on the ac plane. The successive contour lines represent intervals of one electron per A^2., the one electron line being dotted.

B. RESULTS OBTAINED FROM X-RAY ANALYSIS OF THE ABOVE COMPOUNDS.

(1) Coronene, $C_{24}H_{12}$.

Crystal Data: M, 300.3; m.p. 434-436°; d, calc. 1.381, found 1.377; monoclinic prismatic, a = 16.10 ±0.05, b = 4.695 ±0.005, c = 10.15 ±0.05 A., β = 110.8° ±0.2°. Absent spectra, (h0l) when h is odd; (0k0) when k is odd. Space group, $C_{2h}^5(P2_1/a)$. Two molecules per unit cell. Molecular symmetry, centre. Volume of the unit cell, 717.1 $A.^3$. Absorption coefficient for X-rays, λ = 1.54, μ = 7.30 per cm. Total number of electrons per unit cell = F(000) = 312. The crystals are long and needle shaped, elongated in the direction of the b-axis. Normally the crystals are very thin, and have only the (001) face well developed, but the best specimens obtained showed the (100), (101) and $(20\bar{1})$ faces in addition.

Crystal Structure.

The structure was first found approximately by trial methods and then refined by two successive Fourier syntheses of the (h0l) zone which gave clear resolution of all the atoms in the molecule. The contour map calculated from the final Fourier is shown in Fig. 1. As described in the Experimental Section the complete orientation of the molecule can be calculated from this map on the assumptions that the central ring is regular, the molecule is flat and the molecular axes L and M (Fig. 1b) are at right angles. The orientation of the molecule in the crystal is given in Table I where X_L, ψ_L, ω_L; X_M, ψ_M, ω_M; and X_N, ψ_N, ω_N, are the angles which the molecular axes L and M (Fig. 1b) and N their perpendicular make with the crystallographic axes a and b and c' the perpendicular to a and b.

Facing p. 26.

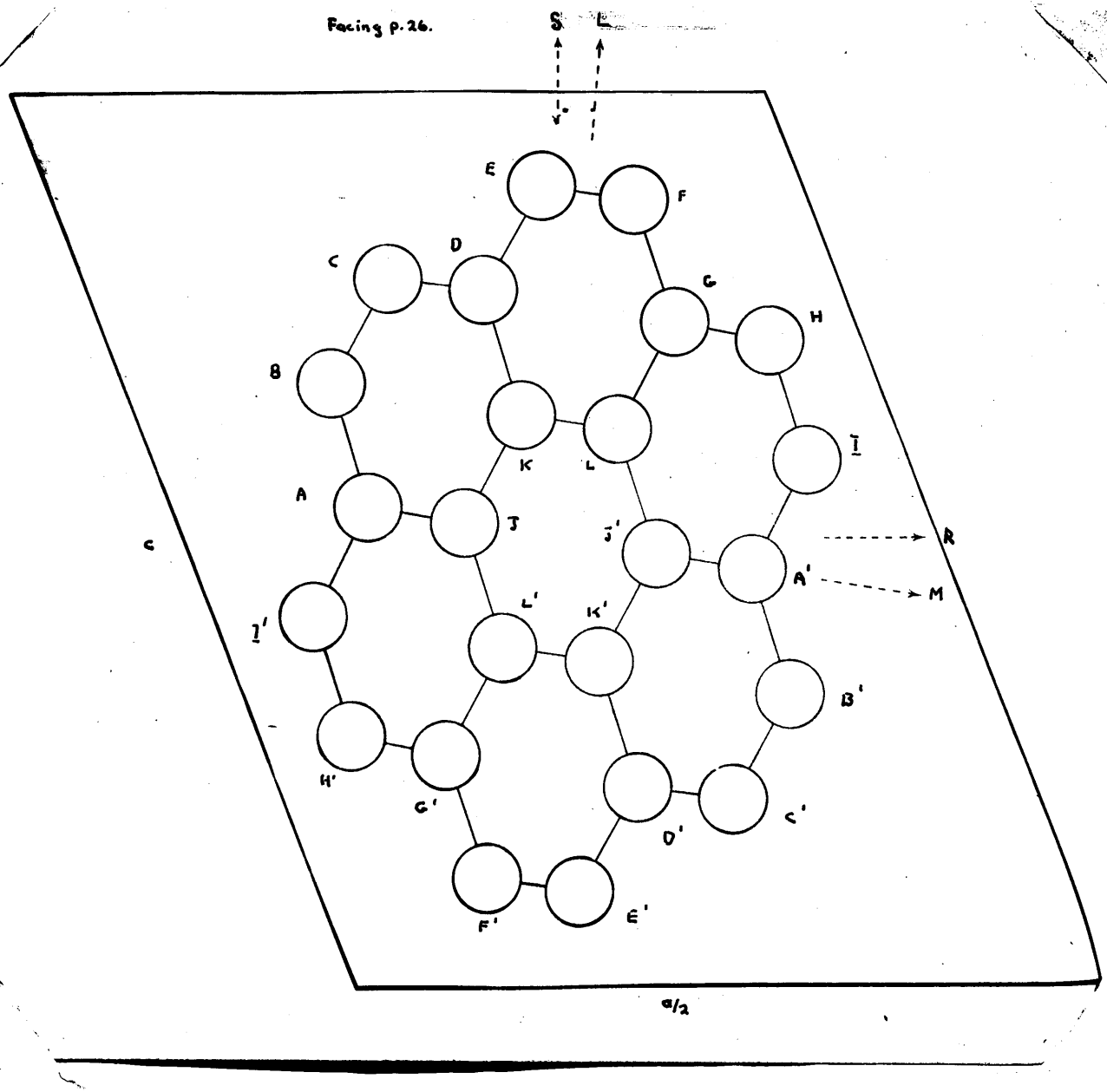

TABLE I.

Orientation of the molecule in the crystal.

$\chi_L = 84.8^\circ$	$\cos\chi_L = 0.0912$
$\psi_L = 85.6^\circ$	$\cos\psi_L = 0.0765$
$\omega_L = 6.9^\circ$	$\cos\omega_L = 0.9928$
$X_M = 44.2^\circ$	$\cos X_M = 0.7174$
$\psi_M = 46.7^\circ$	$\cos\psi_M = 0.6865$
$\omega_M = 96.8^\circ$	$\cos\omega_M = -0.1188$
$X_N = 133.7^\circ$	$\cos X_N = -0.6905$
$\psi_N = 43.7^\circ$	$\cos\psi_N = 0.7233$
$\omega_N = 89.6^\circ$	$\cos\omega_N = 0.0078$

The angle between the plane of the molecule and the (010) plane expressed by ψ_N is 43.7°, very close to the value of 44.2° found by Robertson in the structure of phthalocyanine(39). The perpendicular distance between molecular planes is 3.40Å. almost identical with the interplanar distance in graphite(29).

Fig. 2 shows a group of six coronene molecules in the b axis projection. The interlocking of atoms in the translation along a probably accounts for the poor development of the (100) plane in most crystals. The two molecules accommodated in one complete translation along the a-axis are identical in this projection, but the tilts of neighbouring molecules to the projection plane are in opposite directions and each alternate molecule is translated $\frac{b}{2}$ above the plane of the others. In Fig. 1, R represents the line of maximum inclination of the molecular plane to the projection plane, and the molecular axis S lies in the projection plane (010).

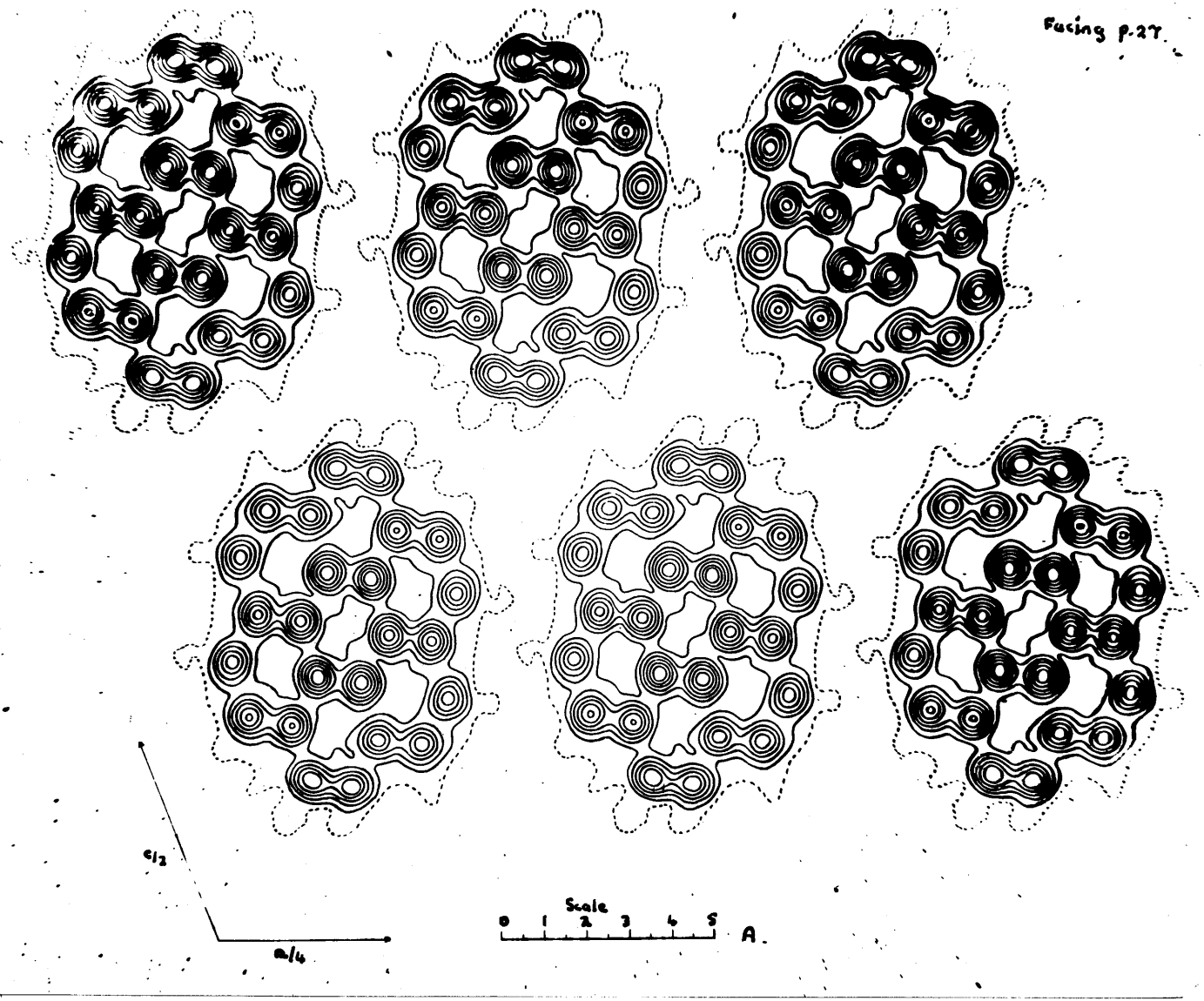

Fig. 2. A group of six coronene molecules in the b axis projection.

R is almost parallel to a hence when the structure is viewed along the c' axis an end view of the molecules is obtained as shown roughly in Fig. 3.

Co-ordinates and Dimensions.

A study of the contour map in Fig. 1 shows that the molecule approximates to a higher symmetry than that required by the centre of inversion, and by averaging certain bond distances into groups as described in Section C the most probable atomic positions have been assigned. These co-ordinates are collected in Table II under (a). The independent estimates for the x and z co-ordinates, measured directly from the projection map, are collected under (b). Only half the atoms in the molecule, those in the asymmetric unit, are listed. The other atoms in the unit cell may be derived from these by the operations:

$$(x, y, z),\ (-x, -y, -z),\ \left(x + \frac{a}{2}, -y + \frac{b}{2}, z\right),\ \left(-x + \frac{a}{2}, y + \frac{b}{2}, -z\right)$$

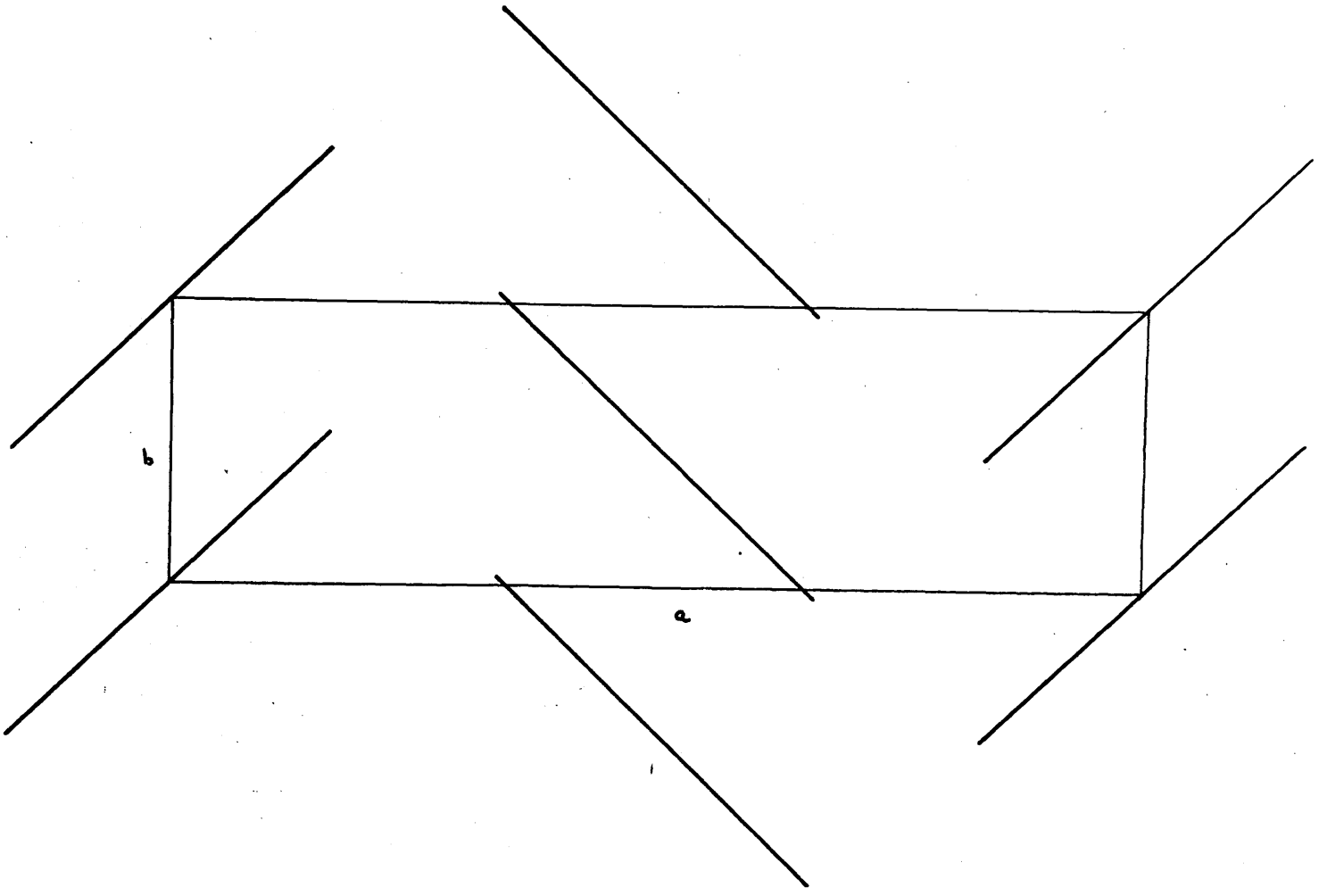

Fig. 3. End view of coronene molecules.

TABLE II. Co-ordinates. Centre of symmetry as origin.

Atom (cf. Fig.1)	x, A. (a)	x, A. (b)	$\frac{2\pi x}{a}$ (a)	y, A. (a)	$\frac{2\pi y}{b}$ (a)	z, A. (a)	z, A. (b)	$\frac{2\pi z}{c}$ (a)
A	-1.922	-1.922	-43.0°	-1.967	-150.8°	0.364	0.352	12.9°
B	-1.800	-1.804	-40.3	-2.337	-179.3	1.770	1.794	62.4
C	-0.768	-0.752	-17.2	-1.769	-135.6	2.956	2.960	104.8
D	0.198	0.198	4.4	-0.794	-60.9	2.806	2.818	99.7
E	1.258	1.256	28.2	-0.194	-14.9	4.000	3.996	141.9
F	2.188	2.190	49.0	0.758	58.1	3.826	3.824	135.7
G	2.118	2.118	47.4	1.172	89.9	2.448	2.448	86.8
H	3.054	3.046	68.3	2.141	164.2	2.232	2.220	79.2
I	2.958	2.954	65.9	2.527	193.7	0.870	0.858	30.9
J	-0.962	-0.962	-21.5	-0.983	-75.4	0.182	0.184	6.5
K	0.098	0.084	2.2	-0.397	-30.4	1.402	1.402	49.9
L	1.060	1.062	23.7	0.587	44.9	1.224	1.226	43.4

From the co-ordinates in Table II and the molecular orientation given in Table I the molecular co-ordinates of the atoms can be calculated in terms of the axes L, M and N and are listed in Table III.

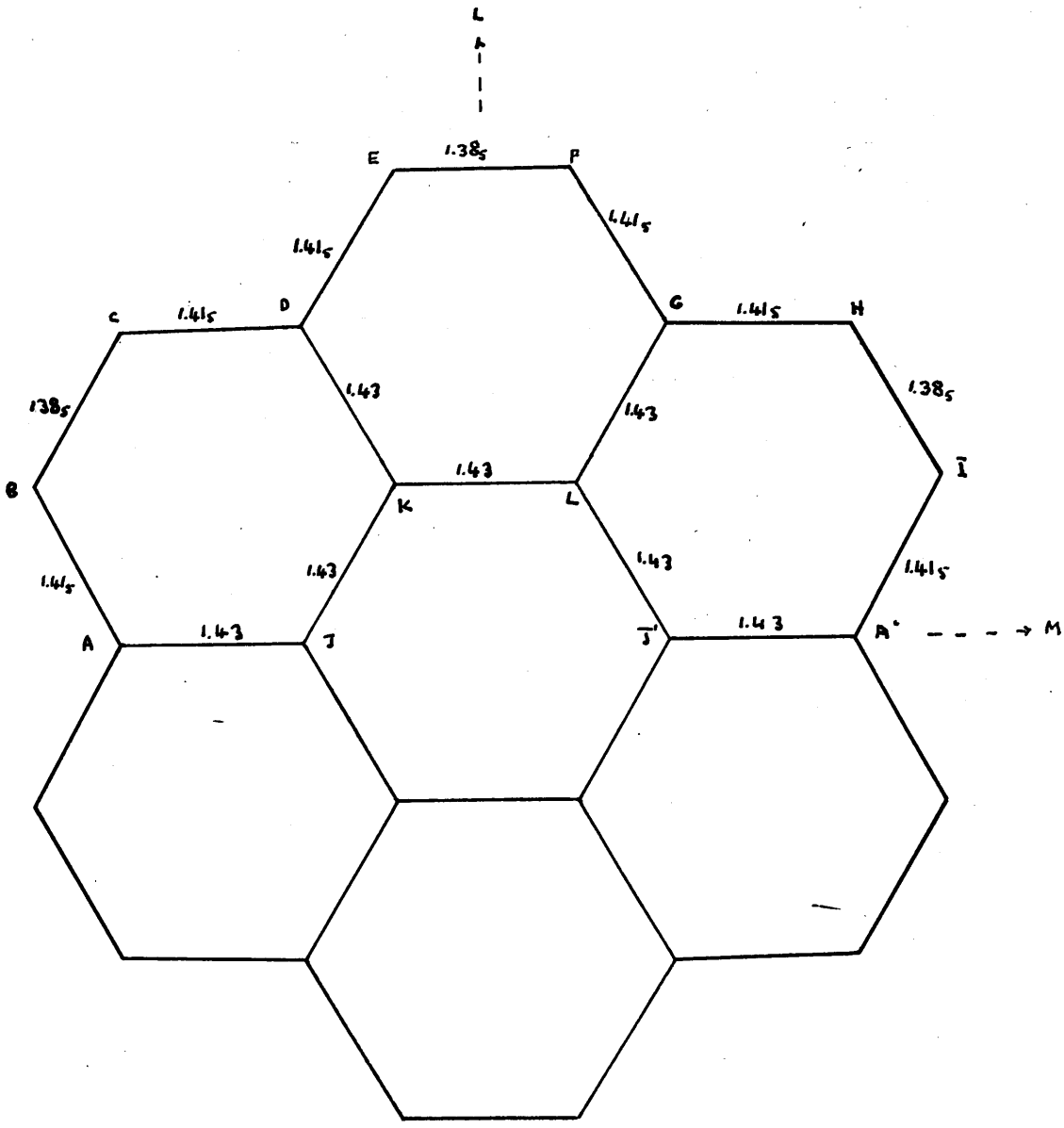

Fig.4. Dimensions of the coronene molecule.

TABLE III.

Co-ordinates with respect to molecular axes.

Atoms	L, A.	M, A.	N, A.
A and A'	0	±2.860	0
B and I	1.243	±3.536	0
C and H	2.441	±2.844	0
D and G	2.476	±1.430	0
E and F	3.684	±0.692	0
J and J'	0	±1.430	0
K and L	1.238	±0.715	0

The molecular model given by these co-ordinates is shown in Fig. 4. The bond lengths vary over a range of about 0.05A. in different parts of the molecule. The central ring and the 'spokes' AJ, KD, LG are 1.43A. compared with 1.38_5A. for the group BC, EF, HI. The other bonds AB, CD, DE, FG, GH and IA' are intermediate in length, being 1.41_5A. The average bond distance is 1.41_5A. The accuracy of these figures is discussed in Part IV in the light of data described in Part III, and the conclusion is that they are probably accurate to ±0.01A., and the distortions indicated above are real. Fig. 5 shows four atoms in the upper part of the molecule. If the whole molecule were regular these atoms would lie in a straight line and the deviation from such a line can be clearly seen.

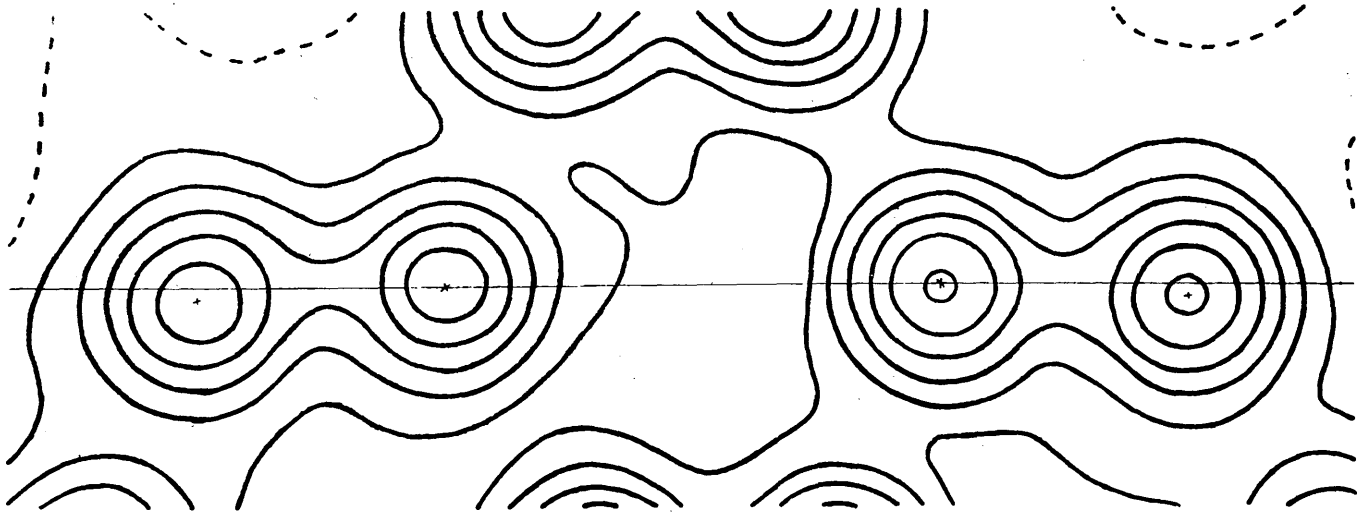

Fig. 5. Enlargement of upper part of the coronene molecule.

Intermolecular distances.

The shortest distances between carbon atoms of adjacent molecules occur between those separated by unit translation along the b axis. Fig. 6 shows a normal projection of two such molecules and the tendency to avoid overlapping of atoms is obvious. The closest approaches are between atoms J' and J_1, and between G and D_1, where the distance is 3.43A., between K and B_1, and between I and L_1, it is 3.44A. The other pairs of atoms are more than 3.5A. apart. Between other molecules the distances are greater. From atom E on the standard molecule to E' on the molecule, one translation along the c axis, the distance is 3.87A., and from E to C' on the same pair of molecules the distance is 3.93A. From atoms I on the standard molecule to B on the reflected molecule at $(\frac{1}{2}a, \frac{1}{2}b)$ the distance is 3.77A. and from I to I' on the same pair, 3.97A. All other distances between atoms of neighbouring molecules appear to be greater than 4A.

(2) Pyrene $C_{16}H_{10}$.

Crystal Data: M, 202.2°; m.p. 150°; d, calc. 1.288, found (Dhar and Guha) 1.27; monoclinic prismatic, a = 13.60 ±0.05, b = 9.24 ±0.03, c = 8.37 ±0.10A., β = 100.2° ±0.2°. Absent spectra (h0l) when h is odd, (0k0) when k is odd. Space group, C_{2h}^5($P2_1/a$). Four molecules per unit cell. No molecular symmetry. Volume of the unit cell 1035A^3. Absorption coefficient for X-rays, λ = 1.54, μ = 6.76 per cm. Total number of electrons per unit cell = F(000) = 424.

The lattice constants given above for pyrene were measured by Professor J.M. Robertson and differ appreciably from those given by Dhar and Guha(2).

Facing P. 31.

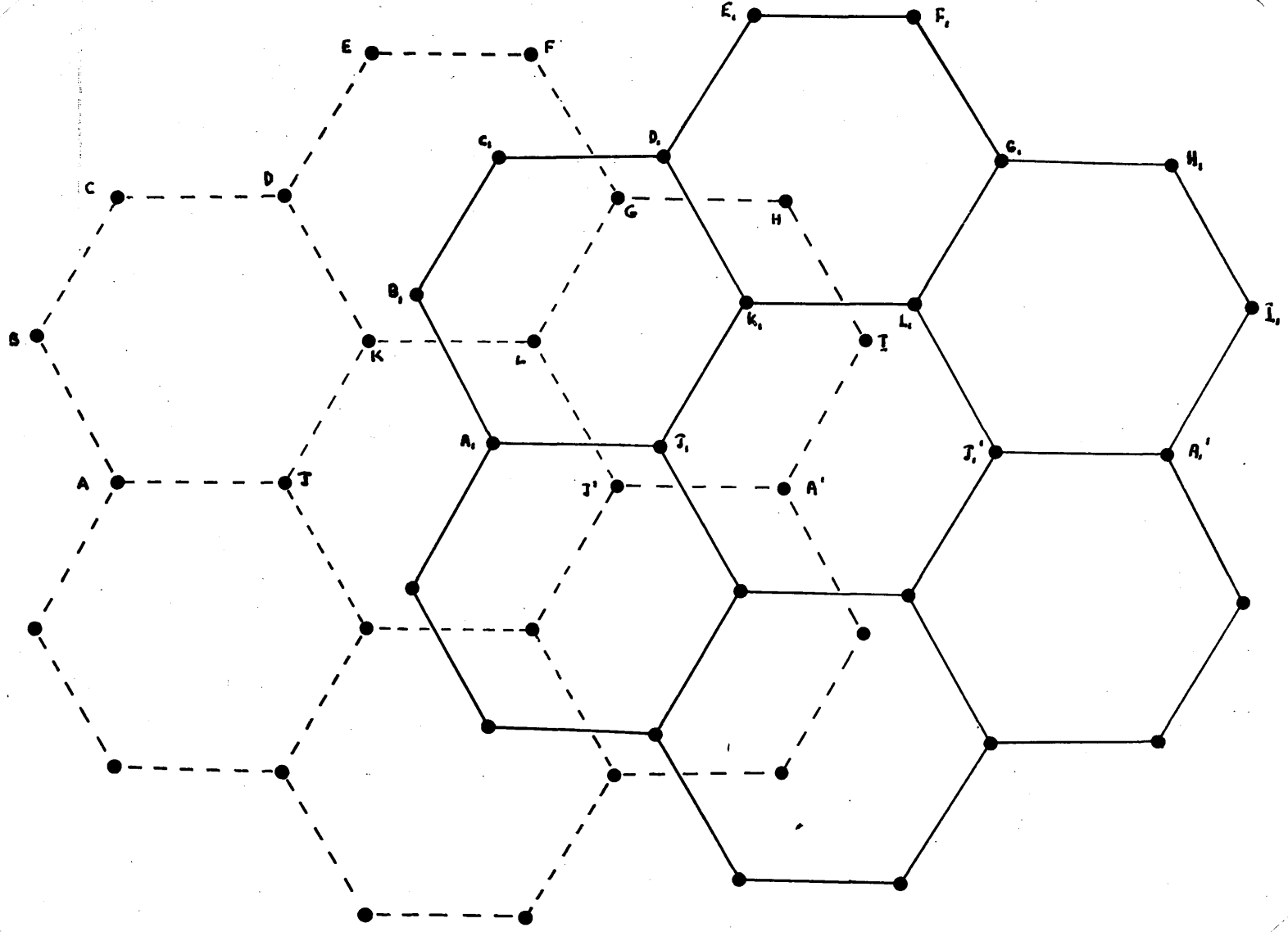

Fig.6. Normal projection of two parallel coronene molecules.

Crystal Structure.

The structure was first obtained approximately by trial methods and then the co-ordinates were refined by a Fourier projection of the (h0l) zone. The results are shown in the contour map of Fig. 7(a). Only 9 out of the 16 crystallographically independent atoms are separately resolved. The others are obscured by overlapping effects of adjoining molecules as indicated in Fig. 7(b). The y co-ordinates of all atoms and the x and z co-ordinates of the 7 unresolved atoms cannot be measured directly, but can be calculated on the assumptions that the molecule is planar, the axes L and M are at right angles(Fig. 7(b)), and the molecule is symmetrical about these axes. A projection down a is shown in Fig. 8. No individual atoms are resolved, but the centres of the molecules can be estimated fairly accurately and the general appearance of the contours indicates that the molecule does contain an inherent centre of symmetry, although this centre is not used crystallographically. It will be seen from Figs. 7 and 8 that the arrangement in the crystal is essentially the same as that found in coronene except that in pyrene two molecules instead of one are grouped about each symmetry centre. The asymmetric unit in pyrene is one complete molecule and its centre has free translations from the centre of symmetry along the three crystallographic axes.

Orientation, Co-ordinates and Dimensions.

By assuming a planar, centro-symmetrical model and averaging certain distances as described in Section C the orientation of the molecule was calculated. The results are collected in Table IV

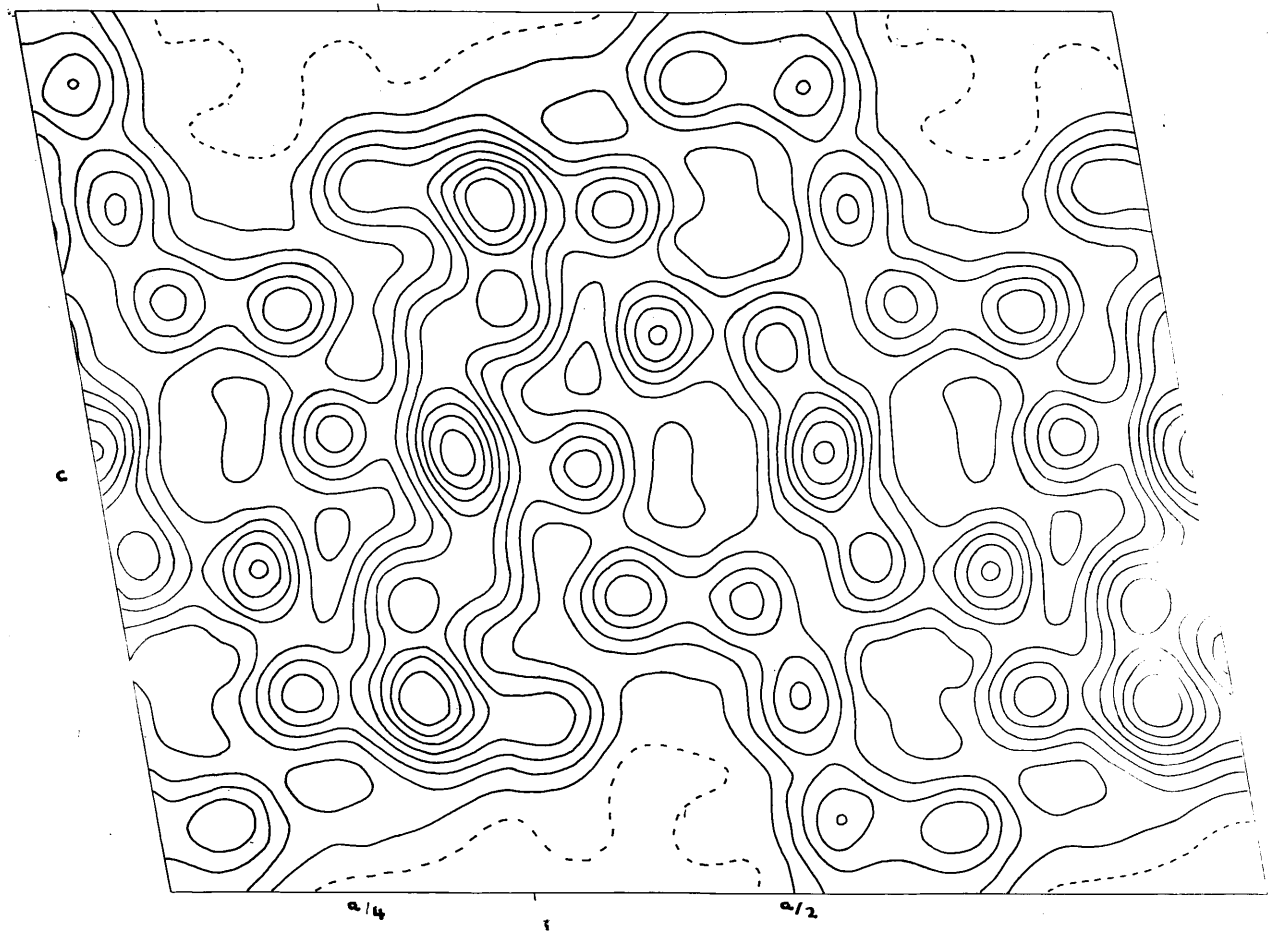

Fig. 7 a.

Fig. 7. Projection of the pyrene structure on the ac plane. Three quarters of the unit cell is included.

where X, ψ and ω are the angles which the molecular axes L and M (Fig. 7b) and N their perpendicular made with the crystallographic axes a, b and c' (c' is perpendicular to a and b). The inclination of the molecular plane to the (010) plane is 40.2° (given by ψ_N), rather less than the corresponding angle in coronene (43.7°). The perpendicular distance between successive molecular planes is given by b $\cos\psi_N$ = 3.53A., rather larger than the interplanar spacing in graphite (3.41A.) or coronene (3.40A.).

TABLE IV

Orientation of the molecule in the crystal.

$X_2 = 61.1^\circ$	$\cos X_2 = 0.4834$	$X_M = 52.2^\circ$	$\cos X_M = 0.6130$
$\psi_2 = 77.7^\circ$	$\cos \psi_2 = 0.2130$	$\psi_M = 52.4^\circ$	$\cos \psi_M = 0.6101$
$\omega_2 = 31.9^\circ$	$\cos \omega_2 = 0.8487$	$\omega_M = 120.1^\circ$	$\cos \omega_M = -0.5017$

$X_N = 128.7^\circ$	$\cos X_N = -0.6248$
$\psi_N = 40.2^\circ$	$\cos \psi_N = 0.7630$
$\omega_N = 80.5^\circ$	$\cos \omega_N = 0.1648$

The co-ordinates with respect to the crystal axes are collected in Table V. The x and z co-ordinates of the nine resolved atoms can be measured directly from the projection in Fig. 7, and these values are underlined. The other crystal co-ordinates follow from the assumption that the molecule is planar and symmetrical about the L and M axes. The figures in Table V give the co-ordinates of all the carbon atoms (A-P) in one pyrene molecule. The other three molecules in the unit cell can be derived by the operations of the space group $P2_1/a$, given above for coronene.

Facing p. 33.

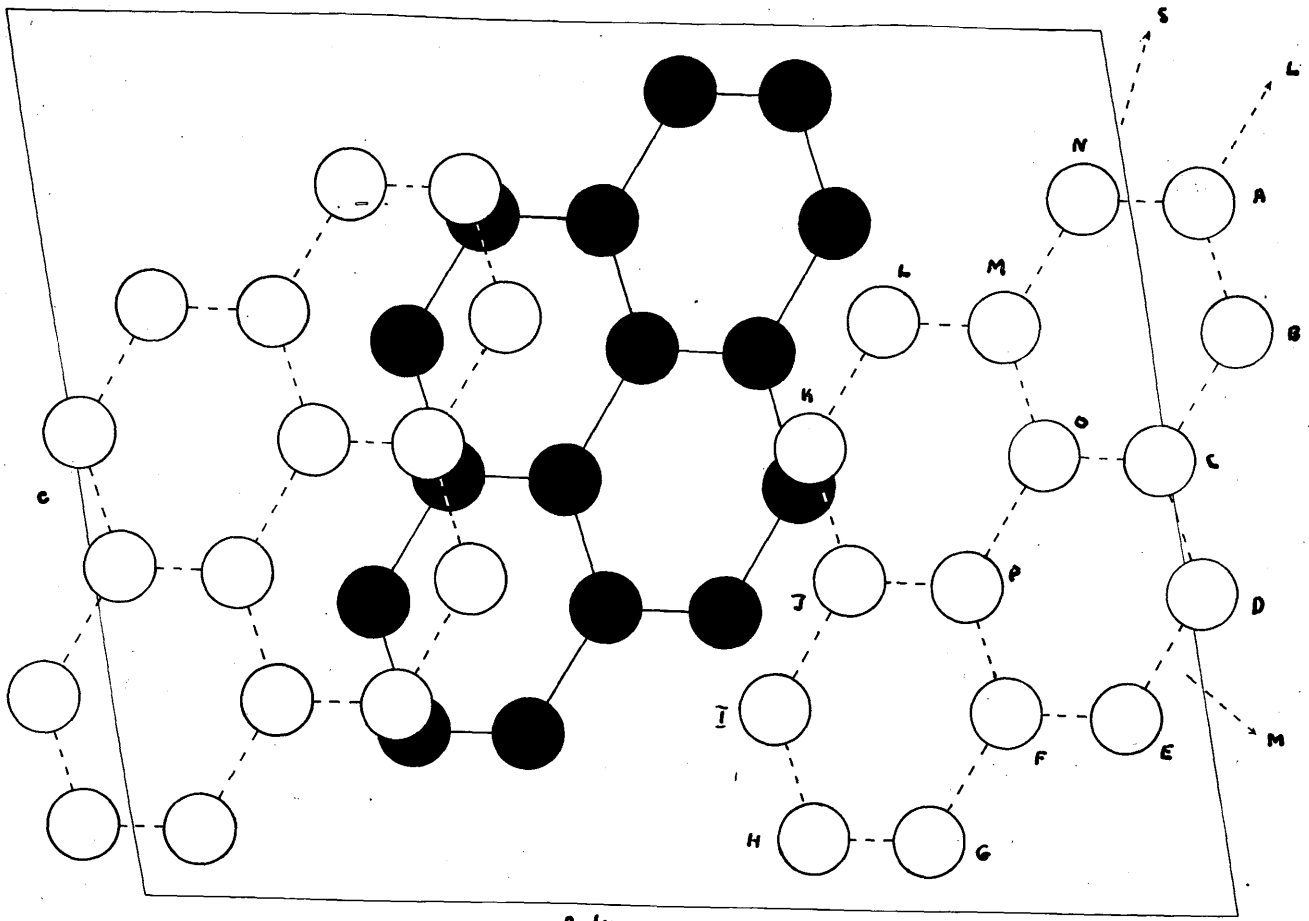

fig. 7β.

TABLE V.

Co-ordinates. Centre of symmetry as origin. x, y, z, are referred to the monoclinic crystal axes. x', y and z' are rectangular co-ordinates referred to the a and b crystal axes and their perpendicular c'.

$$x = x' - z' \cot \beta$$
$$z = z' \operatorname{cosec} \beta$$

Atoms cf. Figs 7 & 9.	x, A.	y, A.	z, A.	x', A.	z', A.	2πx/a	2πy/b	2πz/c
A	3.85	-0.41	3.51	3.229	3.463	101.9°	-16.0°	151.0°
B	4.04	0.18	2.31	3.630	2.271	106.9	7.1	99.4
C	3.14	-0.12	1.08	2.943	1.065	83.1	-4.6	46.5
D	3.33	0.49	-0.18	3.664	-0.181	88.1	19.3	-7.9
E	2.45	0.19	-1.38	2.692	-1.361	64.9	7.7	-59.4
F	1.33	-0.73	-1.37	1.571	-1.345	35.2	-28.5	-59.0
G	0.43	-1.03	-2.59	0.884	-2.551	11.4	-40.2	-111.4
H	-0.65	-1.91	-2.58	-0.189	-2.537	-17.2	-74.8	-111.0
I	-0.83	-2.50	-1.37	-0.590	-1.345	-22.0	097.8	-59.0
J	0.07	-2.20	-0.14	0.097	-0.139	1.9	-86.0	-6.0
K	-0.12	-2.81	1.12	-0.324	1.107	-3.2	-109.9	48.2
L	0.76	-2.51	2.32	0.348	2.287	20.1	-98.3	99.8
M	1.88	-1.59	2.31	1.469	2.271	49.8	-62.1	99.4
N	2.78	-1.29	3.53	2.156	3.477	73.6	-50.5	151.8
O	2.06	-1.01	1.09	1.874	1.078	54.5	-39.5	46.9
P	1.14	-1.31	-0.15	1.170	-0.152	-30.2	-51.2	-6.5
Centre of molecule p.	1.604	-1.160	0.470	1.520	0.463	42.5	-45.3	19.9

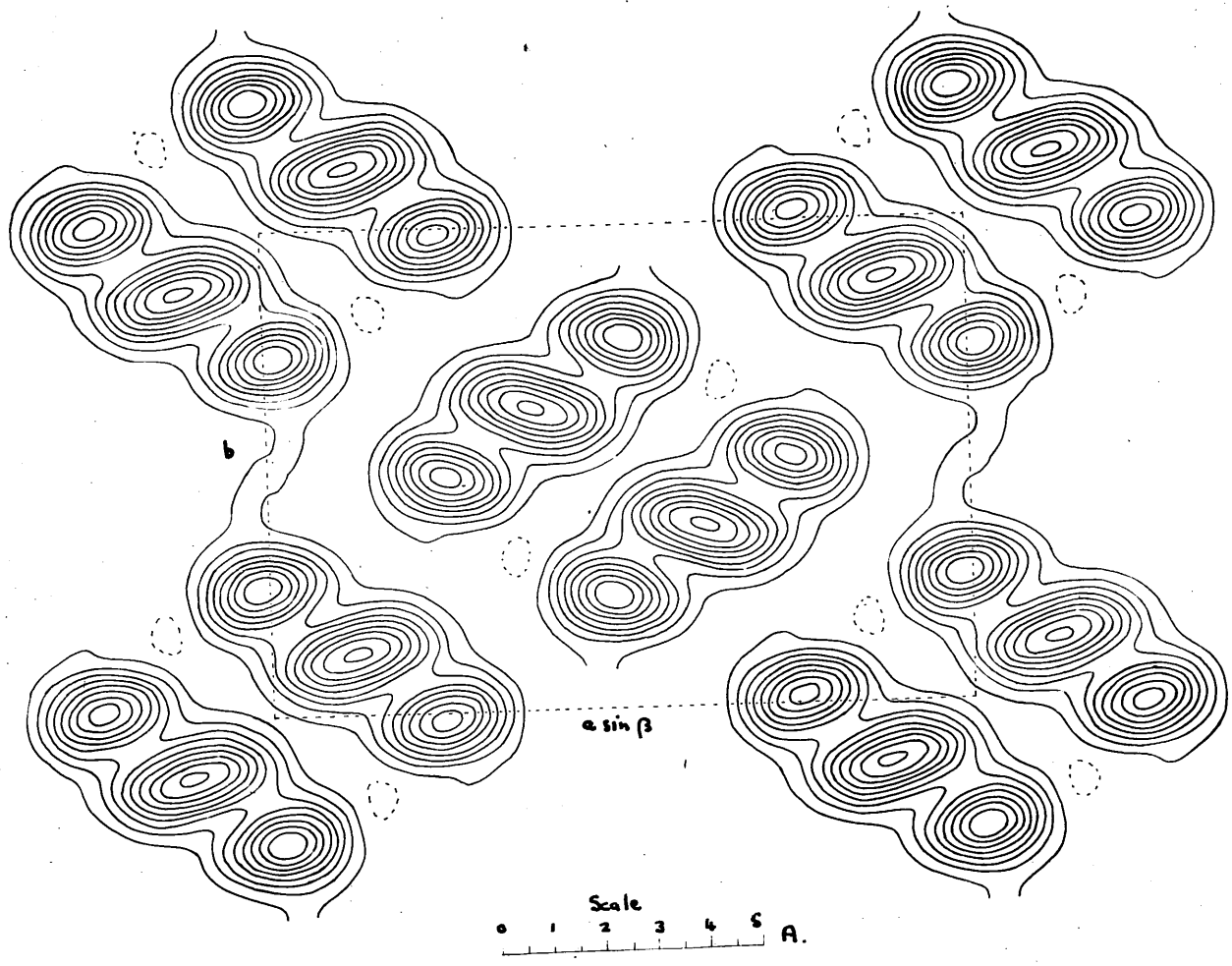

Fig. 8a.

Fig 8. A group of ten pyrene molecules in the c-axis projection.

The molecular dimensions and bond lengths may be calculated from these co-ordinates, and the results are shown graphically in Fig. 9. The ringed atoms A, B, C, E, F, M, N, O, P are separately resolved in Fig. 7 and the bond distances are obtained by direct measurement combined with the orientation angles of Table IV. The other bond lengths can be derived by assuming exact symmetry about L and M and the justification for this procedure is discussed in Section C. It will be seen that the measured values of the bonds OP and EF are unusually large at 1.45A. The hexagon angles do not differ appreciably from 120°.

The molecular structure may be summarised by giving the atomic co-ordinates with respect to the molecular axes L, M and N. These are collected in Table VI. These figures can be combined with the orientation angles and the crystal co-ordinates of the molecular centre (x'_p, y_p, z'_p) to give the co-ordinates of Table V by the relations

$$x = L\cos\chi_L + M\cos\chi_M + N\cos\chi_N + x'_p$$

$$y = L\cos\psi_L + M\cos\psi_M + N\cos\psi_N + y_p$$

$$z = L\cos\omega_L + M\cos\omega_M + N\cos\omega_N + z'_p$$

Facing p. 35.

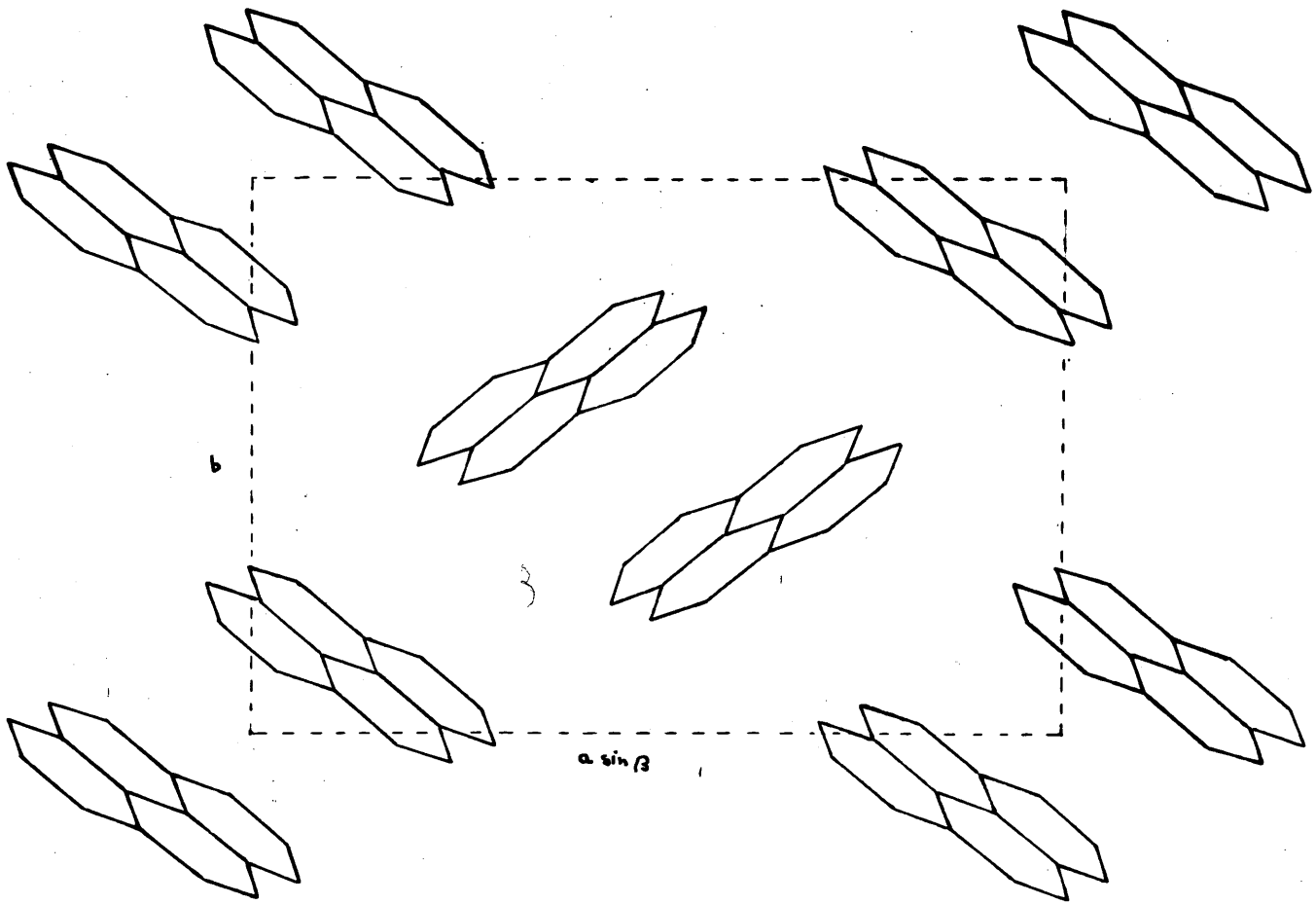

Fig. 86.

TABLE VI.

Co-ordinates with respect to molecular axes.

Atoms	L, A.	M, A.	N, A.
A, H	±3.535	0	0
B, G, I, N	±2.840	±1.203	0
C, F, J, M	±1.420	±1.203	0
D, E, K, L	±0.695	±2.459	0
O, P	±0.725	0	0

Intermolecular Distances.

The closest approach between adjacent molecules occurs along the b axis. Fig. 10 shows the normal projection of one molecule in the plane of the molecule related by the centre of symmetry. The staggered arrangement noted in coronene is illustrated here also. The pairs PP', MG', CI' and KE' nearly coincide in this projection and for these atoms the distance of approach is 3.54A. The other pairs are at rather greater distances.

From atom D on the standard molecule to atom O' (inverted) on the reflected molecule half a translation along the a axis the distance is 3.61A., and from D to P' it is 3.64A. From A on the standard molecule to N' (inverted) on the reflected molecule half a translation along a and one translation along c the distance is 3.96A. All other intermolecular distances appear to be greater than 4A.

Facing p. 36.

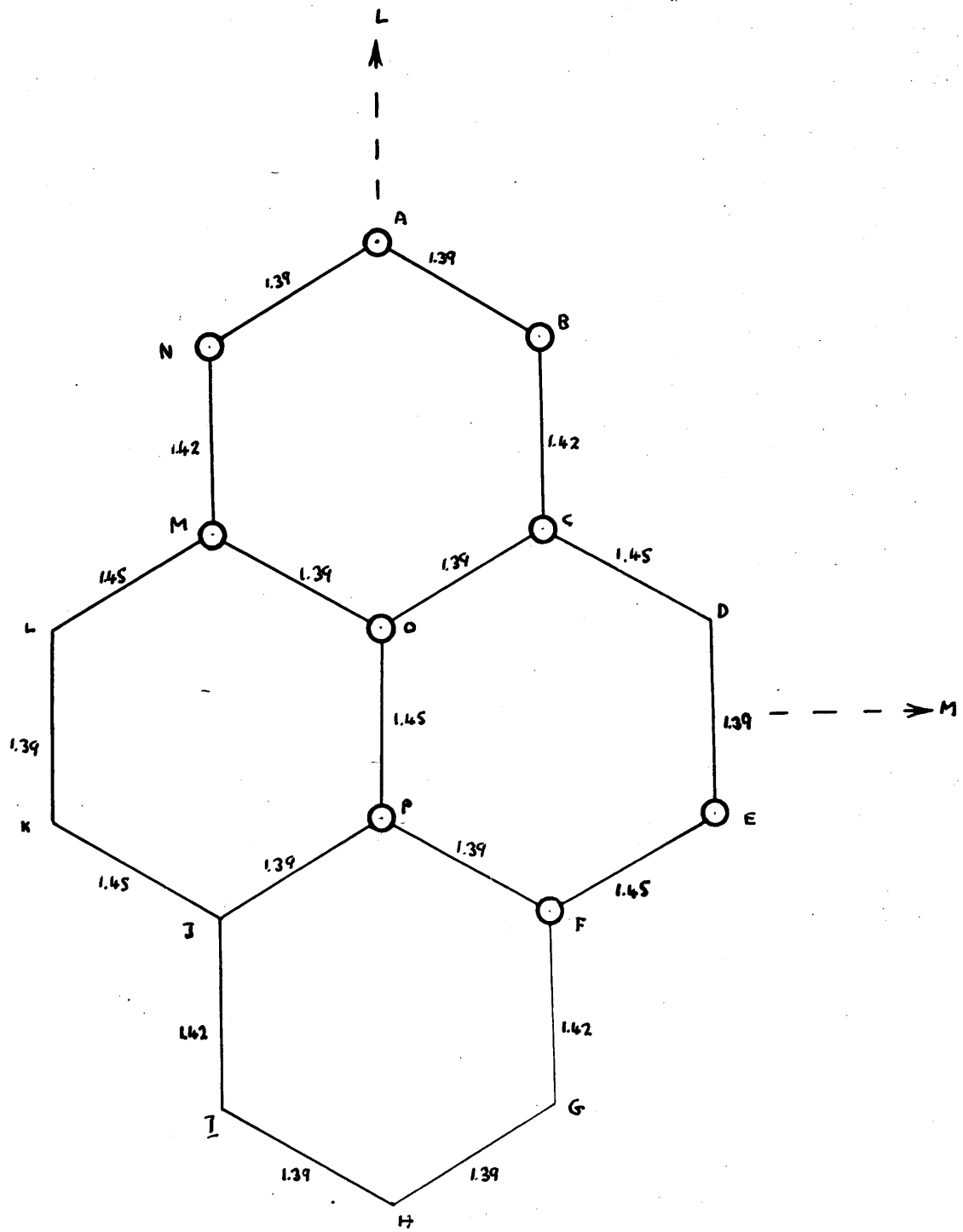

Fig. 9. Dimensions of the pyrene molecule.

(3) 1.2:5.6 Dibenzanthracene (orthorhombic), $C_{22}H_{14}$.

Crystal Data: M, 278; m.p. 260°; d, calc. 1.294, found 1.282; orthorhombic bipyramidal; a = 8.22, b = 11.39, c = 15.14A. Absent spectra (0kl) when l is odd, (h0l) when h is odd, hk0 when k is odd. Space group Q_h^{15}, (Pcab). Four molecules per unit cell. Molecular symmetry, centre. Volume of the unit cell 1418A^3. Absorption coefficient for X-rays, λ = 1.54, μ = 6.78 per cm. Total number of electrons per unit cell = F(000) = 584.

The cell dimensions and space group listed above are those given by Iball(37).

Crystal Structure.

The structure was first found by trial on the basis of the magnetic measurements of Krishnan and Banerjee(38) and the atomic co-ordinates refined by two successive Fourier syntheses of the (0kl) zone. A subsequent correction for the incompleteness of the Fourier series was made as suggested by Booth(40). The results of the second Fourier projection of the (0kl) zone are shown in the contour map of Fig. 11(a). Nine out of the eleven crystallographically independent atoms are resolved, the other two lying almost exactly under the corresponding atoms in adjoining molecules as illustrated in Fig. 11(b). The relative tilts to the projection plane of all the molecules shown in Fig. 11 are illustrated by Fig. 12 which shows diagrammatically a projection of the structure viewed down the b axis. The lines in Fig. 12 represent the L-axes of the different molecules (see Fig. 11(b)). Figs. 11 and 12 together give a complete three dimensional picture of the symmetry elements of the space group Pcab.

Facing p. 37

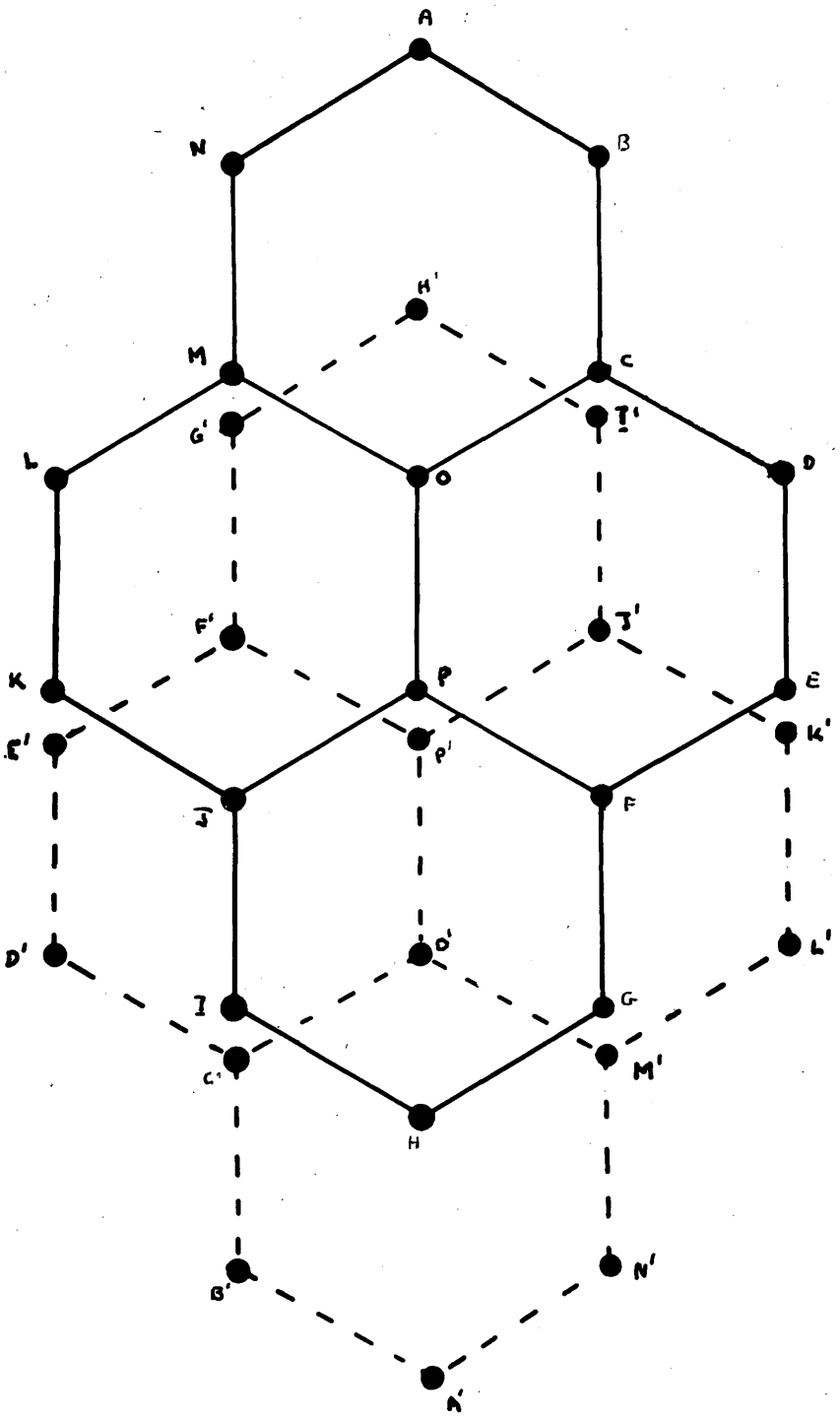

Fig. 10. Normal projection of two parallel pyrene molecules.

Orientation, Co-ordinates and Dimensions.

By assuming a planar model and averaging certain distances in the contour map of Fig. 11 it is possible to calculate the complete orientation of the molecule in the crystal. The results are given in Table VII where χ, ψ and ω are the angles which the molecular axes L and M (Fig. 11(b)) and N their perpendicular made with the crystallographic axes a, b and c.

TABLE VII

Orientation of the Dibenzanthracene Molecule in the crystal.

$\chi_L = 92.1^\circ$	$\cos \chi_L = -0.0374$	$\chi_M = 58.8^\circ$	$\cos \chi_M = 0.5180$
$\psi_L = 106.1^\circ$	$\cos \psi_L = -0.2771$	$\psi_M = 35.3^\circ$	$\cos \psi_M = 0.8162$
$\omega_L = -16.2^\circ$	$\cos \omega_L = 0.9601$	$\omega_M = 75.2^\circ$	$\cos \omega_M = 0.2558$

$\chi_N = 31.3^\circ$	$\cos \chi_N = 0.8545$
$\psi_N = 120.5^\circ$	$\cos \psi_N = -0.5069$
$\omega_N = 96.5^\circ$	$\cos \omega_N = -0.1130$

The co-ordinates with respect to the crystal axes are collected in Table VIII. y_1 and z_1 are the co-ordinates of the resolved atoms measured directly from the second Fourier projection while y_2 and z_2 are the values finally adopted as being most probable after correction for the incompleteness of the Fourier series. The co-ordinates of the two atoms C and I (Fig. 11(b)) cannot be measured directly because of overlapping effects and the co-ordinates adopted for these atoms are those which they would have in a regular hexagonal model in the orientation of Table VII. These positions are in agreement with the appearance of the double peaks shown in Fig. 11(a), but the centres cannot be assigned any

Facing p. 28.

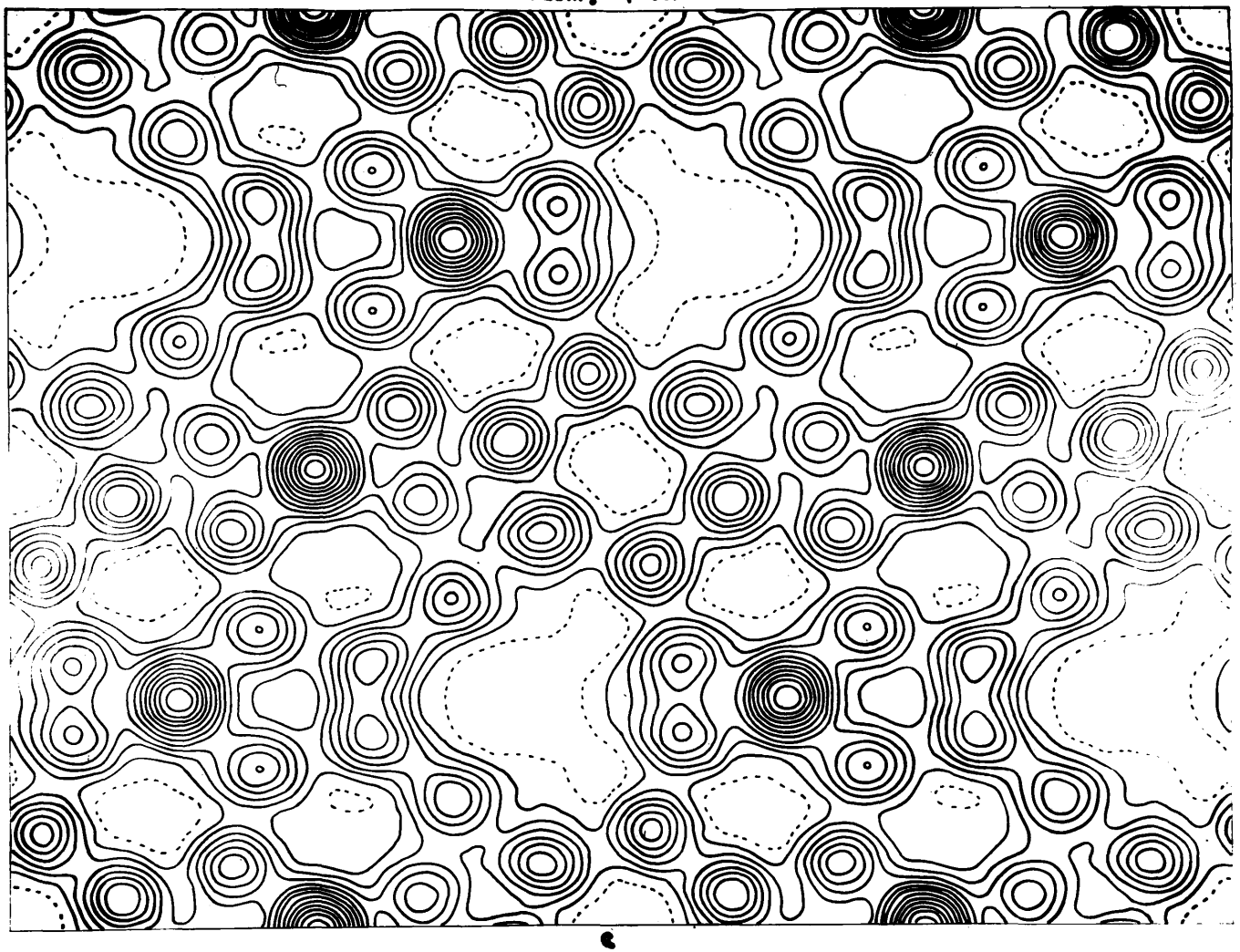

Fig. IIa.

Fig. II. Projection of the dibenzanthracene structure on the bc plane.

more accurately for these two atoms. The other three molecules in the unit cell may be derived from the one given by the symmetry operations of the space group Pcab, the co-ordinates of all related atoms in the cell being given by the relations:

$$\pm\left(x,\ y,\ z;\ \tfrac{1}{2}+x,\ \tfrac{1}{2}-y,\ z;\ x,\ \tfrac{1}{2}+y,\ \tfrac{1}{2}-z;\ \tfrac{1}{2}-x,\ y,\ \tfrac{1}{2}+z\right)$$

TABLE VIII

Co-ordinates assigned to atoms. $\underline{x}$, $\underline{y}$ are the co-ordinates measured directly from the second Fourier projection, x_2, y_2 the corrected values finally adopted.

Atoms	x, A.	y_1, A.	y_2, A.	z_1, A.	z_2, A.	$2\pi x/a$	$2\pi y_2/b$	$2\pi z_2/c$
A	-0.215	-1.580	-1.584	5.465	5.476	-9.4^{o}	-50.1^{o}	130.3^{o}
B	0.444	-0.380	-0.392	5.094	5.108	19.4	-12.4	121.4
C	0.504	0.020	0.020	3.723	3.723	22.1	0.6	88.5
D	-0.095	-0.776	-0.770	2.738	2.740	-4.2	-24.3	65.1
E	-0.028	-0.370	-0.354	1.382	1.392	-1.2	-11.2	33.2
F	0.600	0.786	0.794	0.992	0.978	26.2	25.0	23.3
G	0.647	1.198	1.172	-0.384	-0.376	28.3	37.1	-8.9
H	1.328	2.400	2.404	-0.760	-0.740	58.2	76.0	-17.6
I	1.381	2.794	2.794	-2.097	-2.097	60.5	88.3	-49.8
J	0.769	1.980	1.978	-3.076	-3.063	33.7	62.6	-73.0
K	0.827	2.380	2.388	-4.452	-4.448	36.2	75.3	-105.9

The molecular dimensions and bond lengths may be calculated from these co-ordinates and are shown graphically in Fig. 13. The ringed atoms A, B, D, E, F, G, H, J, K are separately resolved in Fig. 2 and only the bond distances between those atoms can be

Facing p. 34

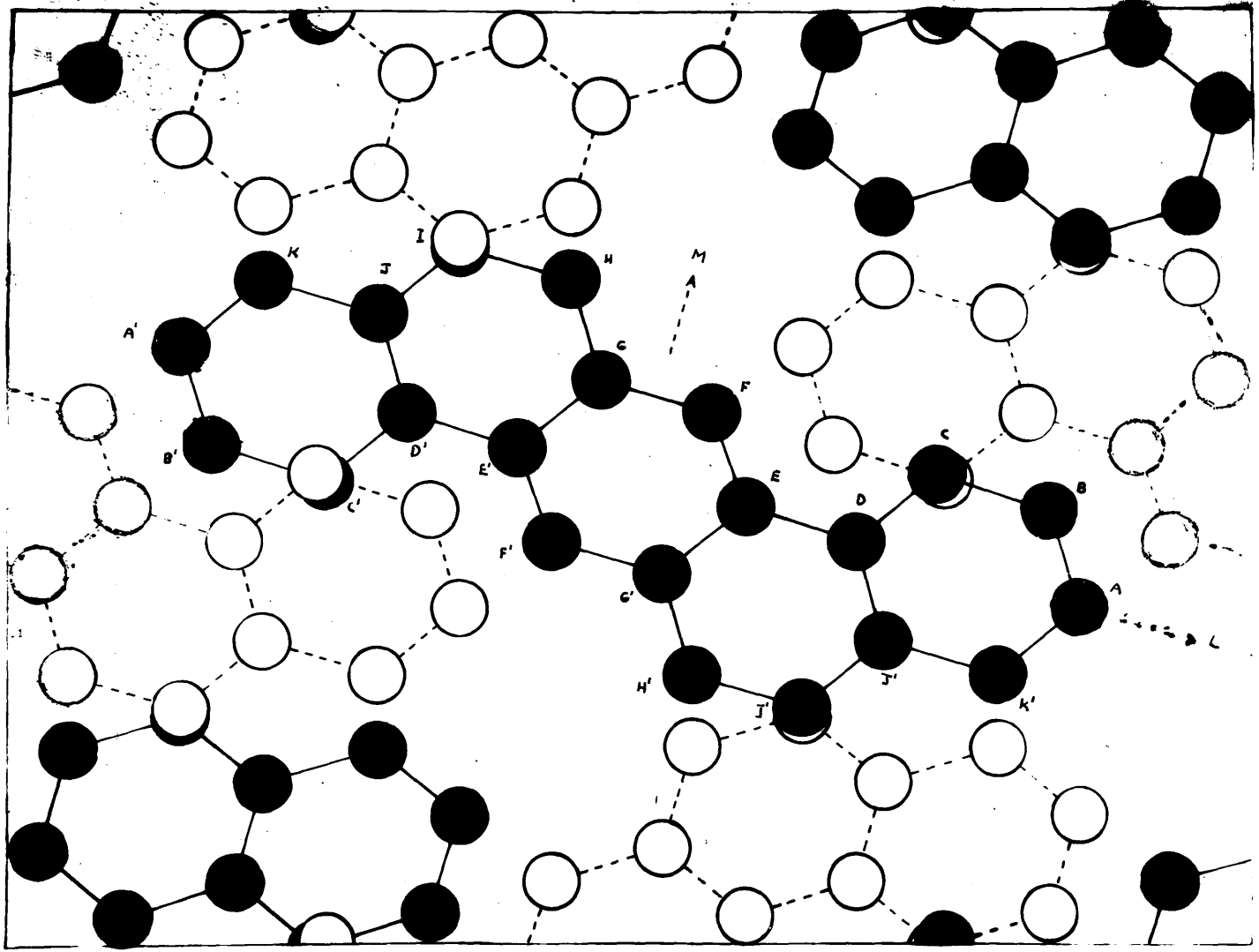

Fig 11. b.

directly measured. The unusually large values found for GH, JK and K'A are very difficult to assess, as the atoms H and K are so distorted by their proximity to the corresponding atoms in the reflected molecule that their centres are rather more uncertain than the others and these values must be considered rather doubtful. The central ring, however, is free from such distortion effects and the values here should be more reliable. The question is discussed more fully in Part IV.

From the molecular orientation given in Table VII and the co-ordinates of Table VIII the molecular co-ordinates of the atoms can be calculated and are collected in Table IX.

TABLE IX

Co-ordinates with respect to molecular axes.

Atoms	L, A.	M, A.	N, A.	Atoms	L, A.	M, A.	N, A.
A	5.703	-0.003	0	G	-0.708	1.196	0
B	4.996	1.218	0	H	-1.427	2.460	0
C	3.550	1.230	0	I	-2.840	2.460	0
D	2.847	0.023	0	J	-3.520	1.229	0
E	1.435	0.050	0	K	-4.964	1.240	0
F	0.696	1.209	0				

Intermolecular Distances.

The closest distance of approach between atoms of different molecules occurs between the standard molecule and the molecule at $(\frac{1}{2}x, \frac{1}{2}z)$. Between c on the first molecule and J on the

Facing p. 40.

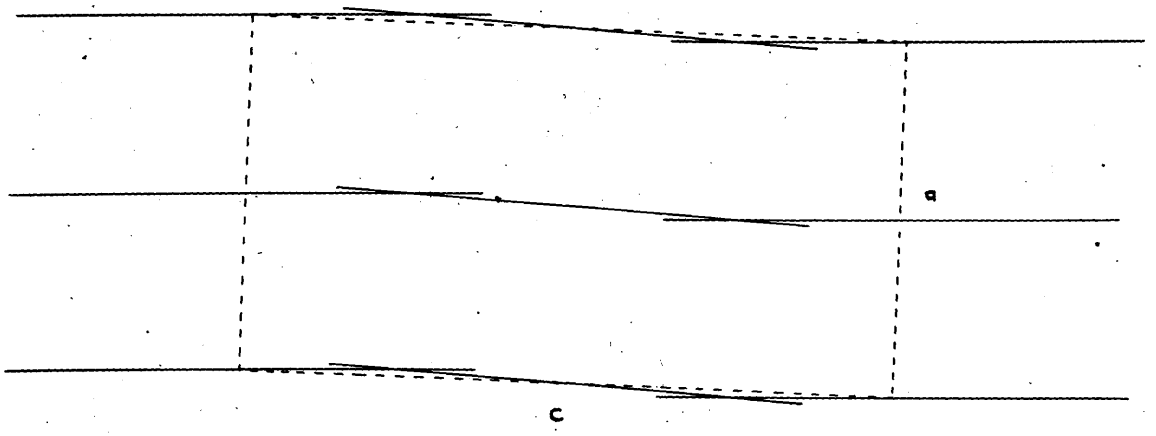

Fig. 12. End view of dibenzanthracene molecules.

translated molecule the distance is 3.54A. while between F and A'(inverted) the separation is 3.56A. Other distances in this direction are CD' 3.76A., CK 3.71A., EB' 3.87A. and FK 3.78A.

The distances are rather longer between the standard molecule and the reflected molecule at $(\frac{1}{2} + x, \frac{1}{2} - y, z)$ where the atom I on the standard molecule is 3.59A. from D' on the reflected molecule, 3.75A. from J and 3.82A. from E'.

All other pairs of atoms are more than 4A. apart.

Facing p. 41.

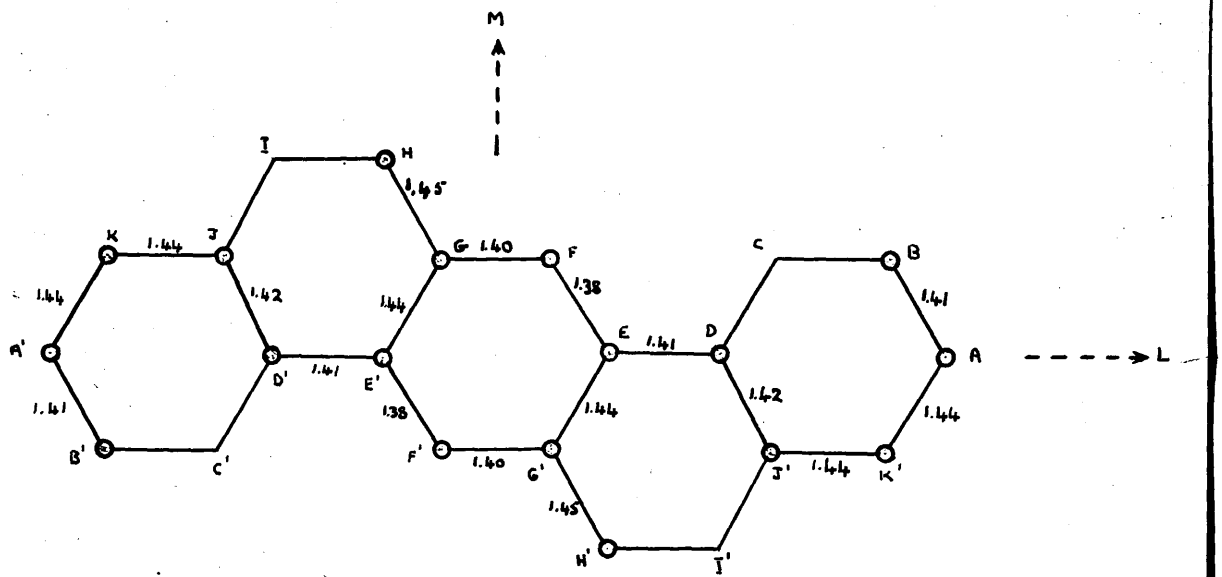

Fig. 13. Dimensions of the dibenzanthracene molecule.

C. EXPERIMENTAL.

(1) Coronene.

The crystals were obtained by slow cooling of a solution in tetrahydro-naphthalene.

Determination of Cell Constants and Space Group.

Copper K_α radiation, $\lambda = 1.54$, was employed for all measurements. Rotation, oscillation and moving film photographs were taken. Only the (020) of the (0k0) reflections could be observed, so long exposure oscillation photographs were taken, but neither the (010) nor the (030) reflections appeared and the space group $P2_1/a$ was assumed. The density of the crystals was found by flotation in calcium chloride solution.

Measurement of intensities.

Moving film photographs of the (h0l) and (hk0) zones were taken from crystals rotating about the b and c axes. The multiple film technique(41) was used in order to correlate the strongest reflections with the weakest. The total range of intensities recorded was about 10,000 to 1. Apart from a few of the weakest reflections which were estimated visually, all intensity measurements were made on the Dawton Scan Photometer(42). The circuit of this photometer was modified by Mr. A.M. Mathieson, and the instrument was thoroughly tested by independent measurement of photographs previously measured on the Robinson Photometer(43). Satisfactory agreement was obtained.

Extremely small crystals were used, and completely immersed in a uniform X-ray beam. The two specimens mainly employed for the (h0l) zone were cut to just over 1 mm. in length (along b) and had

cross-sections of 0.16 mm. by 0.32 mm. and 0.15 mm. by 0.24 mm. respectively. Absorption corrections were made graphically by drawing and measuring a mean path of the X-ray beam through the crystal for each reflection. This method is only approximate but should be quite accurate enough for the (h0l) zone in view of the small crystal dimensions involved. The calculated correction factors ($e^{+\mu t}$) varied from 1.10 to 1.24. In the (hk0) zone the crystal specimen had the rather more extreme cross-section of 0.13 mm. by 0.63 mm. and the absorption correction factors varied from 1.10 to 1.51.

There was little evidence of extinction but the intensities of the three strongest reflections, 200,001 and $20\bar{1}$, varied a little in different crystal specimens and the highest values were adopted as being the most probable.

Trial Analysis.

The short b axis of coronene (4.695A.) and the general crystal habit are extremely similar to those of the phthalocyanine series (44, 45). As coronene, although very different chemically, is also a large, planar molecule, it seemed probable that the crystal structure, and in particular the inclination of the molecules to the (010) plane was similar in both cases.

Assuming a tilt of about 45° to this plane, therefore, there remained only two degrees of freedom to be fixed. From moving film photographs of the (h0l) zone it was observed that the following small-spacing planes give outstandingly strong reflections: (16,00), (16,$0\bar{1}$), 14,$0\bar{8}$), (10,$0\bar{3}$), (602), (40$\bar{5}$), and (207). By making different projections of the coronene molecule on the (010)

Facing p. 43.

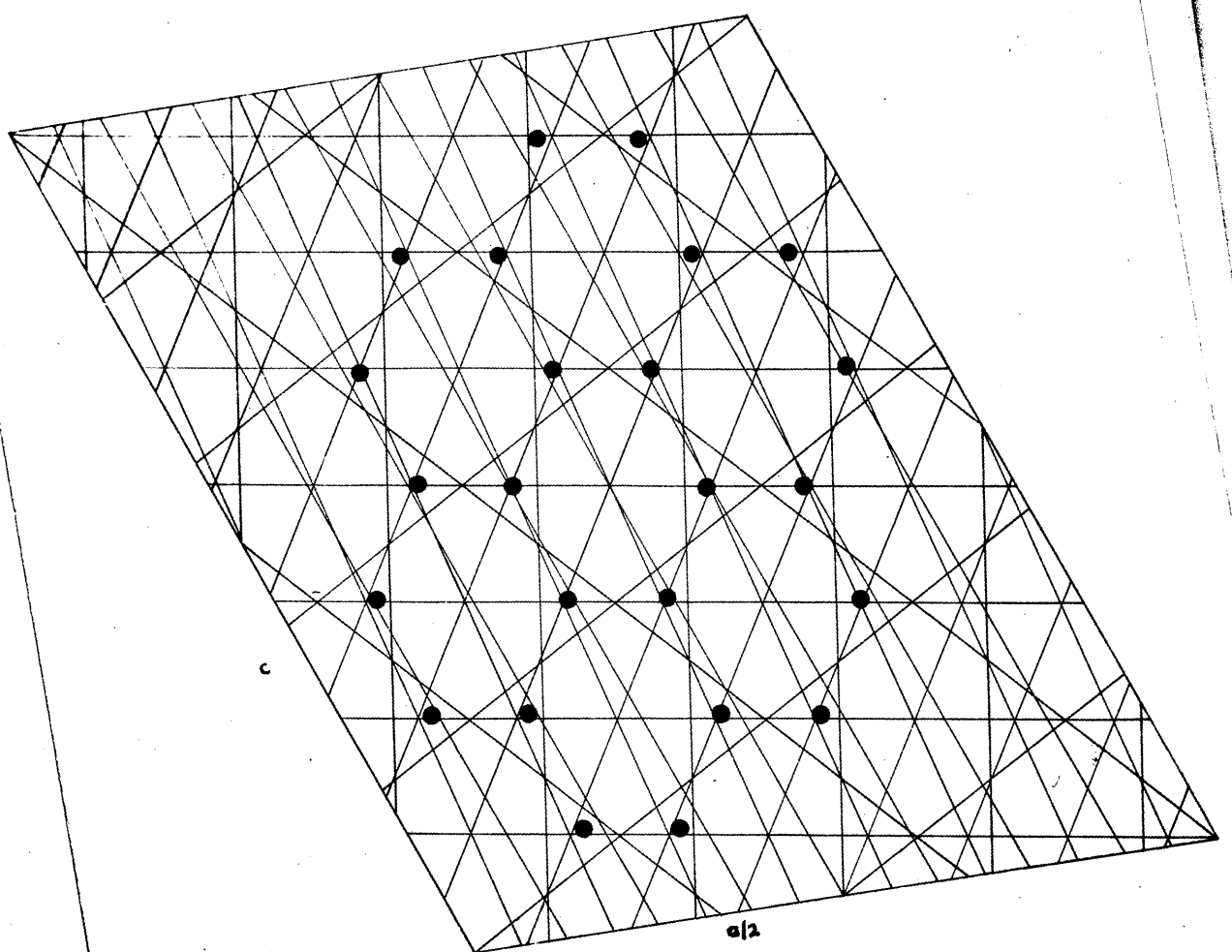

Fig. 14. Prominent (hoℓ) reflections for coronene.

plane it was found that only one orientation could completely account for the enhancement of these reflections. The final diagram used is shown in Fig. 14 and it can be seen that the atoms are grouped very closely near these planes. In this position the agreement between calculated and observed structure factors was good enough to proceed immediately to refinement by double Fourier series methods.

Fourier Analysis.

The electron density on the ac plane was computed at 900 points on the asymmetric unit from the series

$$\rho(x, z) = \frac{1}{ac \sin \beta} \sum_{-\infty}^{+\infty} \sum_{-\infty}^{+\infty} F(hol) \cos 2\pi(hx/a + lz/c)$$

Both the a and the c axes were divided into 60 parts, the intervals along a being 0.268Å., and along c, 0.169Å., and the summation was carried out by means of three figure strips(46). The positions of the contour lines were obtained by graphical interpolation from the summation totals by making sections of the rows and columns.

In the first series 78 terms were included, and in the second, the result of which is shown in Fig. 1(a), 129 terms, all those which could be observed with the exception of the very weak (2,0.11) plane.

Calculation of Orientation.

The central ring of coronene(Fig. 1) fulfilled quite accurately the conditions necessary for it to be the projection of a regular, planar hexagon and it was possible to calculate the orientation of the molecule from this without assuming regularity for any of the

other rings. The best value for the radius of this central hexagon was found to be 1.43A., from consideration of measured distances in directions close to S (Fig. 1(b)).

The tilt of the axis M to $\underline{b}$ (ψ_M) is given by $\sin \psi_M = \frac{r}{R}$ where r is the measured length of a line in the M direction and R its real length. Taking r as the mean of KL and one half of JJ' (Fig. 1) and R as $1.43A_2$, $\psi_M = 46.7^\circ$. Now ψ_L is so close to 90° that it varies very rapidly with regard to its sine and hence cannot be determined accurately by the same method; ψ_L however may be calculated from the observed angle between L and M in projection (94.2°) and the assumption that these molecular axes are actually at right angles in the molecule. Let η_L and η_M be the angles which L and M make with the $\underline{a}$ axis in projection. η_L is found to be $84.75^\circ \pm 0.15^\circ$ by taking the mean direction of the lines DJG', GJ'D', and the line joining the mid-points of EF and KL to the origin. η_M is found to be -9.4°, the angle which AJJ'A' makes with $\underline{a}$. The complete orientation of the molecule may then be obtained from the relations

(1) $\cos^2\chi_L + \cos^2\psi_L + \cos^2\omega_L = 1$
(2) $\cos^2\chi_M + \cos^2\psi_M + \cos^2\omega_M = 1$
(3) $\cos^2\chi_N + \cos^2\psi_N + \cos^2\omega_N = 1$
(4) $\cos\chi_L\cos\chi_M + \cos\psi_L\cos\psi_M + \cos\omega_L\cos\omega_M = 0$
(5) $\cos\chi_L\cos\chi_N + \cos\psi_L\cos\psi_N + \cos\omega_L\cos\omega_N = 0$
(6) $\cos\chi_M\cos\chi_N + \cos\psi_M\cos\psi_N + \cos\omega_M\cos\omega_N = 0$
(7) $\cos\omega_L = \cos\chi_L \tan\eta_L$
(8) $\cos\omega_M = \cos\chi_M \tan\eta_M$
(9) $\psi_M = 46.7^\circ$

The results of this calculation are given in Table II.

Facing p. 45.

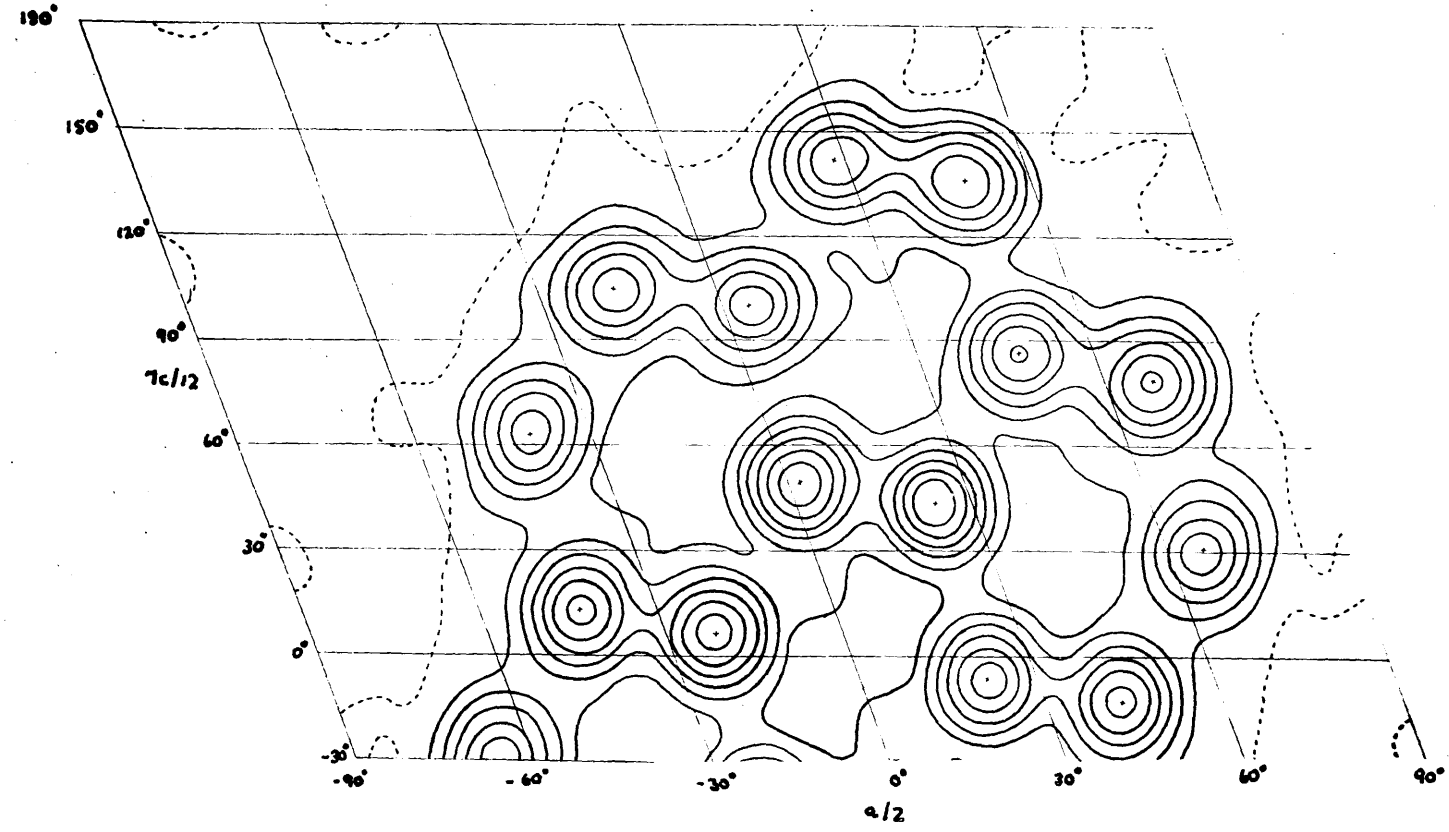

Fig. 15. Co-ordinates assigned to atoms in coronene.

Co-ordinates of Atoms and Molecular Dimensions.

If all the hexagons in the coronene structure were regular and of the same size all parallel bond lengths in projection would be equal, but this is not found to be the case. The 'spokes', KD, LG etc. are not significantly different from the corresponding parallel bonds of the central ring, but the outermost bonds BC, EF and HI when compared with JK, KL and LJ' respectively show a shortening of 3.2 $\pm$0.4%. The other outer bonds are fairly consistently decreased but to a smaller extent viz., A'I, 2.0%; HG, 0.8%; GF, 1.7%; ED, 2.2%; DC, 2.7%; and BA, -1.3% (expansion). The differences between individual members of the groups do not appear to be significant and by taking an average value for each group the molecular model shown in Fig. 4 was deduced. When the molecular co-ordinates of Table III are combined with the orientation angles according to the relations

$$x' = L\cos\chi_L + M\cos\chi_M \qquad x = x' - z'\cot\beta$$
$$y = L\cos\psi_L + M\cos\psi_M \qquad z = z'\cot\beta$$
$$z' = L\cos\omega_L + M\cos\omega_M$$

we obtain the rectangular crystal co-ordinates (x', y, z') and the monoclinic crystal co-ordinates (x, y, z). The latter are collected in Table II in the columns headed (a) and are plotted on the contour map of Fig. 15. The columns headed (b) contain the independently estimated atomic co-ordinates, and it will be seen that the deviations are small.

Structure Factors.

The co-ordinates of Table II(a) were used for a final calculation of the structure factors using the anthracene scattering

curve(47). The scale of the observed F's was obtained by correlation with the calculated values, hence the scale of the contour map may not be quite correct owing to a possible difference of temperature coefficient between coronene and anthracene. The positions of the atoms, however, are in no way affected by this. The final calculated values of the structure factors are collected in Table X under 'F, calc.'. The mean discrepancy between the calculated and observed values, expressed as the sum of all the discrepancies divided by the sum of all the measured structure factors, is 14.0% for the (h0l) zone and 13.1% for all the reflections.

TABLE X

Measured and calculated values of the structure factor for coronene.

hkl	sinθ(λ=1.54)	F, meas.	F, calc.
200	0.103	65	+65
400	0.205	30	-31
600	0.307	7	+7
800	0.409	<2	0
10,00	0.512	5	+5
12,00	0.614	5	-6
14,00	0.716	6	+5
16,00	0.818	17	+18
18,00	0.921	<2	+2
020	0.328	16	+19
040	0.656	<8	0
001	0.082	60	+60
002	0.163	29	-31
003	0.245	8	+10
004	0.326	2	-2
005	0.408	8	+8
006	0.489	8	-9
007	0.571	7	+8
008	0.652	13	+13
009	0.734	6	-6
00,10	0.815	4	+3
00,11	0.897	2	-1
00,12	0.978	6	-5
14,01	0.747	<2	-4
12,01	0.646	5	+3
10,01	0.545	7	+9
801	0.444	10	-10
601	0.344	6	-4
401	0.244	23	+19
201	0.152	32	-28
$20\bar{1}$	0.106	58	+55
$40\bar{1}$	0.191	30	-27
$60\bar{1}$	0.288	13	+8
$80\bar{1}$	0.389	<2	0
$10,0\bar{1}$	0.487	<2	+3
$12,0\bar{1}$	0.588	<2	-1
$14,0\bar{1}$	0.688	<2	-2
$16,0\bar{1}$	0.790	23	+24
$18,0\bar{1}$	0.890	13	+17
18,02	0.988	<1	+1
16,02	0.887	<2	+2
14,02	0.788	<2	+2
12,02	0.687	<2	0
10,02	0.588	6	+6
802	0.489	17	-19
602	0.395	48	-48

hkl	sinθ(λ=1.54)	F, meas.	F, calc.
402	0.304	4	0
202	0.219	12	+9
$20\bar{2}$	0.158	28	-27
$40\bar{2}$	0.211	24	-27
$60\bar{2}$	0.290	21	+17
$80\bar{2}$	0.382	8	-3
$10,0\bar{2}$	0.476	21	-21
$12,0\bar{2}$	0.574	5	+6
$14,0\bar{2}$	0.672	3	-1
$16,0\bar{2}$	0.772	<2	-3
$18,0\bar{2}$	0.872	6	+4
$20,0\bar{2}$	0.973	<1	+1
16,03	0.928	<2	0
14,03	0.831	<1	+1
12,03	0.733	<2	0
10,03	0.637	<2	+1
803	0.545	<2	-2
603	0.454	18	-17
403	0.370	16	-18
203	0.296	2	+1
$20\bar{3}$	0.229	27	+24
$40\bar{3}$	0.258	14	+14
$60\bar{3}$	0.317	5	+7
$80\bar{3}$	0.395	9	-7
$10,0\bar{3}$	0.481	39	-39
$12,0\bar{3}$	0.571	14	-17
$14,0\bar{3}$	0.667	4	+4
$16,0\bar{3}$	0.763	<2	+2
$18,0\bar{3}$	0.860	<2	+2
16,04	0.979	<1	0
14,04	0.884	6	-8
12,04	0.788	10	-12
10,04	0.695	2	-3
804	0.609	<2	2
604	0.520	6	+8
404	0.442	10	+12
204	0.375	5	+5
$20\bar{4}$	0.306	18	-16
$40\bar{4}$	0.317	16	-12
$60\bar{4}$	0.359	3	-2
$80\bar{4}$	0.422	<2	0
$10,0\bar{4}$	0.499	3	-4
$12,0\bar{4}$	0.581	5	-5
$14,0\bar{4}$	0.671	2	-1
$16,0\bar{4}$	0.764	<2	+1
$18,0\bar{4}$	0.858	2	+3
$20,0\bar{4}$	0.955	<1	+3
14,05	0.938	<2	+1
12,05	0.848	8	-9
10,05	0.759	<2	0

hkl	sinθ(λ=1.54)	F, meas.	F, calc.
805	0.673	2	+4
605	0.590	6	-8
405	0.517	7	-7
205	0.454	5	-6
20$\bar{5}$	0.382	14	-12
40$\bar{5}$	0.386	55	-53
60$\bar{5}$	0.414	15	-18
80$\bar{5}$	0.463	6	+7
10,0$\bar{5}$	0.528	3	+4
12,0$\bar{5}$	0.603	3	+7
14,0$\bar{5}$	0.683	<2	+4
16,0$\bar{5}$	0.771	<2	-1
18,0$\bar{5}$	0.860	<2	-4
20,0$\bar{5}$	0.955	4	-6
12,06	0.908	<2	0
10,06	0.821	<2	+2
806	0.743	<2	+3
606	0.663	<2	-5
406	0.594	11	+10
206	0.532	5	+5
20$\bar{6}$	0.461	9	+12
40$\bar{6}$	0.457	11	-10
60$\bar{6}$	0.475	8	-10
80$\bar{6}$	0.514	7	+10
10,0$\bar{6}$	0.565	6	-6
12,0$\bar{6}$	0.631	6	-7
14,0$\bar{6}$	0.706	3	-6
16,0$\bar{6}$	0.763	<2	-1
18,0$\bar{6}$	0.870	<2	+2
20,0$\bar{6}$	0.961	6	-8
12,07	0.973	<1	-1
10,07	0.892	<2	0
807	0.813	<2	+1
607	0.739	6	-7
407	0.673	20	+19
207	0.615	46	+51
20$\bar{7}$	0.545	6	-8
40$\bar{7}$	0.535	6	+6
60$\bar{7}$	0.543	<2	0
80$\bar{7}$	0.572	6	+6
10,0$\bar{7}$	0.615	6	-6
12,0$\bar{7}$	0.672	7	+6
14,0$\bar{7}$	0.739	15	+15
16,0$\bar{7}$	0.810	<2	-2
18,0$\bar{7}$	0.890	2	0
10,08	0.965	2	-3
808	0.885	<2	+1
608	0.815	<2	+1
408	0.752	5	-4
208	0.696	16	+19

hkl	sinθ(λ=1.54)	F, meas.	F, calc.
20$\bar{8}$	0.624	2	-7
40$\bar{8}$	0.610	<2	+3
60$\bar{8}$	0.614	<2	-1
80$\bar{8}$	0.635	<2	+2
10,0$\bar{8}$	0.671	3	-3
12,0$\bar{8}$	0.717	6	+1
14,0$\bar{8}$	0.778	28	+29
16,0$\bar{8}$	0.844	12	+16
18,0$\bar{8}$	0.920	<2	-2
809	0.963	7	-8
609	0.893	<2	+2
409	0.828	<2	-1
209	0.779	7	-6
20$\bar{9}$	0.706	4	-6
40$\bar{9}$	0.740	3	+5
60$\bar{9}$	0.689	3	-3
80$\bar{9}$	0.703	5	-7
10,0$\bar{9}$	0.731	2	+5
12,0$\bar{9}$	0.773	<2	-3
14,0$\bar{9}$	0.827	5	+1
16,0$\bar{9}$	0.887	4	+7
18,0$\bar{9}$	0.951	3	-2
60,10	0.970	5	-4
40,10	0.909	<2	+1
20,10	0.859	2	+1
20,$\bar{1}$0	0.788	2	0
40,$\bar{1}$0	0.770	2	+3
60,$\bar{1}$0	0.764	6	-3
80,$\bar{1}$0	0.774	15	-16
10,0,$\bar{1}$0	0.796	4	-4
12,0,$\bar{1}$0	0.830	<2	+3
14,0,$\bar{1}$0	0.873	3	-3
16,0,10	0.926	2	-3
40,11	0.849	<2	+1
20,11	0.939	2	-1
20,$\bar{1}$1	0.869	<2	0
40,$\bar{1}$1	0.849	<2	0
60,$\bar{1}$1	0.844	<2	0
80,$\bar{1}$1	0.848	3	-4
10,0,$\bar{1}$1	0.865	3	-4
12,0,$\bar{1}$1	0.894	<2	+1
14,0,$\bar{1}$1	0.929	<2	+1
20,$\bar{1}$2	0.949	10	-10
40,$\bar{1}$2	0.928	3	-4
60,$\bar{1}$2	0.920	<2	+1
80,$\bar{1}$2	0.913	2	+2
10,0,$\bar{1}$2	0.934	2	+3
110	0.172	10	+9
210	0.193	57	-56
310	0.225	56	+53

hkl	sinθ(λ=1.54)	F, meas.	F, calc.
410	0.262	19	-16
510	0.304	<5	-3
610	0.348	8	+7
710	0.395	< 6	+3
810	0.441	<7	-4
910	0.489	<7	-1
10,10	0.536	<7	-3
11,10	0.586	<8	0
12,10	0.628	13	+15
13,10	0.685	20	+24
14,10	0.735	13	+14
15,10	0.790	<8	+7
120	0.332	<5	0
220	0.344	9	-10
320	0.363	5	+3
420	0.385	<6	-5
520	0.416	6	+7
620	0.449	5	0
720	0.486	<7	+2
820	0.525	7	-9
920	0.565	<7	+4
10,20	0.607	16	+17
11,20	0.651	14	+12
12,20	0.696	<9	+4
13,20	0.741	8	+7
14,20	0.794	8	-8
15,20	0.839	<7	0
130	0.495	15	-19
230	0.502	<6	+6
330	0.516	8	+10
430	0.546	<7	+1
14,30	0.876	<7	+5
15,30	0.910	7	-5
140	0.659	8	+8
240	0.665	9	-9
340	0.674	9	+10
440	0.687	8	-8

(2) Pyrene.

X-ray Measurements.

The measured values of the structure factors for the three main zones of pyrene were obtained from Prof. J.M. Robertson. The work had been carried out with copper k_α radiation ($\lambda = 1.54$) and small crystals employed, which rendered relative absorption corrections unnecessary. The intensity measurements had been made by means of the Robinson type of photometer(43) and put on an absolute scale by comparison with standard crystals by means of the two crystal moving-film spectrometer(48).

As the cameras used in this work had only permitted observations to be made up to about $2\sin\theta = 1.7$ the range was extended for the (h0l) zone by the present writer up to the limit of copper radiation. Long exposure moving-film photographs were taken, but very few additional reflections appeared, and these were estimated visually and correlated with the absolute measurements.

Trial Analysis of the Structure.

The space group $P2_1/a$ with four molecules in the unit cell implies that the asymmetric unit consists either of one complete molecule, or two halves of separate, crystallographically independent molecules, as was found in stilbene(49). As the normal chemical formula suggests a centro-symmetrical molecule, either of these possibilities may occur, but it should be noted that the two structures are radically different, and it is hardly conceivable that both could give even qualitative agreement with the experimental data. The asymmetric unit was considered first as being one complete molecule and this was found to be the correct solution.

The length of the b axis is 9.24A., very nearly twice that of coronene. Both structures belong to the same space group, but coronene has only two molecules per unit cell. It seemed a reasonable assumption, therefore, that in pyrene the molecular planes might have a similar tilt to the b axis (about 45°) but with two molecules instead of one accommodated in each b translation. These two molecules would be grouped about one crystallographic centre of symmetry.

Five degrees of freedom remain to be fixed, viz. two other orientation angles and the co-ordinates (x_p, y_p, z_p) of the molecular centre with regard to the centre of symmetry. The other orientation angles can be fixed by consideration of certain outstandingly strong reflections from small-spacing planes of the (h0l) zone. A diagram similar to Fig. 14 can be constructed for pyrene making use of the planes (007), (206), (403), $(80\bar{1})$, $(12,0\bar{6})$ and (12,01) and it is found that only one orientation of a regular, planar model will account for the enhancement of reflections from all these planes. The almost complete quarterings of the (h00) and (0k0) series of reflections fix the molecular centre at approximately $\frac{a}{8},\frac{b}{8}$ ($x = 1.70$A. $y = 1.16$A.) from the centre of symmetry. A small translation of about 0.5A. along the c axis is also necessary to account for the observed structure factors of the $(20\bar{1})$ and $(20\bar{2})$ reflections.

Trial calculations based on the observations outlined above led to excellent agreement between the calculated and observed values of the structure factors and refinement by Fourier series methods could be undertaken immediately.

Fourier Analysis.

The Fourier series were set up and the positions of the contour lines obtained as described above under coronene. For the projection on the (010) plane 50 terms were included, and the electron density was computed at 450 points on the asymmetric unit, the a axis being divided into 60 parts (intervals of 0.227A.) and the c axis into 30 parts (intervals of 0.279A.). For the projection along the c axis each axis was divided into 60 parts giving intervals of 0.154A. along b and 0.223A. along $a\sin\beta$. 36 terms were included in this series.

Orientation of the Molecule and Co-ordinates.

From a consideration of the lengths in projection of ON and parallel distances (Fig. 7(b)), which can be only slightly tilted, it was found that the best average radius of the hexagon was 1.41A. With this average radius and the assumptions that the axes L and M are at right angles the orientation can be calculated by the same procedure as given above in the coronene analysis.

In pyrene $\psi_M = 52.4^\circ$ from the mean value of NB, MC and PE which is 1.938 $\pm$0.030A. η_L is taken as the mean of the angles which BCP, AOP and NM make with a. These are 60.2°, 60.0° and 61.3°. The last is given only half the weight of the other two angles as the line is drawn through only two atoms, and the mean value is 60.34°. η_M is the mean of the angles which NB, MC and PE make with a and is observed as $-39.3^\circ \pm 0.4^\circ$.

From the calculated orientation of the molecule the actual bond lengths can be found by reducing each line for its calculated tilt. As only nine of the sixteen crystallographically independent

Facing p. 55.

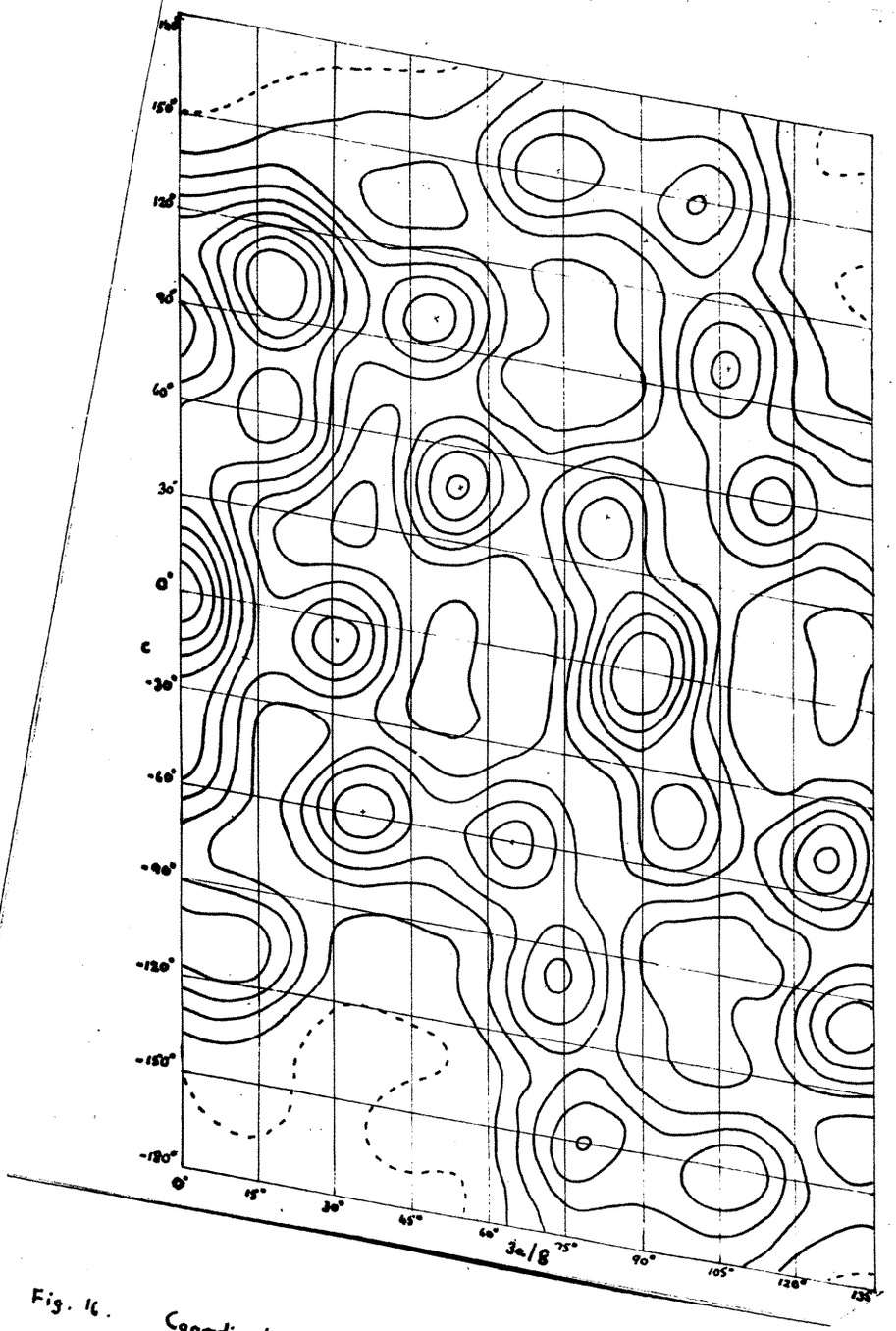

Fig. 16. Coordinates assigned to resolved atoms in pyrene.

atoms are resolved in Fig. 7, the co-ordinates of the others can only be deduced by assuming a molecular centre of symmetry. This assumption is confirmed by the shape of the contours in the map of Fig. 8 and also by consideration of the following bond distances which should be equal if the molecule is symmetrical about L and M.

AN = 1.40A.	AB = 1.38A.	Mean value,	1.39A.
NM = 1.43A.	BC = 1.42A.	"	"	1.42A.
MO = 1.38A.	CO = 1.42A.	"	"	1.39A.
PF = 1.38A.	CO = 1.42A.	"	"	1.39A.

The deviations from the mean values are not greater than 0.03A. and little significance can be attached to them. The mean values have therefore been adopted in constructing the model shown in Fig. 9. The finally adopted centres for the resolved atoms are plotted on the contour map in Fig. 16. Table V gives the finally accepted co-ordinates of all the atoms and includes the co-ordinates (x_p, y_p, z_p) of the centre of the molecule. This position can be accurately estimated from Fig. 7, and rather less precisely estimated from Fig. 8. In practice therefore y_p was found by calculation of the hk0 structure factors and confirmed from the c axis projection (Fig. 8).

From the final co-ordinates given in Table V the structure factors were recalculated and the results are given in Table XI under 'F, calc.'. The scattering curve deduced from the anthracene structure(47) was found rather unsuitable for pyrene as there was a very definite tendency for high order reflections to fall off more rapidly than in anthracene. A difference in temperature factor between the two compounds seems rather unlikely, but the effect may be due to some disorder in the structure. The following scattering curve was used for pyrene (max. f_c = 100).

$\sin\theta(\lambda = 1.54)$ =	0.1	0.2	0.3	0.4	0.5	0.6	0.7	0.8	0.9
f_c =	70	56	43	30	19	12.5	8.5	5	3.5

The average discrepancies between calculated and observed structure factors, expressed as for coronene (see above), are 14.3% for the (h0l) structure factors, 12.9% for the (hk0) structure factors, 8.8% for the (0kl) structure factors and 12.6% for all structure factors.

TABLE XI

Measured and calculated values of the structure factor for pyrene.

hkl	sinθ(λ=1.54)	F, meas.	F, calc.
200	0.115	7.5	+7
400	0.230	47	+46
600	0.345	<2	-4
800	0.460	3	-6
10,00	0.575	<3	-1
12,00	0.690	3	-1
14,00	0.805	4.5	+2
020	0.167	<1.5	+2
040	0.333	19	+23
060	0.500	<3	+1
080	0.667	3.5	+5
0,10,0	0.833	<3	0
001	0.094	65	+66
002	0.187	32.5	-31
003	0.281	5	+6
004	0.374	<2	-2
005	0.468	<2.5	-3
006	0.561	9.5	+14
007	0.654	33	+33
008	0.748	4.5	+1
009	0.841	4	-4
011	0.125	13	+12
012	0.205	<5	-4
013	0.293	9	+9
014	0.383	10.5	-11
015	0.475	<8	+7
016	0.567	<9	-9
017	0.660	11	-13
018	0.752	<10	+1
021	0.191	< 5	-2
022	0.251	8.5	+7
023	0.326	26.5	-25
024	0.409	24	-14
025	0.496	<8	+7
026	0.585	<9	-3
027	0.675	<10	-1
031	0.267	<6	-1
032	0.312	11.5	+10
033	0.376	35	+30
034	0.450	12	-12
035	0.530	<9	0
036	0.614	<10	+4
037	0.701	<10	+2
041	0.346	9	+14
042	0.382	13.5	-15
043	0.436	6.5	-6

hkl	sinθ(λ=1.54)	F, meas.	F, calc.
044	0.501	<9	-3
045	0.574	<9	+2
046	0.652	<10	+2
047	0.734	<10	+4
051	0.427	10.5	-7
052	0.457	<8	-4
053	0.502	<9	+3
054	0.560	<9	-7
055	0.626	<10	+3
056	0.698	<10	+3
061	0.509	7.5	-5
062	0.534	<9	-3
063	0.574	<9	-5
071	0.591	9	+9
072	0.613	<10	+2
073	0.647	<10	+6
$20\bar{9}$	0.830	<3	-2
$20\bar{8}$	0.737	<3	-1
$20\bar{7}$	0.647	7	-7
$20\bar{6}$	0.552	<3	+5
$20\bar{5}$	0.462	2.5	-12
$20\bar{4}$	0.370	19.5	+21
$20\bar{3}$	0.285	15.5	+16
$20\bar{2}$	0.202	40.5	-35
$20\bar{1}$	0.135	48	+43
201	0.160	6.5	+6
202	0.235	18	-15
203	0.320	22	+25
204	0.409	7	+1
205	0.500	10.5	-12
206	0.591	21.5	+24
207	0.683	6.5	+6
208	0.775	<3	+1
209	0.868	<3	0
$40\bar{8}$	0.743	<3	+3
$40\bar{7}$	0.657	<3	+8
$40\bar{6}$	0.567	<3	+2
$40\bar{5}$	0.484	6.5	+4
$40\bar{4}$	0.403	<3	-2
$40\bar{3}$	0.330	3	-7
$40\bar{2}$	0.270	12.5	+19
$40\bar{1}$	0.233	38	+32
401	0.264	20.5	-16
402	0.320	27.5	+29
403	0.393	40.5	+40
404	0.472	<3	+1
405	0.555	<3	0
406	0.641	<3	+3

hkl	sinθ(λ=1.54)	F, meas.	F, calc.
407	0.729	<3	+3
408	0.820	<3	-2
60$\bar{8}$	0.767	<3	0
60$\bar{7}$	0.685	<3	+2
60$\bar{6}$	0.605	<3	+4
60$\bar{5}$	0.531	17	-14
60$\bar{4}$	0.461	17	-14
60$\bar{3}$	0.405	<3	-1
60$\bar{2}$	0.362	3.5	-5
60$\bar{1}$	0.342	9.5	-11
601	0.373	<2	-1
602	0.421	17.5	-13
603	0.482	9	-9
604	0.550	<3	+1
605	0.625	<3	-3
606	0.707	<3	-3
607	0.790	<3	-1
608	0.875	<3	+1
80$\bar{9}$	0.885	4	+4
80$\bar{8}$	0.806	5	+10
80$\bar{7}$	0.732	<3	+1
80$\bar{6}$	0.660	<3	+3
80$\bar{5}$	0.595	<3	+6
80$\bar{4}$	0.540	<3	+2
80$\bar{3}$	0.494	<3	+3
80$\bar{2}$	0.466	23.5	+20
80$\bar{1}$	0.455	35	+31
801	0.486	<3	+4
802	0.528	9	+12
803	0.580	5.5	+6
804	0.641	<3	0
805	0.710	<3	-2
806	0.785	<3	+2
10,0$\bar{6}$	0.730	<3	-1
10,0$\bar{5}$	0.675	3	+10
10,0$\bar{4}$	0.630	<3	-2
10,0$\bar{3}$	0.593	<3	-6
10,0$\bar{2}$	0.574	22	+17
10,0$\bar{1}$	0.569	<3	-2
10,01	0.600	<3	0
10,02	0.637	<3	+3
10,03	0.683	<3	-3
10,04	0.738	<3	0
10,05	0.802	5.5	+7
10,06	0.870	<3	-3
12,0$\bar{7}$	0.865	<3	-3
12,0$\bar{6}$	0.809	14	+14
12,0$\bar{5}$	0.764	10.5	+13

hkl	sinθ(λ=1.54)	F, meas.	F, calc.
12,0$\bar{4}$	0.725	<3	-2
12,0$\bar{3}$	0.698	<3	0
12,0$\bar{2}$	0.682	<3	0
12,0$\bar{1}$	0.682	<3	-2
12,01	0.715	27	+28
12,02	0.749	18	+16
12,03	0.792	<3	-4
12,04	0.840	<3	0
12,05	0.885	<2	0
14,0$\bar{7}$	0.944	<2	0
14,0$\bar{6}$	0.897	4.5	-4
14,0$\bar{5}$	0.856	4	-1
14,0$\bar{4}$	0.828	<3	-1
14,0$\bar{3}$	0.806	<3	-1
14,0$\bar{2}$	0.795	<3	+3
14,0$\bar{1}$	0.798	<3	-4
14,01	0.830	4	+3
14,02	0.861	<3	0
14,03	0.898	2.5	0
14,04	0.943	<2	-1
110	0.102	43	+46
120	0.176	42	+45
130	0.257	12.5	-21
140	0.338	14.5	-10
150	0.421	21.5	-22
160	0.503	15	-14
170	0.586	6	+6
180	0.669	<3	0
210	0.142	42	+43
220	0.203	83	-107
230	0.275	32.5	+33
240	0.353	2.	-3
250	0.432	17	-18
260	0.513	17	-18
270	0.594	3.5	-4
280	0.677	<3	0
310	0.192	26.5	-22
320	0.240	35.5	+32
330	0.304	22	+23
340	0.375	17.5	+13
350	0.451	6.5	-6
360	0.529	2.5	-4
370	0.608	<3	-3
380	0.689	<3	0
410	0.245	11	-10
420	0.284	<3	+5

hkl	sinθ(λ=1.54)	F, meas.	F, calc.
430	0.340	20	+20
440	0.405	30.5	+30
450	0.476	9	+7
460	0.551	<3	-1
470	0.627	<3	-2
480	0.705	<3	+2
510	0.300	10	-11
520	0.333	7.5	-6
530	0.381	<3	+1
540	0.440	10.5	+8
550	0.506	<3	0
560	0.577	3	-4
570	0.650	<3	+3
610	0.355	10	-11
620	0.383	15	-14
630	0.426	<3	+3
640	0.480	<3	-1
650	0.541	5	-5
660	0.607	<3	+3
710	0.411	<3	+4
720	0.436	<3	+4
730	0.474	<3	+4
740	0.523	<3	-1
750	0.580	<3	+2
760	0.642	<4	-7
770	0.709	<3	-4
780	0.	<3	-2
810	0.468	<3	-2
820	0.490	<3	+1
830	0.524	<3	+2
840	0.568	<3	-4
850	0.621	<3	+1
860	0.679	<3	-1
910	0.524	<3	-3
920	0.544	<3	-1
930	0.575	<3	-1
940	0.616	<3	-4
950	0.665	<3	0
10,10	0.581	<3	+1
10,20	0.599	3	+6
10,30	0.627	<3	-1
10,40	0.665	<3	-1
11,10	0.638	<3	0
11,20	0.654	<3	+4
11,30	0.680	<3	+3

(3) Dibenzanthracene.

Measurement of Crystal Data.

The cell constants and space group are those published by Iball(37). The absolute values of F were obtained from Prof. J.M. Robertson. They had been measured photometrically and put on an absolute scale by ionisation spectrometer measurements. As in the case of pyrene, the present writer extended the range of observations to the limits of copper radiation for the most important zone (Okl), but in this case only one additional reflection, the 0,13,2, appeared and this was estimated visually by comparison with the other reflections.

Structure Analysis.

The space group Pcab with only four molecules in the unit cell involves a molecular centre of symmetry coinciding with the crystallographic centre of symmetry. The asymmetric unit, therefore, consists of one half of the molecule, or eleven carbon atoms neglecting hydrogen atoms. As a first approximation a regular planar structure can be assumed, in accordance with the usual chemical formula.

The magnetic measurements of Krishnan and Banerjee(38) give the tilt of the molecular plane to the (011) plane as 29°, while these authors predict that the long axis of the molecule (L in Fig. 11(b)) is lying along the c axis of the crystal. The first of these measurements is probably fairly accurate, but the second can be only an approximation.

Bearing these factors in mind, only one degree of freedom remains to be fixed, the angle which L makes in projection with

one of the crystallographic axes b or c. A projection of a regular planar model tilted at about 30° to a about the L axis can be pivoted at the centre of symmetry and swung round the bc plane until the best position is found. In practice the (020) plane was used as an indicator as its reflection is comparatively weak and extremely sensitive. When the molecule is placed with L coinciding with c the calculated value of the (020) structure factor is much too large, but it can be reduced to the correct positive value by a rotation of the molecule of about 16°. A further fairly small rotation would make this reflection negative, but this possibility was ruled out on consideration of the other (0kl) structure factors. Detailed calculations on this basis gave such good agreement between the measured and calculated values of the structure factors that it was possible to proceed immediately to refinement by double Fourier series methods.

Fourier Analysis.

The Fourier series were set up, the summations carried out and the positions of the contour lines found as described above for the coronene structure. The electron density was computed at 450 points on the asymmetric unit. Both the b and the c axes were divided into 60 parts giving intervals of 0.190Å. along b and 0.252Å. along c. In the first Fourier series 50 terms were included and the refinement was sufficient to fix the signs of the remaining observed reflections of the (0kl) zone. The second Fourier series included 56 terms.

The resulting contour map is shown in Fig. 11(a), the whole unit cell being included. A further Fourier analysis was then

carried out on the calculated values of the structure factors and the final co-ordinates arrived at by adding the small resulting changes in atomic positions to those obtained from Fig. 11, but with the opposite sign.

Orientation of the Molecule and Co-ordinates.

From an inspection of the observed distances in projection of ED and parallel lines, which can be only slightly tilted, it was found that the best average radius of the hexagons is 1.42A. With this average value and the assumptions that L and M are at right angles in the molecule and that the molecule itself is planar, it was possible to calculate the orientation of the molecule with regard to the crystallographic axes. The calculation was carried out by means of the nine relations given above for coronene. χ, ψ, ω and β have the same meanings as before, but in the case of dibenzanthracene η_L, η_M are the angles which L and M make with the c axis. χ_M is found to be 58.8° by averaging the distances FG', EH' and BK' (2.102 $\pm$.040A.) and taking the mean length of these distances in the molecule as 2.46A. η_L was taken as $-16.1^\circ \pm 0.6^\circ$, the mean of the angles made with c by the three lines through A, D, E and the origin; B and F; and K'J' and G'. η_M is $72.6^\circ \pm 0.3^\circ$, found by taking the mean value of the angles made with c by BK', EH' and FG'. The result of the calculation is given in Table VII.

When a regular hexagonal model of dibenzanthracene is placed in this orientation the discrepancy between calculated and observed values of the structure factors is 16.1% for the (0kl) zone. When the observed centres of the atoms are taken (from Fig. 11) this decreases to 15.0% and after correction for the incompleteness of

Facing p. 65.

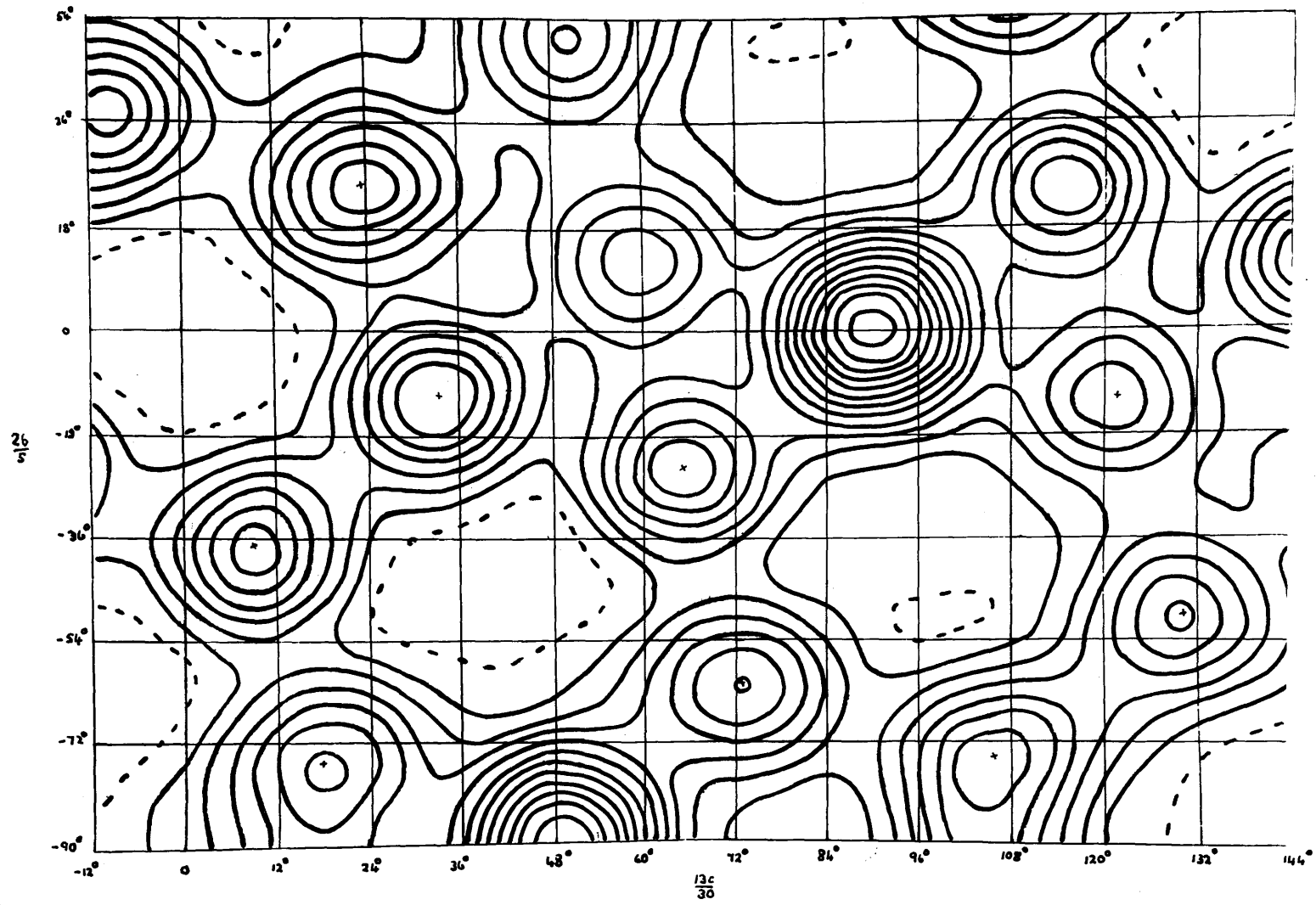

Fig. 17. Coordinates assigned to resolved atoms in dibenzanthracene.

the Fourier series (the small changes made after the Fourier on the calculated structure factors) there is a further improvement to 13.8% for this zone. Hence these final co-ordinates were adopted as most probable and are collected in Table VIII under $\underline{y}_2$, $\underline{z}_2$. The co-ordinates actually estimated from the second Fourier are listed under $\underline{x}_1$, $\underline{y}_1$ in Table VIII. Throughout, the co-ordinates of C and I, which cannot be measured, directly, have been taken as the positions which these atoms would occupy in a regular model in the above orientation, and this is in accordance with the shapes of the double peaks in Fig. 11(a). The finally adopted centres for the resolved atoms are plotted on the contour map of Fig. 17.

The molecular co-ordinates of Table IX were obtained by combining the final y and z co-ordinates of Table VIII with the orientation angles given in Table VII. The bond distances shown in Fig. 13 were calculated directly from these molecular co-ordinates.

In calculating the structure factors from the final co-ordinates the usual hydrocarbon scattering curve(47) was again found rather unsuitable. There was a distinct falling off of the intensities of reflections from the small-spacing planes, while on the other hand the small angle reflections were in general higher than their calculated values. In order to retain the upper part of the usual scattering curve all the absolute F's were multiplied by a scale correction factor of 0.84 and an empirical scattering curve was drawn for the range $\sin\theta = 0.5$-0.9.

The values used for this range are given below (max. $f_c = 100$)

$\sin\theta$ (λ=1.54)	=	0.5	0.6	0.7	0.8	0.9
f_c	=	23.5	15.0	9.5	7.0	4.5

and the calculated structure factors collected in Table XII under "F, cale". The general agreements between the calculated and observed values are very good. The mean discrepancies (expressed as for the previous structures) are 13.8% for the (0hl) zone, 12.0% for the (0k0) zone and 13.2% for the (h0l) zone. For all reflections the mean discrepancy is 12.6%.

TABLE XII

Measured and calculated values of the structure factors for dibenzanthracene.

hkl	sinθ(λ=1.54)	F, meas.	F, calc.
002	0.102	50	-49
004	0.203	13	-14
006	0.303	10	+16
008	0.407	30	-27
00,10	0.508	16	-19
00,12	0.610	<5	-6
00,14	0.711	<5	+3
00,16	0.812	<4	+2
00,18	0.916	<3	-3
020	0.135	24	+34
040	0.270	55	+50
060	0.406	10	-7
080	0.541	15	-6
010,0	0.676	<5	0
012,0	0.810	<4	-1
014,0	0.946	<3	+2
200	0.188	153	+170
400	0.375	7	-5
600	0.562	<5	-3
800	0.749	5	-8
012	0.122	28	+35
022	0.169	4	-2
032	0.227	43	-36
042	0.289	40	-38
056	0.354	37	+30
062	0.419	45	-43
072	0.484	<4	-7
082	0.551	<4	-1
092	0.617	<5	-2
010,2	0.684	<5	+2
011,2	0.750	<5	-3
012,2	0.817	5	-5
013,2	0.883	6	+6
014,2	0.952	<3	-3
014	0.214	26	+22
024	0.244	4	+5
034	0.287	34	-29
044	0.338	4	-5
054	0.394	6	+4
064	0.454	7	+13
074	0.515	4	+4
084	0.578	<4	-5
094	0.642	11	+11
010,4	0.707	24	+23
011,4	0.772	26	+23

hkl	sinθ(λ=1.54)	F, meas.	F, calc.
012,4	0.835	<4	+3
013,4	0.901	<4	-2
014,4	0.968	<2	+2
016	0.311	19	+23
026	0.333	35	-27
036	0.366	36	+33
046	0.407	29	-28
056	0.456	40	-40
066	0.508	19	-19
076	0.563	5	+6
086	0.621	<5	-2
096	0.681	6	-4
010,6	0.740	4	-7
011,6	0.795	<5	+2
012,6	0.867	<4	-1
013,6	0.930	<3	-1
014,6	0.994	<2	-2
018	0.410	20	+21
028	0.427	<3	+2
038	0.454	21	-25
048	0.488	7	+4
058	0.529	5	+8
068	0.574	8	+12
078	0.624	28	-27
088	0.677	34	+31
098	0.731	13	-14
010,8	0.789	<5	0
011,8	0.848	<4	0
012,8	0.906	<3	-3
013,8	0.968	<2	-2
01,10	0.510	8	+7
02,10	0.524	7	-6
03,10	0.545	<4	+2
04,10	0.573	6	-11
05,10	0.608	<5	+8
06,10	0.648	<5	+5
07,10	0.693	6	-6
08,10	0.740	9	-11
09,10	0.793	<5	0
0,10,10	0.847	<4	+1
0,11,10	0.901	<4	0
0,12,10	0.957	<3	-2
01,12	0.611	8	+7
02,12	0.623	31	+42
03,12	0.641	27	+32
04,12	0.665	9	+9
05,12	0.696	<5	+1
06,12	0.731	4	+3
07,12	0.772	<5	+4
08,12	0.815	<4	+2

hkl	sinθ(λ=1.54)	F, meas.	F, calc.
09,12	0.861	<4	-1
0,10,12	0.910	<3	-2
0,11,12	0.962	<3	-1
01,14	0.712	<5	-2
02,14	0.721	13	-14
03,14	0.738	8	+8
04,14	0.760	<5	-3
05,14	0.787	<5	0
06,14	0.818	<4	-1
07,14	0.854	<4	-4
201	0.194	52	+54
202	0.212	50	-41
203	0.240	9	+11
204	0.275	10	-13
205	0.314	7	-5
206	0.356	<5	+5
207	0.400	41	+36
208	0.446	18	-12
209	0.492	<7	+3
20,10	0.539	<7	+5
20,11	0.587	30	+37
20,12	0.635	14	+14
20,13	0.684	13	-14
20,14	0.732	<8	+4
20,15	0.786	7	+5
401	0.378	17	-18
402	0.388	<6	+4
403	0.405	23	-20
404	0.426	36	-37
405	0.453	9	-12
406	0.482	7	+2
407	0.516	14	+10
408	0.551	<7	+8
409	0.590	15	-13
40,10	0.630	<8	+1
40,11	0.671	28	+29
40,12	0.714	15	+16
40,13	0.760	<8	+1
40,14	0.800	<8	-6
40,15	0.853	10	+6
601	0.565	12	-14
602	0.570	10	+10
603	0.582	9	+11
604	0.597	39	-31
605	0.616	8	-9
606	0.638	<8	+3
607	0.664	<8	-2
608	0.691	<8	+4
609	0.722	<8	+3
801	0.753	<8	0

hkl	sinθ(λ=1.54)	F, meas.	F, calc.
802	0.760	<8	2
803	0.766	16	+12
804	0.780	10	-5
120	0.165	71	-71
140	0.287	36	+34
160	0.417	17	-20
180	0.549	21	+19
1,10,0	0.682	<8	0
220	0.232	108	+108
240	0.330	10	-8
260	0.448	13	+15
280	0.574	13	-7
2,10,0	0.703	<9	-3
320	0.312	86	-76
340	0.389	16	+15
360	0.494	<7	-2
380	0.610	19	+15
3,10,0	0.733	16	+7
420	0.399	60	+60
440	0.463	10	-9
460	0.553	9	+5
480	0.659	<8	+2
4,10,0	0.773	15	-9
520	0.487	20	-19
540	0.541	<8	-12
560	0.620	16	+16
580	0.716	<9	0
5,10,0	0.823	11	+7
620	0.578	9	-10
640	0.624	14	+11
660	0.693	7	-7
680	0.780	<8	+4
720	0.670	<8	0
740	0.710	<9	-2

PART III. ERRORS IN ATOMIC CO-ORDINATES OBTAINED BY DOUBLE FOURIER SERIES METHODS.

In Fourier projection maps the centres assigned to atoms may not correspond to the true centres. Such errors can arise from: (1) inaccurate intensity measurements (including absorption errors if the crystal specimens are too large); (2) the incompleteness of the Fourier series, which can include only a limited number of terms; (3) errors arising from inaccurate assignment of the positions of contour lines. The third source of error can be almost eliminated if the intervals of subdivision of the cell are small enough and sections are carefully drawn as described in Part II, Experimental Section. The probable magnitude of all these errors is of obvious importance in connection with the variations in carbon-carbon bond distances found in the work on condensed-ring aromatic hydrocarbons described in Part II. Booth(40) has approached the problem theoretically. By a comparison of intensities of X-ray reflections measured in the investigation of Jeffrey(50) on dibenzyl, with the estimates previously made by Robertson(51) by a totally different method, he arrives at the value of ± 0.6 absolute unit as the probable average error in structure factors for this compound. A calculation of the probable maximum error in atomic position (ε) due to this factor alone, leads to the result $\varepsilon < 0.003$A. When an error proportional to the magnitude of the reflection considered was used the same result was obtained.

With regard to the effect of incompleteness of the series Booth has examined a simple case of two carbon atoms only in the

Facing p.72.

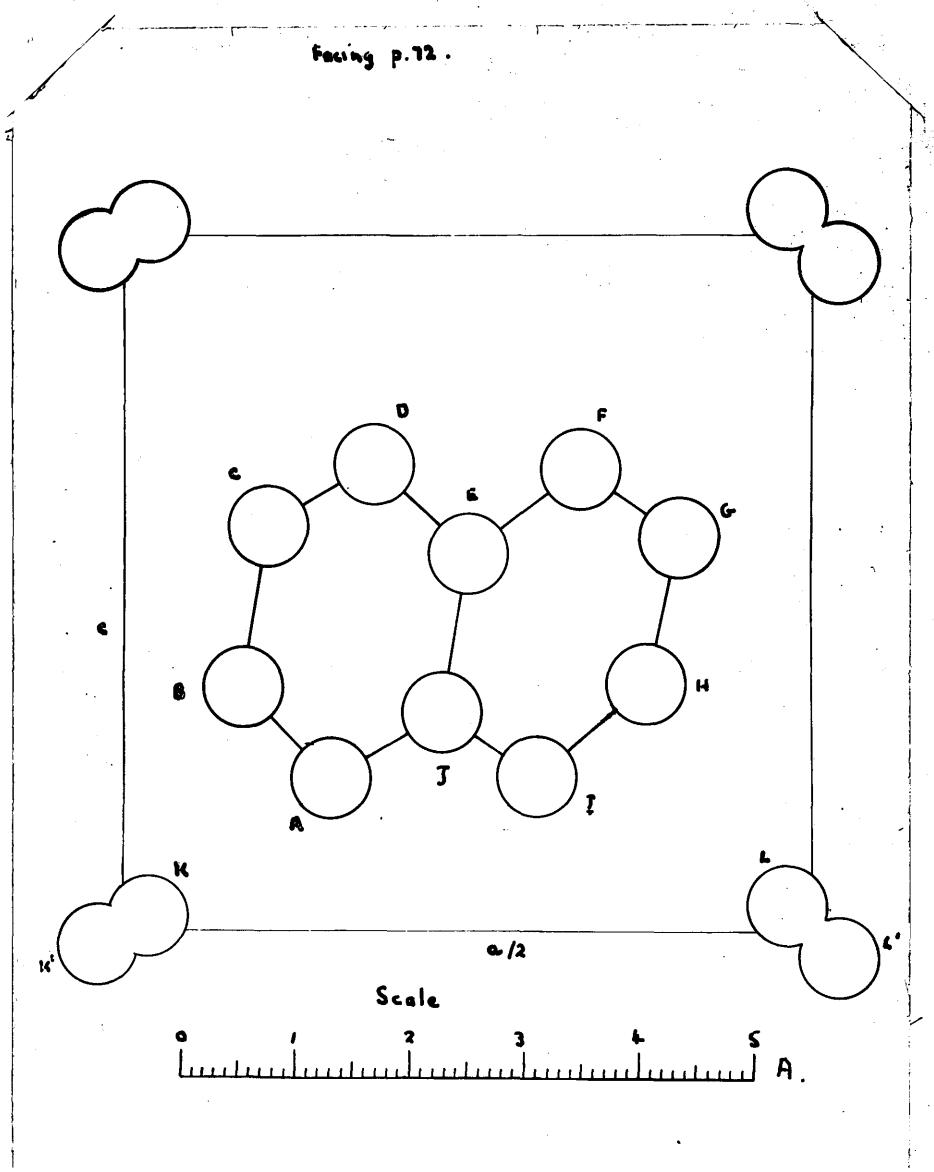

Fig. 18 (a)

Fig. 18.

(a) Hypothetical structure.
(b) 1st Fourier Analysis.
(c) 2nd Fourier Analysis.
(d) 3rd Fourier Analysis.
(e) 4th Fourier Analysis.

unit cell. The results obtained for ε are: < 0.019A. when the series is terminated at $2\sin\theta = 1.5$; < 0.009A. for $2\sin\theta < 1.8$; < 0.005A. for $2\sin\theta < 2.0$. The more complicated cases, however, where there are a large number of atoms in the unit cell, could not be rigorously investigated by the same methods.

In the present investigation a more empirical approach has been made, with the advantage that errors arising in structures of about the same complexity as the hydrocarbons described above can be assessed.

HYPOTHETICAL STRUCTURE.

A two dimensional structure shown in Fig. 18(a) was set up by Prof. J.M. Robertson, the atomic positions being unknown to the author until after the results of the first Fourier analysis were calculated. The lattice constants of this hypothetical structure are: $\underline{a} = 12.00$A., $c = 6.00$A., $\alpha = \beta = \gamma = 90^{\circ}$. Triclinic. Space group C_i^1 - $P\bar{1}$. 2 molecules per unit cell. The atomic co-ordinates given are listed in Table XIII under (x,z) and the bond distances connecting the atoms A-J in Table XIV under (L). The atoms K and L were placed very close to the corresponding inverted atoms in order to test resolution, but the other ten atoms alone were included in the accuracy calculations resulting from successive Fourier analyses.

TABLE XIII

Original Co-ordinates of atoms (x,z) and co-ordinates measures after 1st Fourier (x_1,z_1); 2nd Fourier (x_2,z_2) etc.

Atom (Fig.)	x(A)	x_1(A)	x_2(A)	x_3(A)	x_4(A)	z(A)	z_1(A)	z_2(A)	z_3(A)	z_4(A)
A	1.800	1.806	1.826	1.796	1.808	1.300	1.316	1.282	1.302	1.321
B	1.033	1.040	1.031	1.024	1.054	2.110	2.104	2.116	2.130	2.106
C	1.267	1.254	1.255	1.284	1.262	3.490	3.490	3.498	3.476	3.460
D	2.183	2.180	2.172	2.204	2.192	4.050	4.030	4.081	4.042	4.030
E	3.000	3.004	3.022	3.020	3.018	3.240	3.256	3.236	3.220	3.218
F	4.000	3.992	3.980	4.018	4.016	4.000	3.992	4.022	4.002	3.988
G	4.867	4.854	4.858	4.858	4.854	3.400	3.398	3.416	3.392	3.382
H	4.567	4.562	4.556	4.558	4.578	2.110	2.126	2.107	2.108	2.120
I	3.600	3.600	3.568	3.606	3.608	1.310	1.329	1.322	1.300	1.322
J	2.783	2.776	2.785	2.756	2.770	1.890	1.887	1.884	1.878	1.874
K	0.217					0.130				
L	5.783					0.220				

Facing p. 74.

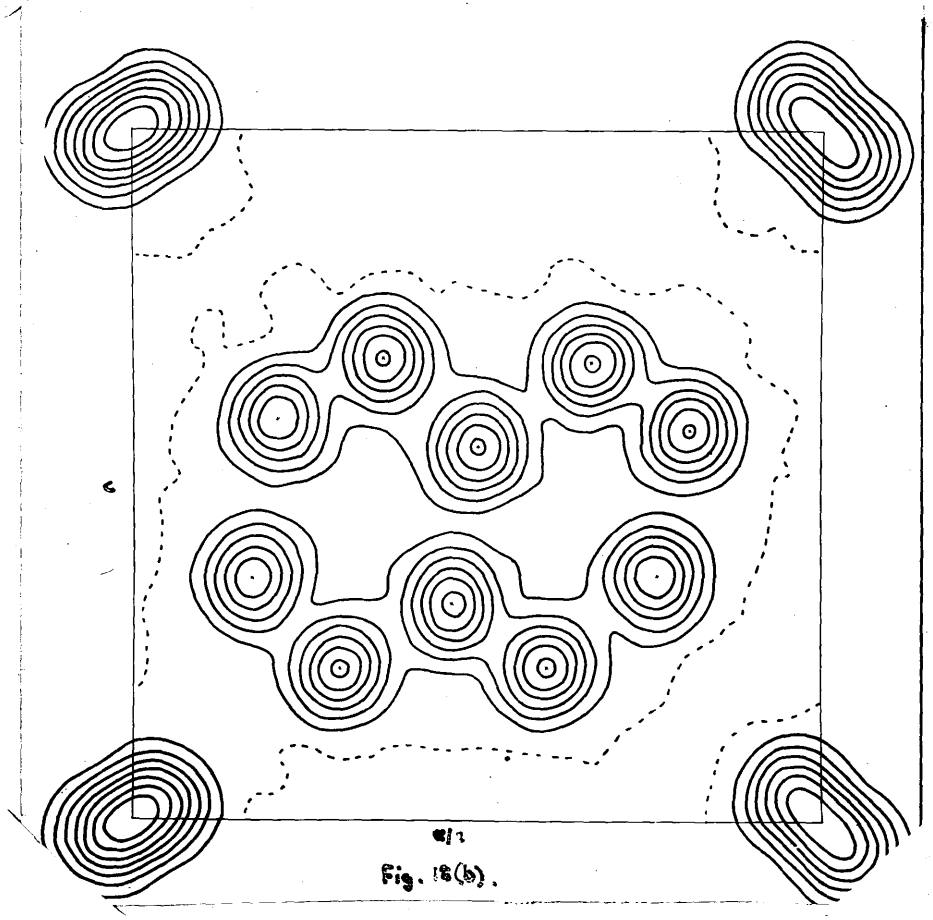

Fig. 18(b).

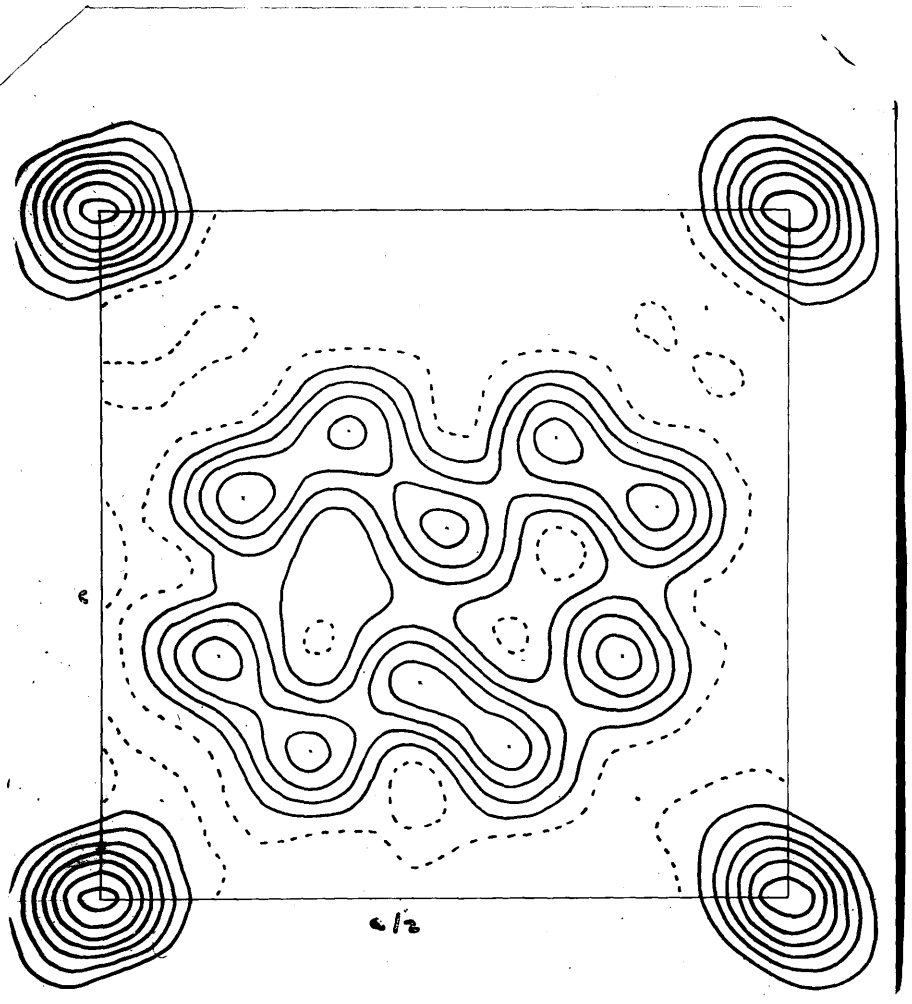

Fig. 18(c).

Scale as in Fig. 18(a).

The structure factors of all (hl) planes reflections from which would occur with copper radiation were calculated using the anthracene scattering curve(47). The first Fourier analysis was carried out using all these terms and the resulting contour map is shown in Fig. 18(b). The atomic positions assigned are indicated on the diagram and the measured co-ordinates are listed under (x_1, z_1) in Table XIII. The bond distances calculated from these co-ordinates are given under (L_1) in Table XIV.

A second Fourier analysis was then carried out on the same values of F, but the reflections for which $2\sin\theta > 1.5$ were omitted. Fig. 18(c) shows the result of this calculation and the measured co-ordinates are collected under (x_2, z_2) in Table XIII and the corresponding bond distances under (L_2) in Table XIV.

TABLE XIV

Bond distances in original structure (L) and as measured after 1st Fourier (L_1), 2nd Fourier (L_2) etc. Δ_1, Δ_2 etc. are the differences between L and L_1, L_1 and L_2 etc.

Bond	L(A)	L_1(A)	L_2(A)	L_3(A)	L_4(A)	Δ_1(A)	Δ_2(A)	Δ_3(A)	Δ_4(A)
AB	1.115	1.099	1.152	1.131	1.090	0.016	0.037	0.016	0.025
CD	1.074	1.072	1.087	1.080	1.090	0.002	0.013	0.006	0.016
EF	1.256	1.232	1.238	1.268	1.262	0.024	0.018	0.012	0.006
FG	1.053	1.046	1.066	1.038	1.034	0.007	0.013	0.015	0.019
HI	1.255	1.249	1.262	1.249	1.256	0.006	0.007	0.006	0.001
JA	1.146	1.126	1.132	1.119	1.111	0.020	0.014	0.027	0.035
BC	1.400	1.402	1.400	1.371	1.372	0.002	0.000	0.029	0.028
DE	1.150	1.130	1.199	1.159	1.160	0.020	0.049	0.009	0.010
EJ	1.368	1.388	1.373	1.367	1.367	0.020	0.005	0.001	0.001
GH	1.324	1.305	1.343	1.318	1.293	0.019	0.019	0.006	0.031
IJ	1.002	0.995	0.964	1.028	1.003	0.007	0.038	0.026	0.001
Mean:						0.013	0.019	0.014	0.016
Max.						0.024	0.049	0.029	0.035

Facing p. 76.

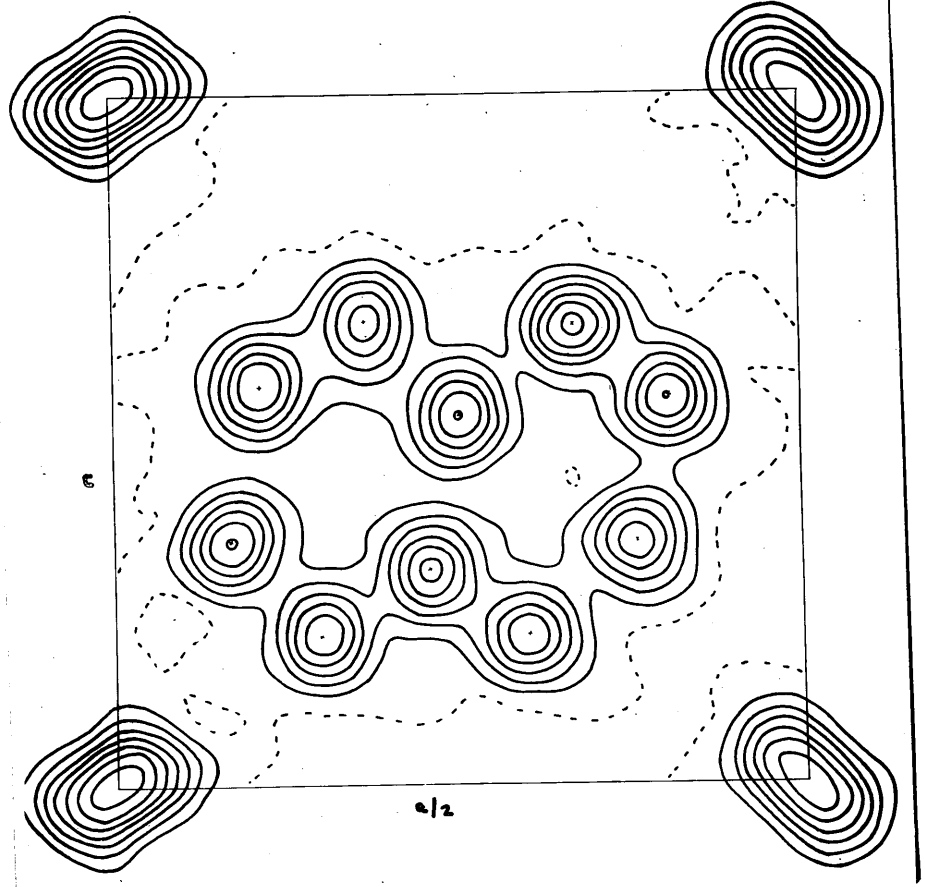

Fig 18(d)

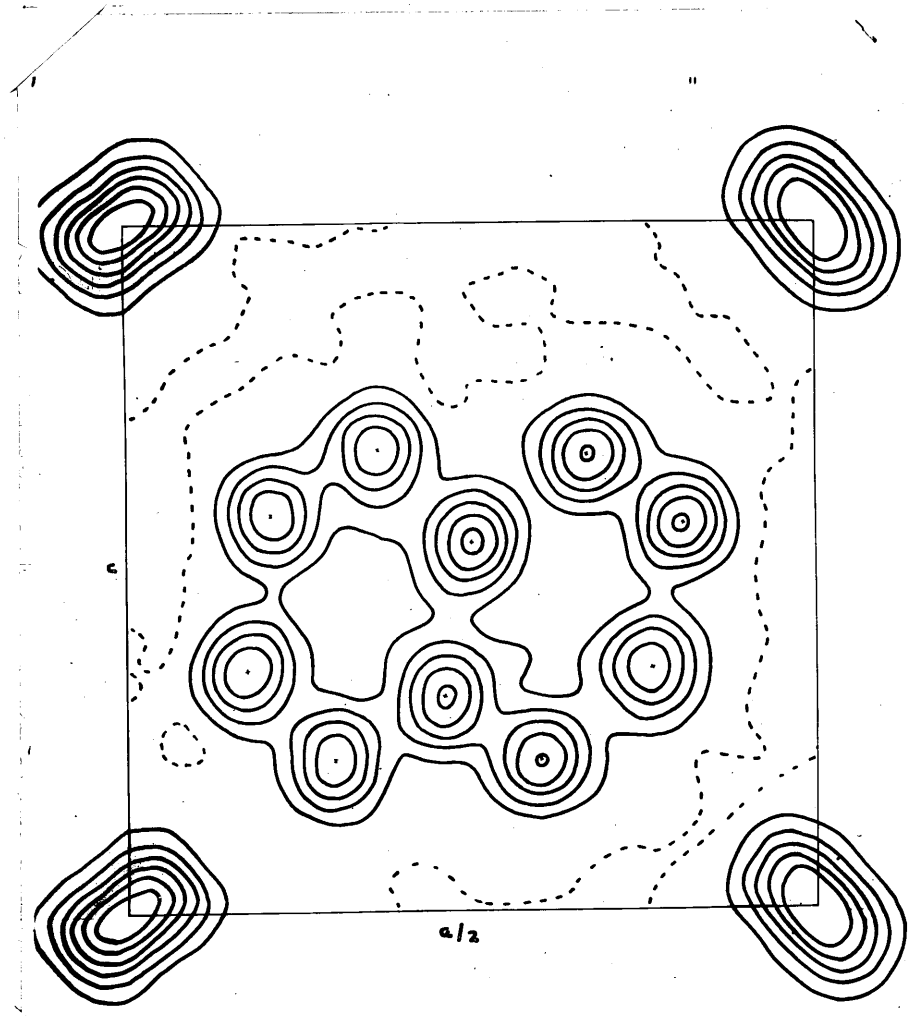

Fig 18(c)

Scale as in Fig 18(a).

Hitherto only errors due to incompleteness of the Fourier series had been considered. The additional effect of errors in intensity measurements was taken into account in the third Fourier analysis shown in Fig. 18(d). Rather large random errors were added to the absolute values of the structure factors, as described more fully in the Experimental Section. All terms which could be observed with copper radiation were included in the series with the exception of those less than 1.5 absolute units. The measured co-ordinates from this analysis are collected under (x_3, z_3) in Table XIII and the bond lengths deduced, in Table XIV under (L_3).

In the fourth analysis a rather different type of intensity error was taken into account. A crystal was assumed which had the rather extreme cross-section of 1.2 mm. x 0.25 mm. Graphical absorption corrections were made and applied in reverse to the absolute values of the structure factors. The same reflections omitted in the third Fourier were omitted in the fourth. The contour map is shown in Fig. 18(e), the atomic co-ordinates measured in Table XIII under (x_4, z_4), and the corresponding bond distances in Table XIV under (L_4).

Table XV shows the total shifts of the atoms from their initial positions as a result of each analysis. Δ_1 is the change from the given co-ordinates to those measured after the first Fourier analysis, Δ_2 the change from the given co-ordinates to those measured from the second Fourier map, and similarly with Δ_3 and Δ_4. A similar nomenclature is used for the changes in bond-lengths, collected in Table XIV. Here

$$\Delta_1 = |L_1 - L|; \quad \Delta_2 = |L_2 - L|; \quad \Delta_3 = |L_3 - L|; \quad \Delta_4 = |L_4 - L|.$$

The mean change and the maximum change in atomic positions and bond lengths are given in the last rows of Tables XV and XIV.

TABLE XV

Shifts of atoms from original position after 1st Fourier(Δ_1), 2nd Fourier(Δ_2), 3rd Fourier(Δ_3) and 4th Fourier(Δ_4).

Atom	Δ_1(A)	Δ_2(A)	Δ_3(A)	Δ_4(A)
A	0.017	0.032	0.004	0.022
B	0.009	0.006	0.022	0.021
C	0.013	0.014	0.022	0.030
D	0.020	0.033	0.022	0.022
E	0.016	0.022	0.028	0.028
F	0.011	0.030	0.018	0.020
G	0.013	0.021	0.012	0.022
H	0.017	0.012	0.009	0.015
I	0.019	0.034	0.012	0.014
J	0.008	0.006	0.029	0.020
Mean Shift:	0.014	0.021	0.018	0.021
Max. Shift:	0.019	0.034	0.029	0.030

CONCLUSIONS

As the anthracene scattering curve(47) was used for calculation of the structure factors, the results are only directly applicable to compounds with rather similar scattering curves. This, however, includes quite a large range of organic compounds, particularly among the aromatic hydrocarbons.

The main feature of the results outlined above is in accordance with the conclusions of Booth(40), viz., that convergence of the Fourier series is of much greater importance than extreme accuracy of intensity measurements. The results of the fourth Fourier, however, show that these errors do add on appreciably when due to unsuitable crystal sizes and shapes, and should be reduced as much as possible.

It would appear that the best determinations of structures by two dimensional Fourier methods should have errors slightly larger than those of the first Fourier analysis but less than those of the third. The mean discrepancy introduced into the structure factors for this third series was 10.3%, which is about 20% in terms of intensity measurements. In the case of small crystal specimens and with photometric, or really careful visual estimates of intensity, the average error in intensity estimation should be distinctly lower than this, hence from Table XIV the probable maximum error in bond length in careful work is <0.03A., but probably >0.02A. If the series is very incomplete these errors may be greater, as would be expected from the appearance of the Fourier map of Fig. 18(c).

An interesting result is obtained when the bond distances are averaged in two sets of six bonds. Ring 1 consists of AB, BC, CD, DE, EJ and JA; ring 2 of EF, FG, GH, HI, IJ and JE. The bond JE is common to both rings.

The results of these averages are collected in Table XVI. The average of the given lengths for these rings are listed under (Av.), the average of those measured from the first Fourier map under (Av_1) and similarly for the second, third and fourth Fouriers. The changes in these averages are given by Δ_1, Δ_2, Δ_3, Δ_4

where $\Delta_1 = |Av._1 - Av.|$; $\Delta_2 = |Av._2 - Av.|$; $\Delta_3 = |Av._3 - Av.|$

$\Delta_4 = |Av._4 - Av.|$

TABLE XVI

Averages of Bond Distances in groups of six.

Ring 1. includes AB, BC, CD, DE, EJ, JA
Ring 2. includes EF, FG, GH, HI, IJ, JE.
Av. = average of original distances.
$Av._1$, $Av._2$ etc. are averages of measured lengths after 1st, 2nd etc. Fouriers

$\Delta_1 = |Av._1 - Av.|$
$\Delta_2 = |Av._2 - Av.|$ etc.

	Av.(A)	$Av._1$(A)	$Av._2$(A)	$Av._3$(A)	$Av._4$(A)	Δ_1(A)	Δ_2(A)	Δ_3(A)	Δ_4(A)
Ring 1	1.209	1.203	1.224	1.205	1.199	0.006	0.015	0.004	0.010
Ring 2	1.210	1.203	1.208	1.211	1.203	0.007	0.002	0.001	0.007
All bonds	1.195	1.186	1.202	1.193	1.185	0.009	0.007	0.002	0.010

It will be seen that in no case except that given by the very incomplete second Fourier series do these errors of average bond

distances exceed 0.010A., and the small random errors in intensity estimation seem to have very little or no effect on the averages. Thus in a careful Fourier analysis, if we can average several independent bond lengths which there is reason to believe are equal, then this average value has a probable maximum error of <0.010A. even although the independent estimates of individual bonds may have errors of about 0.03A.

EXPERIMENTAL.

The Fourier series were set up according to the usual formula given in Part II, Section C. The a axis was divided into 60 parts and the c axis into 30 parts for all analyses, giving intervals of 0.200A. along both axes. The calculations were carried out by means of three figure strips(46). The terms included in the first Fourier are collected in Table XVII. Terms lying outside the line in this Table (with $2\sin\theta>1.5$) were omitted from the second series.

The random errors for the third Fourier series were arranged so that the mean discrepancy in F was 10.3%. The ratio of large to small errors was obtained by constructing a curve of frequency of error against range of magnitude of error. The data for this curve was taken from the comparison of certain estimates of intensities measured both on the Robinson photometer and the Dawton Scan Photometer as described in Part II and the scale of the curve then adjusted so as to give the above mean discrepancy in structure factors. The number of errors lying within different ranges of magnitude are shown below.

No. of errors introduced	Range of magnitude of error in structure factors
50	0.0 - 0.4 absolute units
37	0.4 - 0.8 " "
22	0.8 - 1.2 " "
10	1.2 - 1.6 " "
2	1.6 - 2.0 " "
0	>2.0 " "

The errors were drawn at random, equal numbers of positive and negative errors being introduced in each range with the exception of one extra plane which was given a positive error. All terms, the correct structure factors of which were <1.5 units were omitted from the third Fourier. The terms included in this analysis are collected in Table XVIII.

TABLE XVII

Terms included in 1st Fourier Series.
Values and signs of F(hl).

l \ h	0	1	2	3	4	5	6	7	8	9	10	11	12	13	14	15
7	-1.5	+1.6	+0.7	-1.9	+1.3	-	-1.6	+0.6	-	-	-	-	-	-	-	-
6	+3.4	-4.1	-0.7	-0.7	+1.2	+1.5	+3.2	-3.0	-2.1	-0.3	+0.6	-	-	-	-	-
5	+3.7	+3.2	+4.2	+3.6	-2.1	+0.6	+3.3	-5.1	+0.4	-1.8	+1.6	-0.8	-1.1	-	-	-
4	+0.7	-1.8	+0.6	-5.4	+9.3	-9.4	+1.4	+13.7	+3.7	-3.2	-1.7	-3.9	+0.7	-2.2	-	-
3	+17.5	+13.0	+6.9	+0.8	+0.7	+2.7	+0.4	-13.8	+3.1	+0.5	+4.5	+1.1	+0.2	+0.7	-0.7	-
2	-1.6	-13.2	+18.4	+1.4	+11.6	+6.7	+1.5	-6.7	+4.1	+1.5	-0.5	+0.4	+0.1	-5.7	+1.5	+1.2
1	-24.6	-9.8	+17.0	-1.2	+12.8	-6.2	+18.3	+8.3	-2.5	-4.1	+0.9	-2.3	+2.0	+2.9	-1.8	-2.0
1 0	144.0	+4.1	-9.2	-0.2	-3.4	-1.1	+0.1	-1.7	+5.4	-	+4.2	-0.7	+4.0	+2.7	-2.8	-1.4
$\bar{1}$	-24.6	+11.0	+22.8	-0.8	+20.3	+1.6	+14.2	+0.6	+0.9	+1.3	-2.0	+1.2	-6.8	-2.6	+8.0	+2.1
$\bar{2}$	-1.6	+8.4	+19.5	+0.8	+7.7	-2.6	-11.6	+6.3	+9.7	+0.2	+3.8	+0.5	+2.7	+0.6	-4.5	+0.8
$\bar{3}$	+17.5	-10.7	+3.5	+2.7	+0.4	+4.0	+8.5	-2.7	-2.6	+3.7	-0.4	+2.8	+2.5	-	-1.5	-
$\bar{4}$	+0.7	+2.7	-0.5	+3.8	+7.3	+9.1	+6.4	-4.4	-1.4	+1.6	-0.8	+0.3	-1.1	+3.0	-	-
$\bar{5}$	+3.7	-0.3	+4.9	-2.1	-2.3	-5.6	-1.5	+12.0	+1.7	-	+2.8	+0.3	-0.6	-	-	-
$\bar{6}$	+3.4	+4.9	-1.1	+3.1	+1.8	+2.0	+0.8	-2.3	+1.6	+1.3	-2.2	-	-	-	-	-
$\bar{7}$	-1.5	-0.9	+2.2	+1.1	+1.6	+3.2	-1.7	-0.3	-	-	-	-	-	-	-	-

TABLE XVIII

Terms included in 3rd Fourier Series.
Values and signs of F(hl).

l \ h	0	1	2	3	4	5	6	7	8	9	10	11	12	13	14	15
7	-	+1.4	-	-1.7	-	-	-1.0	-	-	-	-	-	-	-	-	-
6	+4.8	-5.1	-	-	-	-	+3.0	-3.2	-1.9	-	-	-	-	-	-	-
5	+3.5	+5.0	+4.4	+3.0	-1.5	-	+3.9	-4.5	-	-2.0	+1.0	-	-	-	-	-
4	-	-2.4	-	-5.6	+9.9	-8.4	-	+13.5	+2.7	-3.4	-1.9	-3.7	-	-1.2	-	-
3	+17.3	+14.0	+7.1	-	-	+2.9	-	-14.4	+3.7	-	+4.7	-	-	-	-	-
2	-1.4	-13.4	+19.0	-	+10.2	+7.3	-	-6.5	+5.5	-	-	-	-	-5.5	-	-
1	-26.0	-9.6	+15.6	-	+13.8	-5.6	+17.7	+8.9	-3.1	-2.3	-	-1.7	+2.6	+1.9	-1.2	-2.2
1 0	+144.0	+4.7	-8.6	-	-3.2	-	-	-2.7	+6.0	-	+4.8	-	+4.2	+1.7	-2.6	-
$\bar{1}$	-26.0	+12.0	+22.6	-	+19.7	+1.8	+14.4	-	-	-	-1.8	-	-7.0	-1.2	+7.0	+2.3
$\bar{2}$	-1.4	+9.4	+19.3	-	+7.1	-3.6	-12.6	+6.5	+8.7	-	+4.4	-	+2.9	-	-3.9	-
$\bar{3}$	+17.3	-9.7	+3.7	+2.9	-	+4.6	+7.9	-2.9	-2.8	+3.1	-	+1.8	+2.3	-	-	-
$\bar{4}$	-	+2.1	-	+3.6	+7.5	+9.7	+5.4	-3.0	-	+1.4	-	-	-	+2.0	-	-
$\bar{5}$	+3.5	-	+5.1	-3.1	-2.9	-5.4	-	+12.2	+1.5	-	+2.2	-	-	-	-	-
$\bar{6}$	+4.8	+4.7	-	+4.5	+2.4	+1.4	-	-2.9	+0.2	-	-3.2	-	-	-	-	-
$\bar{7}$	-	-	+3.6	-	+14.2	+4.2	-1.5	-	-	-	-	-	-	-	-	-

In the fourth Fourier series a crystal was assumed to have been used which had the cross-section presented to the X-ray beam of 1.2 mm. by 0.25 mm. For each reflection a mean path of the beam through the crystal (t) was drawn and measured and the absolute F values multiplied by $e^{-\mu t}$. μ was taken as 7.0 per cm., about the usual value in the hydrocarbon structures described above. The same planes which had been omitted in the third Fourier series were omitted from the fourth. The values and signs of the structure factors included in the fourth series are given in Table XIX.

TABLE XIX

Terms included in 4th Fourier series.
Values and signs of F(hl).

l \ h	0	1	2	3	4	5	6	7	8	9	10	11	12	13	14	15
7	-	+1.5	-	-1.7	-	-	-1.5	-	-	-	-	-	-	-	-	-
6	+3.0	-3.7	-	-	-	-	+2.8	-2.6	-1.8	-	-	-	-	-	-	-
5	+3.2	+2.8	+3.6	+3.1	-1.8	-	+2.7	-4.1	-	-1.5	+1.3	-	-	-	-	-
4	-	-1.5	-	-4.2	+7.2	-7.3	-	+10.6	+2.9	-2.5	-1.3	-3.0	-	-1.7	-	-
3	+14.2	+9.9	+5.2	-	-	+2.1	-	-11.0	+2.5	-	+3.5	-	-	-	-	-
2	-1.1	-9.7	+14.0	-	+9.9	+5.8	-	-5.8	+3.6	-	-	-	-	-4.4	-	-
1	-16.0	-7.9	+14.9	-	+11.5	-5.6	+16.4	+7.4	-2.2	-3.6	-	-2.0	+1.7	+2.4	-1.4	-1.4
0	+144.0	+3.7	-8.4	-	-3.1	-	-	-1.5	+4.9	-	+3.8	-	+3.5	+2.3	-2.3	-
$\bar{1}$	-16.0	+8.9	+19.9	-	+18.2	+1.4	+12.8	-	-	-	-1.8	-	-5.8	-2.2	+6.4	+1.5
$\bar{2}$	-1.1	+6.2	+14.8	-	+6.5	-2.2	-10.2	+5.5	+8.5	-	+3.3	-	+2.2	-	-3.4	-
$\bar{3}$	+14.2	-8.2	+2.7	+2.1	-	+3.1	+6.7	-2.1	-2.1	+2.9	-	+2.2	-11.9	-	-	-
$\bar{4}$	-	+2.3	-	+2.9	+5.2	+7.0	+4.9	-3.4	-	+1.2	-	-	-	-	-	+2.3
$\bar{5}$	+3.2	-	+14.2	-1.8	-1.9	-4.7	-	+9.8	+1.4	-	+2.3	-	-	-	-	-
$\bar{6}$	+3.0	+4.4	-	+2.7	+1.1	+1.8	-	-2.0	+1.4	-	-1.9	-	-	-	-	-
$\bar{7}$	-	-	+2.0	-	+1.5	+2.9	-1.5	-	-	-	-	-	-	-	-	-

PART IV. DISCUSSION.

CORONENE.

The extremely good resolution of all the atoms in the coronene projection (Fig. 1) indicates that the positions assigned to atomic centres should be as accurate as in the best measurements by similar methods. In conjunction with the results described in Part III, then, we should expect the maximum error in bond length to lie between 0.02A. and 0.03A.

In averaging the bonds into groups, however, this error will be reduced and it is noteworthy that the largest variation of a bond length from the group average is in the bond AB (Fig. 4) which is 0.02_5A. longer than the average, just about the maximum error which would be expected. In the results of Part III bond distances were averaged in groups of six, and the averages in the cases comparable to the present work had errors of less than 0.01A. Now in coronene there is one group of six independent bonds and three of three bonds. The average of the group of six bonds is thus probably not in error by more than 0.01A. In the other groups, however, the bond-distances are even more self-consistent than in the larger group, nowhere deviating from the group average by more than 0.01A. It would appear, therefore, that the finally adopted bond lengths are probably accurate to $\pm$0.01A. and the bonds BC, EF and HI (Fig. 4) are definitely shorter than the central bonds, the "spokes" and the other outer bonds. The differences between these last three groups, however, cannot be said to be outside the limits of experimental error.

Coulson(33) has recently carried out some very detailed calculations on coronene by the molecular orbital method and obtains

a value of 1.418Å. for the central bonds and 1.406 for the average of all bonds in the molecule, compared with the experimental values of 1.43Å. and 1.41_5Å., giving agreement to 0.012Å.

A simpler, though less rigorous treatment of the problem can be made in terms of the 20 stable valency bond structures for coronene. These can be divided into 5 groups as shown below (XIII-XVII) and the double bond character of a given bond computed by dividing the number of times which the bond occurs as a double bond by the total number of structures. The double bond character

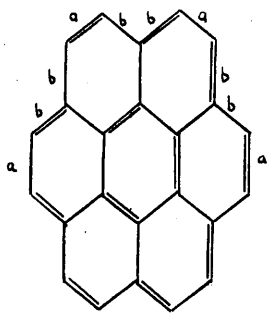

XIII
4 structures

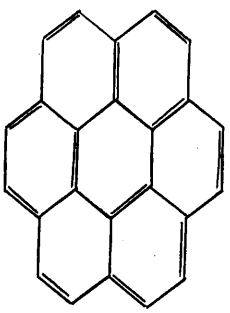

XIV
6 structures

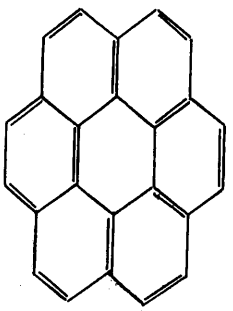

XV
6 structures

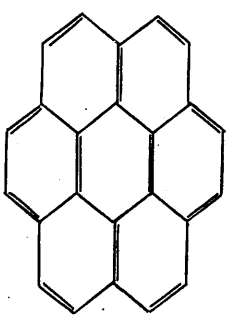

XVI
3 structures

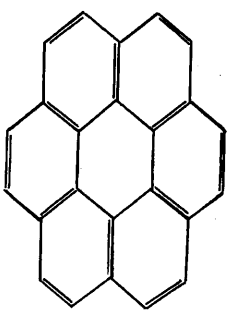

XVII
1 structure

of the outer bonds a (XIII) is 70%, for the other outer bonds b it is 30%, for the six "spokes" 40% and for the inner ring 30%. Thus the a bonds should be shorter than the benzene distance of 1.39A. while the experimental value is 1.38_5A. All the other bonds are both measured and calculated as being very close to the graphite distance of 1.42A., corresponding to 33% double bond character, but the "spokes" are calculated as being slightly shorter than the b bonds while the measured value is slightly longer.

PYRENE.

The finally adopted values for bond distances in pyrene show variations over a range of 0.06A. The bonds OP and the group CD, EF, JK and LM measure 1.45A. while AB, AN, OC, OM, PF, JP, GH, IH, DE and LK (see Fig. 9) are 1.39A. This range is slightly greater than found in coronene, but the accuracy cannot be considered as high in the case of pyrene because of the overlapping of molecules (Fig. 7.b). The result of this is that only nine of the sixteen crystallographically independent atoms are resolved.

In the case of the best resolved atoms we should not expect errors in bond lengths of greater than ±0.03A., but where the atoms are distorted by proximity to related atoms, e.g. the atoms A and B, the error may amount to ±0.04A. This is in agreement with the results described in Part II, Experimental Section, where individual bonds which would be equal if the pyrene molecule were symmetrical about the axes L and M, did not deviate from their mean value by more than ±0.03A.

All that can be stated definitely about the pyrene bond lengths,

then, is that the bonds OP and FE are certainly no shorter than the mean value of 1.41A. and are probably rather longer. These bonds lie between very well resolved atoms and measure 1.45A., hence even assuming the maximum probable error they can hardly be shorter than 1.42A.

A qualitative theoretical treatment of the problem can be made as for coronene. For a fixed position of the carbon atoms there are six ways of arranging the bonds and these six structures (XVIII-XXIII) are considered as making the most important contributions to the structure, and as having equal weight.

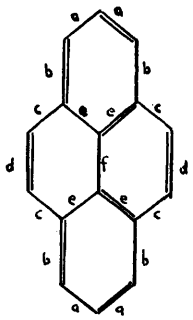

XVIII

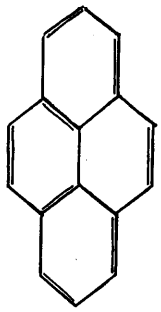

XIX

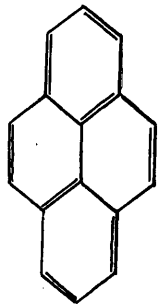

XX

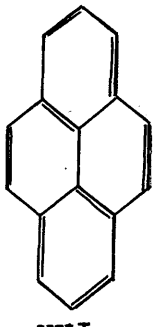

XXI

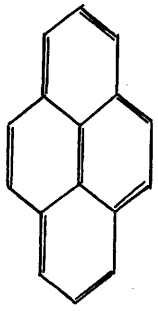

XXII

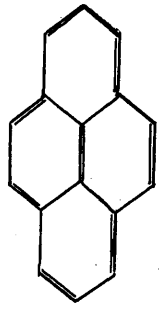

XXIII

The accuracy of these approximations is not easy to estimate but the calculation does give a large amount of agreement with the observed bond lengths. In Table XX the calculated percentage double bond character for each set of bonds is shown above the corresponding bond-distance obtained from the Pauling-Brockway curve(30).

TABLE XX

Bonds(see XVIII)	a	b	c	d	e	f	Average
Double Bond Character	50%	50%	17%	83%	33%	33%	42%
Bond Length calculated (Pauling-Brockway curve)	1.39A.	1.39A.	1.46A.	1.35A.	1.42A.	1.42A.	1.408A.
Bond Length calculated (Coulson)	1.39A.	1.41A.	1.43A.	1.38A.	1.43A.	1.43A.	1.412A.
Bond Length observed	1.39A.	1.42A.	1.45A.	1.39A.	1.39A.	1.45A.	1.412A.

The difference between the c and d bonds is in striking agreement with the measured values, but elsewhere in the molecule the agreement is not so good. The average bond length calculated is 1.408A. in excellent agreement with the observed value of 1.412A. Chemical evidence(52) from the reactivity of different positions in the pyrene molecule suggests that pyrene is best described by structures XVIII-XXI, and if these were given greater weight in the above calculation the length of the central bond would be increased in accordance with the observed data.

Coulson(52) has made some preliminary calculations on the pyrene

bond lengths by similar methods to those he applied to coronene, and his results are also shown in Table XX. These results are in very good agreement with the experimental measurements except for the e bonds, where there is a difference of 0.04Å. For these bonds, however, the experimental error might be of this order.

1.2:5.6 DIBENZANTHRACENE.

The bond lengths measured in dibenzanthracene, as shown in Fig. 13, vary over a range of 0.07Å., which is even larger than in the previous structures discussed. In this case, however, every bond in the asymmetric unit must be considered unique, and the error cannot be reduced by averaging, as was done in coronene, and to a much more limited extent, in pyrene.

The central ring is clearly resolved and the error here should not exceed ±0.03Å. and is probably not greater than 0.02Å. Hence the difference between EG^1 which is 1.44Å. and the other two independent bonds in this ring (1.40Å. and 1.38Å. respectively) is probably real, though this cannot be stated with certainty. Little can be said about the variations in the outer parts of the molecule. The only bonds which differ appreciably from the mean value are GH, JK and K^1A, and these exceptionally large values must be regarded as being rather dubious in view of the distortions caused to the atoms H and K by the nearness of the related atoms in the reflected molecule.

For comparison with the results obtained for coronene and pyrene the calculated percentage double-bond character for each is given below (XXXVI). The twelve stable valency bond structures are shown in XXIV-XXXV and the calculation has been carried out exactly as in the previous structures.

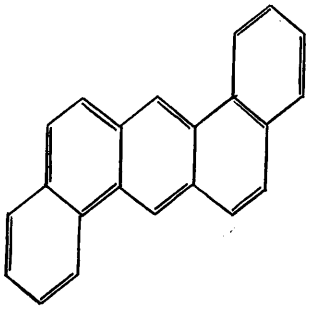

XXIV

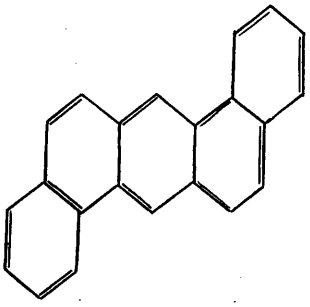

XXV

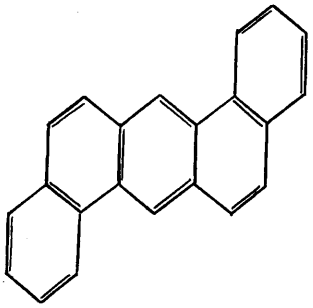

XXVI

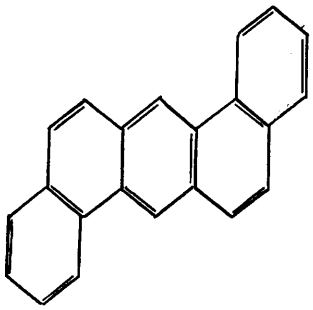

XXVII

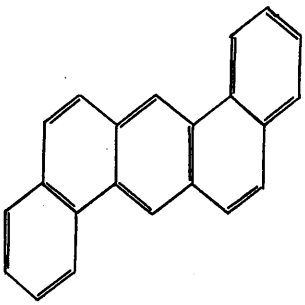

XXVIII

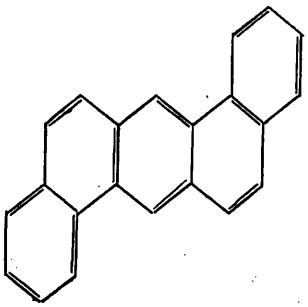

XXIX

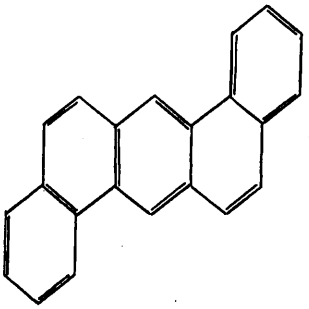

XXX

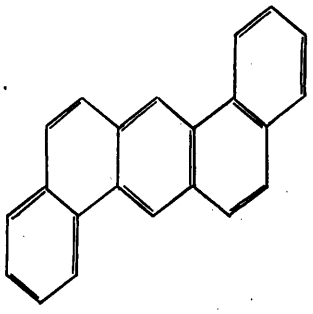

XXXI

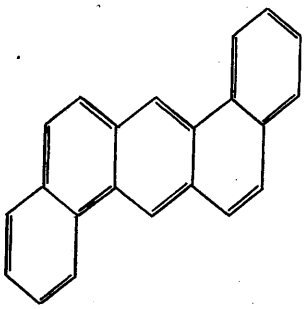

XXXII

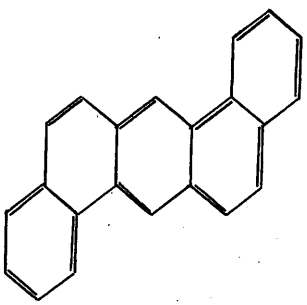

XXXIII

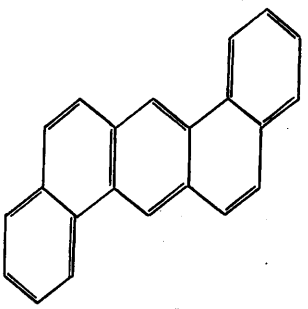

XXXIV

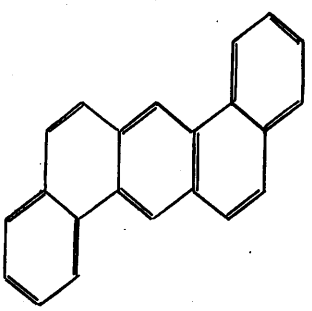

XXXV

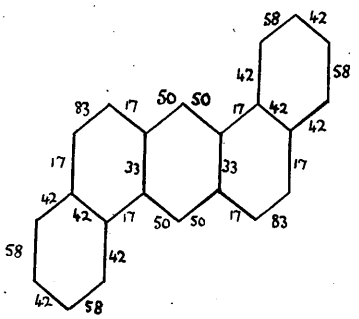

XXXVI

It will be seen that the central ring bears a striking qualitative resemblance to the observed results. EG^1 is calculated to be 1.42A. from the Pauling-Brockway curve(30) (33% double bond character) and measured as 1.44A. The predicted value for both EF and FG is 1.39A. while these bonds were observed to be 1.38A. and 1.40A. respectively. In the rest of the molecule, however, there is little agreement, the biggest discrepancy being for AK^1 (measured 1.44A., calculated 1.38A.) but as pointed out above, the position of K^1 is subject to considerable uncertainty and there may be a fairly large error in the measured value of AK^1.

While this lack of agreement in the outer parts of the molecule may be due partly to experimental error, it is worth noting that no really rigorous calculations have yet been made on a molecule of this shape. It may be that the excited structures play a significant part in this case, whereas in the more symmetrical coronene molecule qualitative agreement with the observed values was obtained even without taking them into account. Further discussion is hardly justified until the experimental data is established more certainly.

CONCLUSIONS.

The main features of the coronene structure can be considered to be definitely established. The shortening of the outermost bonds seems to be beyond experimental error and is in agreement with theoretical calculation.

In the case of pyrene, the two bond groups c and f (XVIII) seem rather definitely longer than the average, also in agreement with the calculated values, but all other variations observed lie within the

limits of possible experimental error, as do all the variations found in dibenzanthracene.

Coronene is the only one of these structures in which two dimensional Fourier methods give clear resolution of all the atoms, and to attain equal, or greater accuracy in the other structures three dimensional work will be required.

In general, the empirical calculations of bond length from the stable valency bond structures do seem to give a certain amount of agreement with observed bond distances, but it is not clear that this would be so in all polycyclic aromatic hydrocarbons. In any case, so far as can be checked, the quantum-mechanical calculations seem to give results rather more in accordance with the experimental data.

REFERENCES.

(1) Oxford: Clarendon Press (1903).

(2) Sitzb. Math. phys. Klasse Bayer. Akad. Wiss. München, p.303, 1912.

(3) Ibid. p.363, 1912.

(4) Proc. Camb. Phil. Soc., 17, 43, 1913.

(5) Nature, 90, 410, 1912.

(6) Proc. Roy. Soc., A, 89, 248, 1913.

(7) Phil. Mag., 27, 315, 1914.

(8) Ibid., 27, 675, 1914.

(9) Geometrische Kristallographie des Diskontinuums, Leipzig, 1919.

(10) The Analytical Expression of the Results of the Theory of Space Groups. Carnegie Institute of Washington, 1930.

(11) Proc. Roy. Soc., A, 88, 428, 1913.

(12) Ibid., A, 89, 246, 1913.

(13) Phil. Trans. Roy. Soc., 215, 253, 1915.

(14) Compton, A.H. and Allison, S.K., X-Rays in Theory and Experiment (1935). London: Macmillan and Co.

(15) Proc. Roy. Soc. A, 123, 537, 1929.

(16) Ibid., A, 140, 79, 1933.

(17) International Tables for the Determination of Crystal Structure (1935). London: Bell and Sons.

(18) Robertson and Woodward, J.C.S. p.36, 1940.

(19) Physical Rev., 1944, 65, 195.

(20) Tilden Lecture 1945, J.C.S. 249 (1945).

(21) Naturw. 9, 337, 1921.

(22) Z. Physik, 23 (1924), 229.

(23) M.J. Buerger, 'X-Ray Crystallography', John Wiley and Sons, New York, 1942.

REFERENCES (continued)

(24) Proc. Phys. Soc. 34, 33, 1921.

(25) R. Wierl, Ann. d. Phys., 8, 521, 1931.

(26) Proc. Roy. Soc. A., 142, 674, 1933.

(27) Ibid. A., 146, 140, 1934.

(28) Eyster, J. Chem. Phys., 6, 580, 1938.

(29) Bernal, Proc. Roy. Soc., 1924, A, 106, 749.

(30) J.A.C.S., 59, 1223, 1937.

(31) The Nature of the Chemical Bond, Cornell 1940, 142.

(32) Proc. Roy. Soc., A, 158, 306, 1937.

(33) Nature, 1944, 154, 797.

(34) Zeit. Krist, 1935, 91, 123.

(35) Chemische Kristallographie, 1919, 5, 437.

(36) Zeit. Krist., 91, 170, 1935.

(37) Nature, 1936, 137, 361.

(38) Zeit. Krist., 1935, 91, 173.

(39) J.C.S., 1936, 1195.

(40) Nature, 1945, 156, 51.

(41) Robertson, J. Sci. Instr., 1943, 20, 175.

(42) Robertson and Dawton, ibid., 1941, 18, 126.

(43) Ibid., 1933, 10, 233.

(44) Robertson, J.C.S., 1935, 615.

(45) Linstead and Robertson, ibid., 1936, 1736.

(46) Robertson, Phil. Mag., 1936, 21, 176.

(47) Robertson, Proc. Roy. Soc., A, 150, 110, 1935.

(48) Robertson, Phil. Mag., 1934, 18, 729.

REFERENCES (continued)

(49) Robertson, Proc. Roy. Soc., 1935, A, 150, 348.

(50) Nature, 1945, 156, 82.

(51) Proc. Roy. Soc., A, 146, 473 (1934).

(52) Cook, Ann. Reports Chem. Soc., 1942, 39, 163.

(53) Coulson, Private Communication.